

UNDERSTANDING TEMPORAL DYNAMICS OF PLANT SPECIALIZED  
METABOLITES IN RESPONSE TO SIMULATED BROWSING IN WINTER

by

Bryanna Hope Bright



A thesis

submitted in partial fulfillment

of the requirements for the degree of

Master of Science in Biology

Boise State University

May 2023

© 2023

Bryanna Hope Bright

ALL RIGHTS RESERVED

BOISE STATE UNIVERSITY GRADUATE COLLEGE

**DEFENSE COMMITTEE AND FINAL READING APPROVALS**

of the thesis submitted by

Bryanna Hope Bright

Thesis Title: Understanding Temporal Dynamics of Plant Specialized Metabolites in Response to Simulated Browsing in Winter

Date of Final Oral Examination: 09 March 2023

The following individuals read and discussed the thesis submitted by student Bryanna Hope Bright, and they evaluated the student's presentation and response to questions during the final oral examination. They found that the student passed the final oral examination.

Jennifer S. Forbey, Ph.D.

Chair, Supervisory Committee

Amy C. Ulappa, Ph.D.

Member, Supervisory Committee

Sven Buerki, Ph.D.

Member, Supervisory Committee

The final reading approval of the thesis was granted by Jennifer Forbey, Ph.D., Chair of the Supervisory Committee. The thesis was approved by the Graduate College.

## DEDICATION

For God and my family, without which I would not have the strength to pull through the hardships of life to get to where I am today.

## ACKNOWLEDGMENTS

A large thank you to Boise State University and the Department of Biological Sciences for the exemplary community and providing access to the graduate and Teaching Assistant programs that helped support my degree progress, without which none of this would have been possible. Specifically, thanks go out to Marie-Anne de Graff as the coordinator for the graduate and Teaching Assistant programs for her help and guidance. I also want to express my appreciation to Shay Gillette and Melanie Purviance for the opportunities they provided me for additional funding. Also, I want to express my gratitude to my committee members, Dr. Amy Ulappa and Dr. Sven Buerki, for their continued support throughout my project. I am extremely grateful to my advisor, Dr. Jennifer Forbey, for accepting me into her lab unexpectedly and providing me endless amounts of support, guidance, and encouragement. She has helped me grow as a person, scientist, and as someone who is faced with many health challenges. I would also like to extend a huge thank you to Britt Pendleton in the Forbey lab who helped provide guidance and assistance throughout my experience in the graduate program. I would not have been able to get through the demanding work as a graduate student without her. My thanks go out to Dr. Gail Patricelli and Alan Krakauer at UC Davis as well as Graham Frye and Marcella Fremgen-Tarantino from Boise State University that assisted with the experimental setup and data collection. Additionally, I would like to thank the other current Forbey lab members, including Debbie Conner and Ashley Martwick, for their support in the laboratory and in the field, as well as other past lab members, specifically

Chelsea Merriman, Brecken Robb, and Karli Graski, for their help in the chemistry data collection and processing. Thank you to Celin Younan and Stephanie Galla who were also able to help read and comment on my thesis to guide it in the right direction. I would also like to extend my thanks to the Biomolecular Research Center (BRC) for support from Dr. Laura Bond for answering my countless statistical questions. Lastly, I would like to specifically thank my family members with my parents Kim and James Bright, many siblings, grandparents, and more, for their continued support on my arduous journey through the many challenges that graduate school, COVID-19, and other health issues have posed. This thesis and the accompanying research was made possible by funding from the National Science Foundation (NSF) Track 2 EPSCoR Program under award number OIA-1826801 (GUTT) and NSF Idaho Track 1 EPSCoR Program under award number OIA-1757324 (GEM3).

## ABSTRACT

Plants are continually defending themselves from the herbivores that consume them, often using an array of plant specialized metabolites (PSMs). Volatile organic compounds, including monoterpenes, are one such type of PSMs that can be emitted and induced by plants in response to mechanical damage and herbivory. These volatiles serve as direct defenses against herbivores and can alert neighboring plants about potential threats, resulting in protection against future attacks. However, how these chemicals change over time in response to browsing by vertebrates in the winter has received limited attention and is crucial to interpreting how monoterpenes defend plants against vertebrate herbivores. To assess induced defenses of plants in the winter, we investigated temporal changes of monoterpenes in Wyoming big sagebrush (*Artemisia tridentata* subsp. *wyomingensis*) naturally occurring in the Wyoming landscape following either a single event of mechanical damage (acute damage) or repeated damage (chronic damage) to leaves that simulated “bites” by the avian herbivore, Greater Sage-grouse (*Centrocercus urophasianus*). We hypothesized that plants would exhibit changes in specific monoterpenes through the process of emission which releases volatiles into the air in response to damage and then through induction which involves biochemical synthesis. We also hypothesized that the intensity of damage would influence monoterpene profiles. Based on these hypotheses, we predicted an initial decrease in the concentration of monoterpenes in leaves soon after damage due to emission which would be followed by increases in monoterpenes in leaves as the time course progressed

associated with induction. We also predicted that treatment plants would be less variable in monoterpene profiles compared to control plants and that higher levels of damage would result in greater changes in monoterpenes. Monoterpene profiles and concentrations were analyzed using gas chromatography. Multiple Principal Component Analyses (PCA) using Euclidean distance, ANOVAs, correlation matrices, and nonparametric Kruskal-Wallis tests were used to compare changes in monoterpenes over time within treatments, between treatment groups, and between levels of collection intensity after an initial simulated browsing event. We identified fourteen potential compounds of interest with the largest vector loadings from the PCAs which were reduced to six compounds of interest based on strong correlation with other compounds. There was no evidence that any compound of interest changed over time after simulated browsing within individual treatment groups. We found no evidence that browsing type or browsing intensity changed monoterpene profiles or concentrations of compound of interest. Results suggest that damage to sagebrush in the winter results in only minor changes in monoterpenes over a six-day time course. However, review of correlation among clusters of compounds following browsing indicate that chronic browsing results in more negative correlations between compounds suggesting conversion of monoterpenes into other metabolites. Lack of induced defenses associated with winter browsing is inconsistent with observed induced defenses in sagebrush damaged in the summer and suggests stable winter chemistry following leaf damage that may explain the relatively high winter foraging fidelity observed in sage-grouse. This research demonstrates the value of a multivariate approach to detect chemicals that might normally be ignored due to their relatively low concentration and rarity in a plant-

herbivore system. The multivariate approach could be used to assess the relative plasticity of chemical defenses as a consequence of gene by environment interactions. Metrics of chemical stability relative to seasonality, climate, or herbivory could be used to inform management decisions of what plant genotypes to select for restoration of disturbed areas and predict how chemical responses will cascade up to influence species of conservation concern and entire communities.

## AUTOBIOGRAPHICAL SKETCH OF AUTHOR

Bryanna Bright was born in Anaheim, California and raised in Nampa, Idaho. She attended Boise State University in Boise, Idaho and graduated with a Bachelor of Science in December 2016 in Biology with an emphasis in Zoology. After graduating, Bryanna spent some time working for the Wildlife Sarari in Winston, Oregon and for the Idaho Department of Agriculture. She joined Boise State University for the Master of Science in Biology degree program in August of 2019 and was introduced to the Sagebrush Steppe ecosystem research projects.

## TABLE OF CONTENTS

DEDICATION .....	iv
ACKNOWLEDGMENTS .....	v
ABSTRACT .....	vii
AUTOBIOGRAPHICAL SKETCH OF AUTHOR.....	x
LIST OF TABLES .....	xiii
LIST OF FIGURES.....	xvii
LIST OF ABBREVIATIONS.....	xxiii
CHAPTER ONE: UNDERSTANDING TEMPORAL DYNAMICS OF PLANT SPECIALIZED METABOLITES IN RESPONSE TO SIMULATED BROWSING IN WINTER.....	1
Introduction .....	1
Methods.....	10
Study Area .....	10
Experimental Design .....	11
Laboratory Methods for Analysis of Monoterpenes .....	13
Data Processing.....	14
Statistical Analyses.....	16
Results .....	19
Exploratory PCAs of Time Points within Treatment Groups.....	19
PCA of Control versus Acute Treatments .....	22

PCA of Control versus Chronic Treatments.....	22
PCA of Collection Intensity .....	23
Correlation Matrices of Compounds of Interest and Standards .....	23
Selection of Compounds of Interest Based on Correlations.....	26
Comparing Time Points and Treatment Groups.....	27
Comparing Collection Intensities .....	27
Discussion.....	28
References.....	40
Tables.....	55
Figures .....	67
<b>CHAPTER TWO: APPLYING KNOWLEDGE OF PLANT INDUCED DEFENSE TO ECOSYSTEM MANAGEMENT, AGRICULTURE, AND PHARMACOLOGY THROUGH USE-INSPIRED RESEARCH IN CHEMISTRY.....</b>	<b>82</b>
References.....	90
APPENDIX A.....	98
APPENDIX B.....	101
APPENDIX C.....	103
APPENDIX D.....	121
APPENDIX E .....	126
APPENDIX F .....	131
APPENDIX G.....	136
APPENDIX H.....	140

## LIST OF TABLES

- Table 1.1. Sampling collection scheme. All sites (Figure 1.1) contained paired plants (Plant ID 1 - 5) with each being assigned to either a simulated browsed treatment (e.g., clipped, hereafter treatment, green left column) or serving as a control (e.g., was not clipped, tan top row). The treatment plants in each pair received a simulated browsing event (represented by the beak icon) at time zero (Hour 0) and then collections of the stems and leaves (represented by the scissors icon) were taken from the treatment plant at the designated time intervals after the simulated browsing event (Hour 1, Hour 24, Hour 48, Hour 144 hr). For each treatment plant's first collection of material, stems and leaves were also collected from the paired control plant. A collection intensity scale was assigned to each sample collection event throughout the time course for each treatment plant with a collection intensity of low indicating that no previous collection had taken place on that plant (low, light red representing acute level of simulated browsing) and a collection intensity of high indicating that three prior sequential collections had been taken on that plant (high, dark red, representing the highest chronic level of simulated browsing). .....55
- Table 1.2. Compound names with retention times (mins) acquired from gas chromatography. Naming the compounds was done to simplify the visualization of all compounds in the figures with known compounds in parentheses determined from co-chromatography with standards. The yellow highlighted compounds were included in the subsequent analyses because they were present in at least 10% of any treatment group. The unhighlighted compounds were excluded from the analyses. ....56
- Table 1.3. Principal Component Analysis (PCA) loadings cutoff tables for comparing time points (1, 24, 48, and 144 hr) within *a*) control, *b*) acute, or *c*) chronic treatment groups separately and comparing *d*) control versus acute, *e*) control versus chronic, and comparing *f*) varying levels of collection intensity at 144 hr. These tables were created from a threshold equation of  $\sqrt{1/\text{ncol}(\text{dataframe})}$  that resulted in the value of 0.132 for all groups (Holland 2019). Similar loading values represent compounds that are correlated within the positive or negative quadrant of the PC dimensions (PC1 or PC2). Only loadings that are above the threshold of 0.132 (in bold) were included. Any loading in either PC1 or PC2 higher than +/-0.3 rounded were considered a compound of interest (indicated by red shading) as they signified a substantial contribution to the variation being

	observed among the groups being compared (Merenda 1997, Peterson 2000). .....	57
Table 1.4.	The number of correlated pairs (Figure 1.10, Figure 1.11) that were above the +/-0.4 threshold for control, acute, and chronic treatment group. ....	59
Table 1.5.	Mean, Standard Error, minimum (Min), and maximum (Max) statistics for the two strongest positive and two strongest negative correlated clusters that occurred throughout the treatment groups.....	60
Table 1.6.	Kruskal-Wallis test results comparing positive and negative correlated values among the control, acute, and chronic treatment groups where only pairs were included if at least one treatment group had an $r^2 > +/-0.4$ . ....	61
Table 1.7.	Pairwise Wilcoxon Rank Sum test to determine which treatment groups of control, acute, and chronic were significantly different from each other when at least one treatment group had an $r^2 > -0.4$ .....	62
Table 1.8.	Kruskal-Wallis test results on the correlation values between the strongest positive and negative correlation clusters to compare strength among the control, acute, and chronic treatment groups.....	63
Table 1.9.	Pairwise Wilcoxon Rank Sum test to determine if the treatment groups of control, acute, and chronic were significantly different from each other when observing the strongest negative correlation cluster.....	64
Table 1.10.	Two-way ANOVA results for the final compounds of interest identified from comparing treatment groups and time points. ....	65
Table 1.11.	One-way ANOVA results from the final compounds of interest from comparing the varying levels of collection intensity. ....	66
Table C.1.	Principal Component Analysis (PCA) loadings cutoff tables for comparing time points (1, 24, 48, and 144 hr) within <i>a</i> ) control, <i>b</i> ) acute, or <i>c</i> ) chronic treatment groups separately and comparing <i>d</i> ) control versus acute, <i>e</i> ) control versus chronic, and comparing <i>f</i> ) varying levels of collection intensity at 144 hr, all with the inclusion of C14. These tables were created from a threshold equation of $\text{sqrt}(1/\text{ncol}(\text{dataframe}))$ that resulted in the value of 0.132 for all groups (Holland 2019). Similar loading values represent compounds that are correlated within the positive or negative quadrant of the PC dimensions (PC1 or PC2). Only loadings that are above the threshold of 0.132 (in bold) were included. Any loading in either PC1 or PC2 higher than +/-0.4 rounded (previous threshold) were considered a compound of interest (indicated by red shading) as they signified a substantial contribution to the variation being observed among the groups being compared (Merenda 1997, Peterson 2000).....	113

Table C.2.	Two-way ANOVA results for the initial compounds of interest identified from comparing treatment groups and time points. These were calculated when C14 was included in the analysis. ....	119
Table C.3.	One-way ANOVA results from the final compounds of interest from comparing the varying levels of collection intensity. These were calculated when C14 was included in the analysis. ....	120
Table E.1.	Correlation matrix and corresponding $r^2$ values for the control group subset. Cells colored in any blue shade indicate positive $r^2$ values $> 0.3$ . Cells colored in any orange shade indicate negative $r^2$ values $> -0.3$ . Red font color indicates that $r^2$ value is above the $\pm 0.4$ threshold which were included to compare the strength of correlations among treatment groups. Blue borders indicate the strongest positive correlation clusters typically over an $r^2 > 0.4$ while orange borders indicate the strongest negative correlation clusters typically over an $r^2 > -0.3$ which were also compared among treatment groups.....	128
Table E.2.	Correlation matrix and corresponding $r^2$ values for the acute group subset. Cells colored in any blue shade indicate positive $r^2$ values $> 0.3$ . Cells colored in any orange shade indicate negative $r^2$ values $> -0.3$ . Red font color indicates that $r^2$ value is above the $\pm 0.4$ threshold which were included to compare the strength of correlations among treatment groups. Blue borders indicate the strongest positive correlation clusters typically over an $r^2 > 0.4$ while orange borders indicate the strongest negative correlation clusters typically over an $r^2 > -0.3$ which were also compared among treatment groups.....	129
Table E.3.	Correlation matrix and corresponding $r^2$ values for the chronic group subset. Cells colored in any blue shade indicate positive $r^2$ values $> 0.3$ . Cells colored in any orange shade indicate negative $r^2$ values $> -0.3$ . Red font color indicates that $r^2$ value is above the $\pm 0.4$ threshold which were included to compare the strength of correlations among treatment groups. Blue borders indicate the strongest positive correlation clusters typically over an $r^2 > 0.4$ while orange borders indicate the strongest negative correlation clusters typically over an $r^2 > -0.3$ which were also compared among treatment groups.....	130
Table G.1.	Two-way ANOVA results for C26 comparing the effects of treatment group, time points, and treatment by time point interactions on the compound concentrations. ....	137
Table G.2.	Two-way ANOVA results for C28 comparing the effects of treatment group, time points, and treatment by time point interactions on the compound concentrations. ....	137

Table G.3.	Two-way ANOVA results for C34 comparing the effects of treatment group, time points, and treatment by time point interactions on the compound concentrations. ....	138
Table G.4.	Two-way ANOVA results for C38 comparing the effects of treatment group, time points, and treatment by time point interactions on the compound concentrations. ....	138
Table G.5.	Two-way ANOVA results for C44 comparing the effects of treatment group, time points, and treatment by time point interactions on the compound concentrations. ....	139
Table H.1.	Two-way ANOVA results for C18 comparing the effects of treatment group and time points on the compound concentrations. ....	141
Table H.2.	One-way ANOVA results for C18 comparing the effects of the varying levels of collection intensity on the compound concentrations. ....	141
Table H.3.	Tukey’s Honestly Significant Difference (HSD) test comparing the multiple means of each treatment group and time point in a pairwise manner for C18 to identify any differences that may be greater than the expected standard error. ....	142

## LIST OF FIGURES

- Figure 1.1. Map of 15 collection patches in Fremont County, Wyoming, USA where the induced defense experiment was conducted. The overlay map in the upper left corner displays the sagebrush biome distribution throughout the western United States. The red star indicates the location of the study area. Sagebrush biome distribution map acquired from the USGS (Jeffries and Finn 2019). .....67
- Figure 1.2. (Left) Overview of induced defense experiment with treatments that mimic natural browsing by sage-grouse on sagebrush where distinct bite marks are made on the leaves. This browsing damage was simulated by cutting 50 leaves from each simulated browsed treatment plant (indicated by bird beak icon) in each collection site at zero hr (T = 0 hr). After the simulated browsing treatment, leaf and stem material was collected using scissors at various time points (0, 1, 24, 48, and 144 hr). Collections were taken from treatment plants and (Right) a spatially and temporally paired control plant that was unique and had never received simulated browsing or prior collections. All paired treatment and control plants were positioned at a minimal distance of 1 m apart. ....68
- Figure 1.3. Diagram of induced defense data structure and the associated number of collection samples in each group. ....69
- Figure 1.4. Chromatogram of a cocktail of monoterpene standards used for co-chromatography. The standards correspond to the compound names (inset) based on the retention times (mins) that they appear on the chromatogram. The first peak corresponds to the solvent methylene chloride used to combine standards into a single sample for gas chromatography.....70
- Figure 1.5. Representative monoterpene chromatograms for sagebrush (*Artemisia tridentata* subsp. *wyomingensis*) (top three lines) and the cocktail of monoterpene standards (bottom blue line). The peaks represent individual compounds with the relative abundance measured as area under the curve (AUC) with the corresponding retention time (RT) in mins. The main compounds of interest and standards are marked using compound names based on associated RTs (Table 1.2). .....71
- Figure 1.6. Consort diagrams that details the decisions made for inclusion and exclusion of samples and monoterpene compounds into the analyses.....72

- Figure 1.7. Principal Component Analyses (PCAs) generated for comparing time points (1, 24, 48, and 144 hr) within *a)* control, *b)* acute, and *c)* chronic treatment groups separately using the calculated centered values. The colored ellipses represent the different time points (hr) after simulated browsing within each treatment and where time points fall across the different PC dimensions. The compounds are represented by the vectors of varying lengths with the longer vectors having a stronger influence on the variation among the samples within the time point category (see Table 1.3 for PCA loadings). ..... 73
- Figure 1.8. PCAs generated for the *a)* control versus acute treatment for all time points and *b)* control versus chronic treatment for all time points using the calculated centered values. The colored ellipses represent the different treatment groups present and where they fall across the different PC dimensions. The compounds are represented by the vectors of varying lengths with the longer vectors having a stronger influence on the variation among the samples within the treatment category (see Table 1.3 for PCA loadings). ..... 74
- Figure 1.9. PCA generated for the different levels of collection intensity (see Figure 1.2 and 1.3) using the calculated centered values. The colored ellipses represent the control and the different levels of collection intensity (low – high) and where they fall across the different PC dimensions. The compounds are represented by the vectors of varying lengths with the longer vectors having a stronger influence on the variation among the samples within the collection intensity category (see Table 1.3 for PCA loadings). ..... 75
- Figure 1.10. Correlation matrices generated from the area under the curve per gram dry weight (AUC/gDW) values of the fourteen main vector loadings that made the cutoff threshold of +/-0.3 (see Table 1.3) and the monoterpene standards. The size of each circle corresponds to the strength of the correlation represented by the correlation coefficients between -1.0 and +1.0 among the respective compounds while the color indicates either a positive (blue) or a negative (red) correlation. All compounds aside from the standards appeared in at least one of the PCA loading tables. The correlation matrices are created through comparing *a)* all samples in the experiment, *b)* time points within control, *c)* time points within acute, *d)* time points within chronic, *e)* control versus acute, *f)* control versus chronic, and *g)* collection intensity. Compound C14 was excluded in the subsequent analyses due to its “oil-can” appearance that bled into C15 (see Appendix C for details). ..... 77
- Figure 1.11. Correlation matrices generated from the area under the curve per gram dry weight (AUC/gDW) values of the compounds of interest that made it above the cutoff of +/-0.3 that signified a substantial contribution to the

	variation being observed among all samples within the experiment (see Table 1.3). The size of each circle corresponds to the strength of the correlation between -1.0 and + 1.0 between the respective compounds while the color indicates either a positive (blue) or a negative (red) correlation. All compounds appeared in at least one of the PCA loading tables as having a loading value above the +/-0.3 cutoff.....	78
Figure 1.12.	Consort diagram that details the decisions made for inclusion and exclusion of the final compounds of interest that made it above the PCA loading cutoff of +/-0.3 for the final analyses (see Table 1.3).....	79
Figure 1.13.	Mean monoterpene concentrations (AUC/gDW) for the final compounds of interest when comparing treatment groups across the time points (hours) after the first simulated browsing event. Each bar graph has associated standard error bars. ....	80
Figure 1.14.	Mean monoterpene concentrations (AUC/gDW) for the final compounds of interest when comparing across the varying levels of collection intensity for plants at 144 hr following the first simulated browsed event. Each bar graph has associated standard error bars. ....	81
Figure A.1.	Original sketch of the field experimental design showing the spatial extent by which plants were treated and how they were paired with control plants. Plant numbers match those in Table 1.1 and the overview layout of Figure 1.2.....	100
Figure C.1.	Stacked chromatograms of randomly selected samples that contained either one or two peaks being recorded for AUC values of C1 and C2 (Table 1.2). C1 and C2 are indicated by their retention time (min). C1 is shown to constantly bleed into C2. ....	106
Figure C.2.	Stacked chromatograms of randomly selected samples that contained either one or two peaks recorded for AUC values of C24 and C25 (Table 1.2). C24 and C25 are indicated by their retention time (min). The peak for C24 is shown to overlap the position for C25 due to its large peak size and range. ....	107
Figure C.3.	Representative chromatograms of monoterpene cocktail standard runs (top for chromatograms) and blanks (bottom 3 chromatograms). The red bar transecting each chromatogram at 13.62 min retention time indicates the location for C14 that appeared randomly throughout the samples with an “oil-can” shape (Figure 1.5, Figure C.4). C14 never occurred in any of the blank or standard cocktail runs suggesting it was not a contaminant. ....	108
Figure C.4.	Representative chromatograms of monoterpenes in sagebrush ( <i>Artemisia tridentata</i> spp.) (top two lines) and the monoterpene cocktail standard	

(bottom line). The peaks represent the initial individual compounds with the relative abundance measured in area under the curve (AUC) with the corresponding retention time in minutes. The main compounds of interest are marked prior to C14 exclusion. Here the “oil-can” appearance of C14 (at 13.62 min) is clearly demonstrated..... 109

Figure C.5. Principal Component Analyses (PCAs) generated for comparing time points (1, 24, 48, and 144 hr) after simulated browsing within *a)* control, *b)* acute, and *c)* chronic treatment groups separately using the calculated centered values with the inclusion of C14. The colored ellipses represent the different time points (hr) within each treatment and where time points fall across the different PC dimensions. The compounds are represented by the vectors of varying lengths with the longer vectors having a stronger influence on the variation among the samples within the time point category. In each PCA, C14 is a strongly pulling vector. .... 110

Figure C.6. PCAs generated for the *a)* control versus acute treatment for all time points and *b)* control versus chronic treatment for all time points using the calculated centered values with the inclusion of C14. The colored ellipses represent the different treatment groups present and where they fall across the different PC dimensions. The compounds are represented by the vectors of varying lengths with the longer vectors having a stronger influence on the variation among the samples within the treatment category. In each PCA, C14 is a strongly pulling vector. .... 111

Figure C.7. PCA generated for the different levels of collection intensity using the calculated centered values with the inclusion of C14. The colored ellipses represent the different levels of collection intensity (zero – high) and where they fall across the different PC dimensions. The compounds are represented by the vectors of varying lengths with the longer vectors having a stronger influence on the variation among the samples within the collection intensity category. In this PCA, C14 is a strongly pulling vector. .... 112

Figure C.8. Correlation matrices generated from the area under the curve per gram dry weight (AUC/gDW) values of the main vector loadings that made the cutoff threshold of +/-0.3 (see Table 1.3) with the inclusion of C14. The size of each circle corresponds to the strength of the correlation between -1.0 and +1.0 among the respective compounds while the color indicates either a positive (blue) or a negative (red) correlation. All compounds aside from the standards appeared in at least one of the PCA loading tables. The correlation matrices are created through comparing *a)* all samples in the experiment, *b)* time points within control, *c)* time points within acute, *d)* time points within chronic, *e)* control versus acute, *f)* control versus chronic, and *g)* collection intensity. .... 116

Figure C.9.	Mean monoterpene concentrations (AUC/gDW) for the initial compounds of interest when comparing treatment groups across the time points (hours) after the first simulated browsing event. Each bar graph has associated standard error bars. These were generated using the four main compounds that displayed the highest vector loadings when C14 was included.....	117
Figure C.10.	Mean monoterpene concentrations (AUC/gDW) for the initial compounds of interest when comparing treatment groups across the varying levels of collection intensity. Each bar graph has associated standard error bars. These were generated using the four main compounds that displayed the highest vector loadings when C14 was included. ....	118
Figure D.1.	Correlation plot of concentration (in area under the curve) for the monoterpene standard 1,8-cineole between Batch 1 (blue) and Batch 2 that occurred after recalibration of the gas chromatography machine (red) for the same 17 sagebrush samples.....	124
Figure D.2.	Comparison of concentration (in area under the curve) for the monoterpene standard 1,8-cineole between Batch 1 (blue) and Batch 2 that occurred after recalibration of the gas chromatography machine (red) for the same 17 sagebrush samples. The repeat of each individual plant samples are connected between the two groups to show potential discrepancy.....	125
Figure F.1.	Boxplots of the positive correlation pairs for each treatment group where only pairs were included if at least one treatment group had an $r^2 > 0.4$ . Each boxplot has an associated median and quartiles for each treatment group.....	133
Figure F.2.	Boxplots of the negative correlation pairs for each treatment group where only pairs were included if at least one treatment group had an $r^2 > -0.4$ . Each boxplot has an associated median and quartiles for each treatment group.....	133
Figure F.3.	Boxplots of the strongest positive correlation cluster for each treatment group. Each boxplot has an associated median and quartiles for each treatment group. ....	134
Figure F.4.	Boxplots of the second strongest positive correlation cluster for each treatment group. Each boxplot has an associated median and quartiles for each treatment group. ....	134
Figure F.5.	Boxplots of the strongest negative correlation cluster for each treatment group. Each boxplot has an associated median and quartiles for each treatment group. ....	135

Figure F.6. Boxplots of the second strongest negative correlation cluster for each treatment group. Each boxplot has an associated median and quartiles for each treatment group ..... 135

## LIST OF ABBREVIATIONS

ANOVA	Analysis of variance
AUC	Area under the curve
AUC/gDW	Area under the curve per gram dry weight
BRC	Biomolecular Research Center
BLM	Bureau of Land Management
C	Celsius
cm	Centimeter
$r^2$	Coefficient of determination
C#	Compound
DW	Dry weight
g	Gram
GC	Gas chromatography
GPP	Geranyl diphosphate
HPLC	High-performance liquid chromatography
hr	Hour
HSD	Honest Significant Difference
LDA	Linear discriminant analysis
MF	Marcella Fremgen
m	Meter
$\mu\text{g}$	Microgram

mph	Miles per hour
mL	Milliliter
mm	Millimeter
min	Minute
NSF	National Science Foundation
NIRS	Near-infrared spectroscopy
NMDS	Nonmetric multidimensional scaling
NMR	Nuclear Magnetic Resonance
PSM	Plant Specialized Metabolites
PCA	Principal Component Analysis
RT	Retention time
SEM	Standard error of the mean
T	Time
WW	Wet weight

CHAPTER ONE: UNDERSTANDING TEMPORAL DYNAMICS OF PLANT  
SPECIALIZED METABOLITES IN RESPONSE TO SIMULATED BROWSING IN  
WINTER

**Introduction**

Plant specialized metabolites (PSMs) mediate plant-plant and plant-animal interactions at ecological and evolutionary scales (Ehrlich and Raven 1964, Heil and Karban 2010, Bouwmeester et al. 2019). Specifically, plants and herbivores have been in a chemical arms race for millennia, co-evolving different bioactive chemicals in plants and subsequent mechanisms in herbivores that counter these defenses (Ehrlich and Raven 1964, Freeland and Janzen 1974, Agrawal 2000, Dearing et al. 2005, Sorensen et al. 2005). For example, the leaf-chewing insect herbivore, *Blepharida*, has adapted to the chemical defenses of the tropical plant species *Bursera* (Burseraceae) by halting the resin flow of the leaf vein canals through cutting prior to feeding on the leaves (Becerra et al. 2009). A well-observed co-evolution example are monarch caterpillars that are adapted to the chemical defenses of milkweed (Asclepiadaceae) which includes latex and cardiac glycosides (Dussourd and Eisner 1987, Birnbaum and Abbot 2018). This co-evolution of defense mechanisms has also been documented in vertebrate herbivores. For example, desert woodrats (*Neotoma lepida*) have duplicated genetically diverse cytochrome P450 genes that result in a detoxification enzyme subfamily capable of combating PSMs in their primary food source creosote (*Larrea tridentata*) (Malenke et al. 2012, Greenhalgh et al. 2022).

Plant-plant and plant-animal interactions also occur across smaller spatial and shorter temporal scales often through the process of emission of volatiles from leaves (Fall et al. 1999, Ameye et al. 2018) and through biosynthetic induction (Baldwin and Schultz 1983, Karban and Myers 1989, Dudareva et al. 2013, Eisenring et al. 2017). Past studies have demonstrated the importance of emitted volatiles as chemical signals that can be detected by and influence the chemistry of neighboring plants (Karban et al. 2000, 2006, Kost and Heil 2006). For example, when lima beans (*Phaseolus lunatus*) were exposed to volatiles emitted by conspecific neighbors, they exhibited less leaf loss to herbivores than the control plants that were not exposed to the volatiles (Kost and Heil 2006). Induced defense strategies are both short-term and long-term (Tuomi et al. 1988, Heil and Karban 2010). For example, after tobacco (*Nicotiana attenuata*) has been damaged, they quickly begin producing nicotine and protease inhibitors to directly defend against herbivory (Steppuhn and Baldwin 2007, Backmann et al. 2019). After the foliage of mountain birch (*Betula pubescens* subsp.) has sustained damage, it not only accumulates phenols in its adjacent leaves, but maintains higher levels of phenolics for 3-4 years after defoliation (Niemi et al. 1979, Tuomi et al. 1984, Backmann et al. 2019). These studies demonstrate the immediate and long-term temporal dynamics of induced PSMs.

The dynamics of PSM emission and induction also occur at varying biological scales and can have cascading spatial effects across a community of species (Glinwood et al. 2004, Heil and Karban 2010, Hussain et al. 2019). Intra-plant communication occurs when plants use their own volatile compounds to communicate among its different branches to coordinate a complete chemical defense across the entire plant (Karban et al.

2006). Intra-species communication occurs when chemo-typically and genetically related individuals have a quicker and more accurate response to emission from a conspecific that has been attacked (Karban et al. 2014a, Hussain et al. 2019). Lima bean plants (*Phaseolus lunatus*) induced both within-plant and caused intra-specific plant signaling after exposure to volatiles from conspecific shoots that were beetle-damaged (Heil and Bueno 2007). Inter-species communication can also occur when one species induces defenses in response to “eavesdropping” on the emissions resulting from herbivore damage on a different plant species (Baldwin et al. 2006). For example, barley plants (*Hordeum vulgare*) exposed to the volatiles released by two types of thistles (*Cirsium arvense* and *Cirsium vulgare*) were less acceptable to aphids due to the induced defenses in barley (Glinwood et al. 2004). Emission of volatiles from plants in response to herbivore damage can influence the behavior of both herbivores (Karban and Baxter 2001, Forbey et al. 2009) and predators of herbivores (Wiens et al. 1991, Heil 2008, Clavijo McCormick et al. 2012). After leaf tissue damage has occurred, tomato plants (*Solanum lycopersicum* Mill.) emit PSMs that both repel herbivores and can attract natural herbivore predators (Unsicker et al. 2009, Raghava et al. 2010).

The majority of induced defense studies focus on invertebrate damage in model plant systems (e.g., tomatoes, tobacco, *Arabidopsis thaliana*) that are fast-growing (Baldwin and Schultz 1983, Karban et al. 2000, Hulten et al. 2006, Heil and Karban 2010). These studies look at the effects that invertebrate herbivores have on PSMs, inspecting various parts of a plant from its roots to its reproductive parts for changes in PSMs, and conducting experiments to assess how plants respond either over a single time point or intervals of time (Zangerl and Rutledge 1996, Karban et al. 2000, Nykänen and

Koricheva 2004, McCall and Karban 2006, Backmann et al. 2019, Chen et al. 2020). Studies in non-model plants often do not assess the time course of chemical profiles (Farmer and Ryan 1990, Karban et al. 2000, Godard et al. 2008) or tend to focus on profiles emitted (Karban et al. 2014a, Tzin et al. 2017) rather than the chemical profiles in the leaf tissue still available to herbivores after damage. In addition, studies often rely on palatability indices that quantify the number of browsed leaves following leaf damage that are not directly linked to changes in chemical concentrations of leaves (Karban and Baxter 2001). There are also a limited number of studies that vary the intensity and timing of damage which may better represent foraging damage by vertebrate herbivores compared to less mobile invertebrates (Underwood 1998, Kant et al. 2004, Pu et al. 2015). Finally, the focus on invertebrates results in few studies investigating induced defenses in winter when low resource availability and lower temperatures may limit capacity for chemical biosynthesis (Hulten et al. 2006, Neilson et al. 2013).

To our knowledge, the foraging consequences of vertebrate herbivores in the winter has yet to be linked to short-term, small-scale dynamic changes in chemistry of plants. It is likely that vertebrate herbivores are responding to volatile cues at small scales. For example, volatile PSMs explained foraging decisions of Greater Sage-grouse (*Centrocercus urophasianus*), where birds selected species, patches, and individual plants with the lowest volatile monoterpenes (Frye et al. 2013). Responses to monoterpenes could include avoidance of plants due to irritation caused by emitted volatiles (Cometto-Muñiz et al. 1998, Forbey et al. 2009, Nobler et al. 2019), increased foraging on plants that are more vulnerable after emission of PSMs that results in lower concentrations in the leaves (Frye et al. 2013, Bouwmeester et al. 2019), leaving a patch before induction

of PSM begins (Basey et al. 1988, Kost et al. 2011), or a delay in returning to a patch that has been induced until enough time has passed for the induced defense to subside (Backmann et al. 2019). Predicting responses by vertebrate herbivores to PSMs requires greater understanding of not only the time course, but also the context in which induction may or may not occur. Induction may be dependent on plant species. For example, lomatium (*Lomatium dissectum*), lupine (*Lupinus polyphyllus*), and California valerian (*Valeriana californica*) did not induce a defense response when neighboring sagebrush (*Artemisia tridentata*) were experimentally clipped, but wild tobacco (*Nicotiana attenuata*) did produce a chemical defense response (Karban et al. 2004). Induction may also be dependent on environmental conditions. Induced defense is more commonly seen in fast growing plants in areas of high resource availability whereas slower growing plants found in environments low in resources may rely more on constitutive defenses (Karban 2011). For example, congeners across multiple genera in glade and white-sand low-resource areas had higher constitutive defenses and overall higher investments in total defenses compared to their respective congeners in non-glade and clay high-resource areas (Fine et al. 2006, Zandt 2007). In subarctic systems, alder (*Alnus*) and birch (*Betula*) shrubs did deter vertebrate herbivory through higher concentrations of PSMs, but willows (*Salix*) were not able to produce a defense response (Bryant and Kuropat 1980, Bryant et al. 2014, Swanson 2015). In addition, induction is often herbivore specific (Kost and Heil 2006). In the shrub *Baccaris salicifolia*, damage by a generalist (*Aphis gossypii*, feeding on many plant species) resulted in a unique emission of PSM blends compared to a specialist (*Uroleucon macolai*, feeding only on *Baccaris salicifolia* and *Baccaris polifolia*) aphid species. This specificity resulted in induced

defense responses in the neighboring plants for the particular species of aphid that was present (Moreira et al. 2018)

The gaps in knowledge surrounding plant induced defenses in the winter must be carefully addressed to better understand and manage the ecological interactions between plants and vertebrate herbivores. The sagebrush steppe represents an ideal system to understand dynamics of induced defenses in the winter that may help understand the foraging ecology of vertebrate herbivores of conservation concern and influence the way in which we manage sagebrush during restoration. First, there is evidence that induced defenses are occurring in sagebrush due to damage by herbivores in the summer (Wiens et al. 1991, Karban et al. 2000). Experimental clipping of sagebrush in the summer resulted in induced defense in conspecifics (Karbon et al. 2006) and neighboring plants such as tobacco (Farmer and Ryan 1990), with neighboring undamaged plants exhibiting less insect herbivory than those farther away from damaged sagebrush (Karbon et al. 2004). Sagebrush is a good plant model to study induced defense responses in the winter because, unlike other plant species from this ecosystem, it is an evergreen and therefore is often the only leaf material available during the winter for vertebrate herbivores of conservation and economic importance. Specifically, vertebrate herbivores such as sage-grouse (*Centrocercus* spp.), pygmy rabbits (*Brachylagus idahoensis*), pronghorn (*Antilocapra americana*), bighorn sheep (*Ovis canadensis*), and mule deer (*Odocoileus hemionus*) can feed almost exclusively on sagebrush in the winter due, in part, to sagebrush being the only leafy vegetation present (Wallestad and Eng 1975, Frye et al. 2013, Dwinnell et al. 2019). As sagebrush in the landscape continues to decline (Reisner et al. 2013), the herbivores that rely on this plant for food will also decline.

Understanding how native and restored sagebrush responds chemically to biotic and abiotic stressors during the winter is important for landscape management and the conservation of vertebrate herbivores of conservation concern. Although several studies demonstrate that individual monoterpene concentrations in leaves influence habitat use and browsing by vertebrate herbivores (Frye et al. 2013, Ulappa et al. 2014, Fremgen 2015), none have addressed how individual monoterpenes in leaves may change relative to browsing events to make plants more or less selected by herbivores in the future.

We used the sagebrush system to demonstrate how an untargeted, discovery-based, multivariate approach can be used to investigate differences in composition and concentrations of chemicals in sagebrush leaves (*Artemisia tridentata* subsp. *wyomingensis*) in response to simulated browsing by Greater Sage-grouse (*Centrocercus urophasianus*) with a focus on changes in monoterpenes throughout a time course in the winter (Heil and Karban 2010, Clavijo McCormick et al. 2014, Bouwmeester et al. 2019). Multivariate techniques allow us to investigate the entire chemical profile (Hervé et al. 2018) to pinpoint when chemical variation may be occurring following damage through differences in the PCA ellipses and correlation matrices. This exploration will expand upon knowledge already gathered from studies that have focused on single time points and single chemical changes, such as the clipping of sagebrush plants and measuring the methyl jasmonate released before and after damage (Karbon et al. 2000), and over large expanses of time, such as phenols being observed to accumulate in birch trees years after defoliation (Tuomi et al. 1988). Exploration of how PSMs change immediately and over a few days is important in understanding how PSM dynamics influence habitat use and foraging of vertebrate herbivores (Tuomi et al. 1988, Nykänen and Koricheva 2004,

Karban et al. 2014a, Backmann et al. 2019, Moreira and Abdala-Roberts 2019).

Currently, there has not been a multivariate analysis to investigate how PSMs in the leaves of sagebrush vary in response to herbivory over time during the winter.

When plants are initially damaged, volatile monoterpenes are emitted to repel herbivores and communicate through intra-plant, intra-specific, and inter-specific ways (Karban et al. 2006, Karban et al. 2014a, Hussain et al. 2019). As such, our first hypothesis is that sagebrush plants will emit PSMs when initially damaged (Karban et al. 2000, Dudareva et al. 2013, Bouwmeester et al. 2019). For example, sagebrush has been shown to emit volatiles one hour after mechanical clipping (Karban et al. 2000). The emission phase is predicted to cause a reduction in PSM concentration in the leaf material early on in the time course. Repeated damage when an herbivore continually returns to the same plant causes an increase in leaf monoterpenes through induced chemical biosynthesis to create potentially toxic concentration in the leaf material to deter herbivores over longer periods of time (Zangerl and Rutledge 1996, Moreira et al. 2018, Bouwmeester et al. 2019). Based on this evidence, our second hypothesis is that after initial emission, sagebrush plants will induce the chemical synthesis of volatiles over time (Karban et al. 2000, Dudareva et al. 2013, Bouwmeester et al. 2019). The induction phase is predicted to cause an increase in specific monoterpenes in the leaf material later on in the time course. To test the emission and induction predictions, we simulated browsing on sagebrush plants and collected samples of the leaves to analyze monoterpenes throughout a time course.

In addition to a time course, we investigated how the intensity of damage would influence PSM dynamics. There are conditions in nature where an herbivore may

continually return to the same plant to browse which may cause greater induction of defenses compared to a single browsing event (Karban 2011). This has been demonstrated in acacia trees (*Acacia sieberiana* var. *woodii*) that exhibit significantly higher concentrations of cyanide (prussic acid) with high browsing intensity by giraffes (*Giraffe camelopardalis*) compared to lower browsing intensity sites (Zinn et al. 2007). Repeated chronic browsing on a single plant is predicted to have a longer lasting effect than acute browsing which would allow the plant to recover and return to baseline, constitutive monoterpene concentrations (Underwood 1998, Karban 2011). For example, soybean plants (*Glycine max*) that were attacked by Mexican bean beetles (*Epilachna varivestis*) exhibited strong resistance to herbivory up to three days after damage, but this resistance tapered off after about 15 days (Underwood 1998). In addition, plants up-regulate a specific suite of monoterpenes that may more precisely target herbivores after being damaged rather than a breadth of baseline monoterpenes associated with a variety of biotic and abiotic factors (Zangerl and Rutledge 1996, Kant et al. 2004, Portillo-Estrada et al. 2015). Based on this evidence, our third hypothesis was that higher intensity of browsing would have a stronger influence on the synthesis of PSMs (Underwood 1998, Karban 2011). As such, we predicted there would be greater monoterpene changes in our chronic treatment that received repeated damage than plants that received no damage or only a single damage event (Heil 2009, Heil and Karban 2010). We also predicted that more intense browsing would reduce variability in monoterpenes profiles and would have more strongly correlated sets of compounds compared to plants with no or low damage (Heil 2009, Heil and Karban 2010). To test the intensity of browsing predictions, we varied the number of repeated browsing events

on plants. We used PCA ellipses to compare monoterpene profiles and ANOVAs to compare peaks of interest between levels of browsing intensity. We used correlation matrices to assess variation and strength of correlation among the compounds of interest.

We propose that understanding the time course of induced defense in the winter from this study may help interpret winter habitat use, diet selection, and movement patterns of vertebrate herbivores within microsites and across landscapes. Knowledge of which plants or plant species are chemically stable or dynamic following damage by different forms of damage (e.g., mowing, insect damage, browsing of leaves versus stem) may inform management decisions on which species are best to use for restoration of disturbed areas.

## Methods

### Study Area

This study was conducted between March 28<sup>th</sup> and April 4<sup>th</sup> of 2015 in Fremont County, Wyoming, 15 miles south of Hudson, Wyoming on Bureau of Land Management lands (N 42.833, W 108.4833, Figure 1.1). The minimum temperature during the study was -8.4°C and maximum temperature was 22.4°C. During the study, there was an average minimum and maximum temperature of 0.1°C and 15.4°C, respectively. The average daily precipitation during the study was 0.3 mm with the highest amount of snow or rain (2.1 mm) during April 2<sup>nd</sup>, 2015. Snow accumulation was recorded as a depth of 1.3 mm average. The minimum and maximum wind speeds were 9.8 mph and 47.2 mph, respectively, with an average wind speed of 24.0 mph. This location was selected because it is dominated by Wyoming big sagebrush (*Artemisia tridentata* subsp. *wyomingensis*) with a mix of Basin big sagebrush (*A. t.* subsp. *tridentata*) and black sagebrush (*A. nova*).

## Experimental Design

Within this location, 15 patches of Wyoming big sagebrush were identified by morphology, lack of fluorescence of leaves (Rosentreter et al. 2021), and taxonomic knowledge provided by local practitioners. Each patch was approximately 20 m in diameter and contained a minimum of 20 sagebrush plants. Each replicate patch was spaced a minimum of 100 m apart. Within each replicate patch, one sagebrush plant in the center of each patch was randomly selected and designated as treatment plant #1. Additional treatment plants (treatment plants #2-5) were assigned in reference to the previously selected treatment plant by selecting the closest plant at a minimum of 1.5 m towards the North, East, South, and West. For each treatment plant, a paired control plant was selected that was approximately 1.0 m away and located in the opposite direction of the other treatment plants radially (see original sketch of experimental design, Appendix A). The pairs of treatment and control plants were spaced at this distance to prevent “eavesdropping” among plants that could induce patch-wise chemical changes in response to simulated damage (Karban et al. 2000, 2006). This 1.0 m minimum distance was decided based on previous evidence that sagebrush plants had no response to clipped sagebrush when at a distance of more than 60 cm (Karban et al. 2006).

For each patch at time zero ( $T = 0$  hr), collections of 5-6 stems with leaves (approximately 5 g wet weight) were taken from the control plant #1. Both stems and leaves were collected by cutting with scissors and placing in coolers to avoid directly damaging the leaves and further inducing volatile release (Fall et al. 1999, Holopainen 2004). The control plant biomass was collected before damaging the paired treatment plant. After the collection of stems with leaves from the control plant #1, simulated

browsing was performed on each treatment plant (plants #1-5) in each patch at time zero ( $T = 0$  hr). Simulated browsing was done by mimicking natural browsing by sage-grouse, which involves breaking clusters of leaves with the beak and not the stems and leaves together (Figure 1.2). Clusters of individual leaves were portioned out and clipped with scissors to simulate sage-grouse biting on each treatment plant, which each received a total of 50 randomly simulated “bites” throughout the plant. The amount of 50 bites on each treatment plant was based on previous studies indicating that heavily browsed sagebrush plants had an average number of 50 bites throughout the plant (Fremgen 2015).

At time zero ( $T = 0$  hr), directly after treatment plant #1 was simulated browsed, collections of 5-6 stems with leaves were collected with scissors. Treatment plant #1 was spatially and temporally paired with unbrowsed control plant #1. After one hr from simulated browsing ( $T = 1$  hr), collections were taken from treatment plant #2 and its spatially and temporally paired unbrowsed control plant #2. At 24 hr after simulated browsing ( $T = 24$  hr), collections were taken from treatment plant #3 and its paired unbrowsed control plant #3 and a second collection was taken from treatment plant #2. At 48 hr after simulated browsing ( $T = 48$  hr), collections were taken from treatment plant #4 and its paired unbrowsed control plant #4, a third collection was taken from treatment plant #2, and a second collection taken from treatment plant #3. At 144 hr after simulated browsing ( $T = 144$  hr), collections were taken from treatment plant #5 and its paired unbrowsed control plant #5, a fourth collection was taken from treatment plant #2, a third collection taken from treatment plant #3, and a second collection taken from treatment plant #4. This design of sample collections allowed for varying levels of collection intensity at 144 hr after initial simulated browsing, where control plant #5

represents zero (no previous collections), treatment plant #4 represents low (one previous collection), treatment plant #3 represents medium (two previous collections), and the treatment plant #2 represents high (three previous collections) levels of increasing collection intensity at 144 hr (Table 1.1, Figure 1.3, but also see original sketch of experimental design in Appendix A).

A total of 16 collections on ten control-treatment paired plants throughout 15 patches were acquired. Sample collections (n = 244) were stored on wet ice in coolers or freezers before being transferred to storage at Boise State University where collections were stored at -20°C prior to being processed for chemical analysis.

#### Laboratory Methods for Analysis of Monoterpenes

Plant collections were manually de-wooded using liquid nitrogen to remove the leaves from the stems. Manually de-wooding occurred by fully submerging individual collections of sagebrush into liquid nitrogen and gently dislodging leaves from stems by hand using clean forceps. The resulting leaves from each individual collection were ground and homogenized using liquid nitrogen and a mortar and pestle to grind the leaves to less than 2 mm diameter particles. Forceps, mortars, and pestles were cleaned between samples using 70% ethanol.

Concentrations of monoterpenes in sagebrush samples were quantified at Boise State University in the Forbey lab using a gas chromatograph (Agilent 6890N, Agilent Technologies; 5301 Stevens Creek Boulevard, Santa Clara, CA 95051, USA) with a headspace auto-sampler (Hewlett-Packard HP7694; 1501 Page Mill Road, Palo Alto, CA 94204, USA) (Nobler 2016) (Appendix B). Homogenized subsamples (0.100 g wet weight [WW]) of each sample were placed in a 20 mL headspace vial.

A cocktail of monoterpene standards that are known to occur in sagebrush was run with the sample vials. Compounds in the cocktail include alpha-pinene (C10), camphene (C11), beta-pinene (C15), 3-carene (C21), p-cymene (C22), 1,8-cineole (C24), terpinolene (C38), and camphor (C53) (Figure 1.4). All cocktail compounds were dissolved in methylene chloride to combine the standards into a single sample for gas chromatography. Cocktail standards and monoterpenes in sagebrush samples had retention times (RT) quantified in minutes (Figure 1.4, Figure 1.5). Corresponding peak areas for each RT were quantified in area under the curve (AUC). HP ChemStation version B.01.00 (Santa Clara, California, USA) was used to calculate both values. The RTs generated by the cocktails were used to identify the compounds in sagebrush samples from co-chromatography (Frye et al. 2013, Fremgen 2015) (Table 1.2). All samples were dried for 24 hr at 60°C to obtain sample dry weights (DW). These values were then used to quantify monoterpene concentrations as AUC/gDW.

There was an equipment failure on the headspace autosampler that required maintenance part way through the chemical analysis, leaving 53 samples that were not analyzed. These 53 samples were excluded from the analysis due to recalibration during the autosampler maintenance, resulting in 191 samples available for statistical analysis. The equipment failure limited inclusion of specific treatment groups or specific time points and prevented us from having repeated measures of monoterpenes for each plant (see Figure 1.6).

### Data Processing

Data processing and statistical analyses were conducted using R 4.0.4 (R Core Team 2021) and RStudio Version 1.4.1717 (RStudio Team 2021). To begin data

processing, we used the *align\_chromatograms* function in the package *GCalignR* (Ottensmann et al. 2018) to align all cocktail and sample chromatograms in R. A cutoff of 22 mins was placed on the inclusion of RTs from the chromatogram alignment to minimize effects of retention time drift influencing AUC values. Once alignment was complete, the resulting dataset was trimmed so that only RTs that were found in at least 10% of the samples in a single control or treatment group were included. Manual adjustment had to be made to certain compounds, C1 and C2 as well as C24 and C25, throughout all samples. C1 and C2 were read as either one peak or two peaks for each sample, however nearly all samples possessed two peaks with the peak for C1 bleeding into the peak for C2. Therefore, the AUC values for C1 and C2 were combined into a single chemical identified as C1 because we could not separate the already merged peaks and wanted our values at this RT to be comparable across samples (Appendix C). Review of chromatograms show that the peaks of C24 and C25 were a single peak instead of the two separate peaks. The AUC values for C24 and C25 were combined into a single chemical identified as C24 and determined to be 1,8-cineole based on co-chromatography (Appendix C). Samples MF656, MF657, MF747, and MF775 were all excluded from the dataset because they were found to have duplicate identities where each duplicate differed in concentrations and therefore could not be properly identified. It was also determined that C14 needed to be excluded from the overall analyses due to C14 appearing to have a portion of the peak dilute into C15 in an “oil-can” shape in the chromatogram (see peak “g” at 13.62 min RT in Figure 1.5) that randomly occurred across samples and batches of runs and never occurred in blank runs or in standard cocktails suggesting it was not a contaminant. It could not be determined if C14 was a

true individual peak, an early elution of the sequential peak of C15, or co-elution from previous injections. Analyses were previously conducted with the inclusion of C14 (Appendix C). This resulted in 186 samples and 46 compounds for the analyses and outcomes of analysis did not differ from analysis where this peak was excluded (Figure 1.6, Table 1.2).

The adjusted dataset of AUC for each compound was divided by biomass of each sample to generate AUC/gDW as our quantitative value following previous methods for quantifying monoterpenes based on biomass of leaf material (following Frye et al. 2013, Fremgen 2015). Log transformation was performed on the resulting AUC/gDW values to assist with the skewed distributions observed (Hervé et al. 2018). Centering was then used on the log transformed values to help with interpretations and visualization analyses of the data for the PCAs (Hervé et al. 2018) (Appendix D).

### Statistical Analyses

To test predictions of the emission hypotheses that we would observe lower concentrations of monoterpenes in leaves early in the time course and the induction hypotheses that we would observe higher concentrations later in the time course, we first compared chemical profiles over time points within each control or treatment group using a Principal Component Analyses (PCAs). We also used PCAs to test our prediction of the browsing intensity hypotheses that monoterpene profiles would change more (e.g., distinct PCA ellipse) and be less variable (e.g., smaller PCA ellipse) than control treatments. Separate PCAs were generated to compare control versus acute and control versus chronic (Figure 1.8). A PCA was also generated to determine the influence of collection intensity levels at time 144 hr ( $T = 144$  hr) and assess the prediction that higher

intensities of browsing would have greater changes in monoterpene concentration (Figure 1.9). These PCAs were generated using the log transformed and centered dataset (Figure 1.7) with the base R function *prcomp* (R Core Team 2021) and the function *fviz\_pca\_biplot* in the package *factoextra* (Kassambara and Mundt 2020). From each subsequent PCA, the vector loading values for each compound were extracted to determine the contribution of each compound to the principal components. A cutoff of +/- 0.3 was established for these loadings to constitute a substantial contribution to the overall variation observed (Merenda 1997, Peterson 2000) (Table 1.3). Any loading value that made it above this cutoff value after rounding was deemed a potential compound of interest.

To test our prediction of the browsing intensity hypotheses that chronic browsing would result in less chemical variation and more strongly correlated chemicals, correlation matrices were generated for each treatment group using the functions *cor* and *corrplot* in the package *corrplot* (Wei and Simko 2021). Correlation matrices were used to assess the degree of correlation among potential compounds of interest extracted from the PCA vector loadings that made it above the +/-0.3 loading cutoff as well as all monoterpene standards (Figure 1.10). A matrix was created for all of the samples within this experiment as well as each subset to correspond with each PCA respectively. For better visualization, a correlation matrix was also generated using only the compounds of interest to better determine the strength of the correlation between high loading compounds (Figure 1.11, Appendix E). Within the control and each treatment group, the total amount of correlated values with an  $r^2 > +/-0.4$  were tallied (Table 1.4, Appendix E). The sets of strongest positive and negative correlation clusters were determined by the

strongest  $r^2$  values within in any one control or treatment group to better compare strongly positive or negative correlation clusters among groups. Nonparametric Kruskal-Wallis tests were used to compare the strength of positive and negative correlations among control and treatment groups using only correlation pairs where at least one of the treatments groups had a pair with an  $r^2 > +/-0.4$  (Appendix F). Nonparametric Kruskal-Wallis tests were also used to compare the correlation values between the two sets of strongest positive and strongest negative correlation clusters based on the  $r^2$  values strengths (Appendix F). If the Kruskal-Wallis test was significant, a Pairwise Wilcoxon Rank Sum test was performed to determine which treatment groups were significantly different from each other.

Correlation values were also used in conjunction with the PCA loadings to determine which compounds that made it above the  $+/-0.3$  loading cutoff were selected for the final analyses (Figure 1.12). After it was determined which compounds were strongly correlated, final compound selection was performed using several criteria. These included being a compound that aligned with a standard using co-chromatography (Figure 1.5), high loading across multiple PCAs (Table 1.3), larger loading values in comparison to the correlated compound loading values throughout the PCAs (Appendix E), and lowest occurrence of zero values within the samples.

To test predictions of the emission, induction, and browsing intensity hypotheses that monoterpenes would be lower in plants immediately after damage (emission hypothesis), higher in plants later in the time course (induction hypothesis), and changes would be higher in chronic treatments, we used two-way ANOVAs on the log transformed and centered dataset of concentrations (AUC/gDW) from final compounds

of interest. Although our experimental design was established to allow for a two-way repeated measures ANOVA (i.e., each plant within each treatment group [acute and chronic] was repeatedly measured over time), we could not use for this approach because of an instrumentation issues that prevented the availability of all time points for each plant (see GC batch comparisons in Appendix D). Instead, we used the function *aov* in the R base package *stats* (R Core Team 2021) to compare time points within treatment groups and between treatment groups. There was no significant interaction between treatment groups and time points (Appendix G and H) and therefore each comparison was analyzed separately for each of the final compounds of interest. One-way ANOVAs were also performed to test the effect of collection intensity at 144 hr on the log transformed and centered dataset of concentrations (AUC/gDW) from final compounds of interest.

## Results

### Exploratory PCAs of Time Points within Treatment Groups

Overall, PCAs reveal only minor differences among time points within treatment groups, between treatment groups, and among levels of collection intensity (Figures 1.7, 1.8, 1.9). PCAs and vector loadings identified several compounds that consistently influenced variation along dimensions of PCAs (i.e., C28 and C34) regardless of treatment and some that were unique influencers of variation within treatments (i.e., C26, C34, C38, and C44).

### PCA of Time Points within Control

Of the total accumulated variation, or eigenvalues, of the PCA from the time points within the control treatment group (Figure 1.7a), 20.0% of the variation was

accounted for across dimension 1 and 18.0% of the variation was accounted for across dimension 2. The four compounds of interest identified from the vector loading values, or eigenvectors, above  $\pm 0.3$  (Table 1.3a) and represented correlated compounds (Figure 1.12) in the time course within the control group PCA were C26, C28, C34, and C44. The ellipse for the zero hr time point was generally neutrally aligned across all positive and negative dimensions 1 and 2 and had the widest dimensional space. Compound C28 contributed most to the one hr ellipse pulling towards the positive quadrant of dimensions 1 and 2. The ellipse for the 24 hr time point was widest across dimension 1 and narrowest across dimension 2 with C26 contributing most to the pull of this ellipse. The ellipse for the 48 hr time point pulled relatively equally across dimension 1 and 2 with C44 contributing most to the pull of this ellipse. Similar to the 24 hr time point, the ellipse for the 144 hr was widest across dimension 1 and narrowest across dimension 2 with C26 contributing most to the pull of this ellipse.

#### PCA of Time Points within Acute

Of the total accumulated variation, or eigenvalues, of the PCA from the time points within the acute treatment group (Figure 1.7b), 24.9% of the variation was accounted for across dimension 1 and 13.3% of the variation was accounted for across dimension 2. The three compounds of interest identified from the vector loading values, or eigenvectors, above  $\pm 0.3$  (Table 1.3b) and represented correlated compounds (Figure 1.12) in the time course within the acute group PCA were C28, C34, and C44. The ellipse for the zero hr time point was narrowest across dimension 1 and widest across dimension 2 with C44 contributing the most to the pull of this ellipse. Similar to the zero hr time point, the ellipse for the one hr time point was narrowest across dimension 1 and widest

across dimension 2 with C44 contributing most to the pull of this ellipse. The ellipse for the 24 hr time point had the smallest dimensional space and is generally neutrally aligned across all positive and negative dimensions 1 and 2 with C28 and C34 contributing most to the pull of this ellipse. Compounds C28, C34, and C44 contributed most to the 48 hr ellipse which had the largest dimensional space across dimension 1. There was no ellipse for the 144 hr time point as there were insufficient samples to generate an ellipse.

#### PCA of Time Points within Chronic

Of the total accumulated variation, or eigenvalues, of the PCA from the time points within the chronic treatment group (Figure 1.7c), 21.1% of the variation was accounted for across dimension 1 and 12.7% of the variation was accounted for across dimension 2. The four compounds of interest identified from the vector loading values, or eigenvectors, above +/-0.3 (Table 1.3c) and represented correlated compounds (Figure 1.12) in the time course within the chronic group PCA were C26, C28, C34, and C38. The ellipse for the one hr time point was generally neutrally aligned across all positive and negative dimensions 1 and 2 with C28, C34, and C38 contributing most to the shape of this ellipse. The ellipse for the 24 hr time point had the widest dimensional space and is widest across dimension 1 and narrowest across dimension 2 with C26 and C28 contributing most to the pull of this ellipse. Compounds C28, C34, and C38 contributed most to the 48 hr time point ellipse with it being generally neutrally aligned across all positive and negative dimensions 1 and 2. In contrast to the 24 hr time point, the ellipse for the 144 hr time point had the smallest dimensional space and is narrowest across dimension 1 and widest across dimension 2 with C26 and C38 contributing most to the pull of this ellipse.

### PCA of Control versus Acute Treatments

Of the total accumulated variation, or eigenvalues, of the PCA from the control versus acute treatment groups (Figure 1.8a), 20.2% of the variation was accounted for across dimension 1 and 15.7% of the variation was accounted for across dimension 2. The four compounds of interest identified from the vector loading values, or eigenvectors, above  $\pm 0.3$  (Table 1.3d) and represented correlated compounds (Figure 1.12) in the time course within the control versus acute PCA were C26, C28, C34 and C61. The ellipse for the control treatment group was generally neutrally aligned across all positive and negative dimensions 1 and 2 with C26 and C61 contributing most to the shape of this ellipse. The ellipse for the acute treatment group was widest across dimension 1 and narrowest across dimension 2 with C28 and C34 contributing most to the pull of this ellipse.

### PCA of Control versus Chronic Treatments

Of the total accumulated variation, or eigenvalues, of the PCA from the control versus chronic treatment groups (Figure 1.8b), 19.0% of the variation was accounted for across dimension 1 and 15.5% of the variation was accounted for across dimension 2. The four compounds of interest identified from the vector loading values, or eigenvectors, above  $\pm 0.3$  (Table 1.3e) and represented correlated compounds (Figure 1.12) in the time course within the control versus acute PCA were C26, C28, C34, and C44. The ellipse for the control treatment group was generally neutrally aligned across all positive and negative dimensions 1 and 2 with C26, C34, and C44 contributing most to the pull of this ellipse. Similar to the control treatment group, the ellipse for the chronic treatment group was generally neutrally aligned across all positive and negative

dimensions 1 and 2 being the widest across dimension 1 and narrowest across dimension 2 with C28, C34, and C44 contributing most to the shape of this ellipse.

#### PCA of Collection Intensity

Of the total accumulated variation, or eigenvalues, of the PCA from the collection intensity levels (Figure 1.9), 20.2% of the variation was accounted for across dimension 1 and 16.0% of the variation was accounted for across dimension 2. The five compounds of interest identified from the vector values, or eigenvectors, above  $\pm 0.3$  (Table 1.3f) and represented correlated compounds (Figure 1.12) in the time course within the control versus acute PCA were C26, C28, C34, C38, and C61. The ellipse for the zero level collection intensity was widest across dimension 1 and narrowest across dimension 2 with C38 and C61 contributing most to the pull of this ellipse. Compounds 28, C34, and C61 contributed most to the low level collection intensity ellipse which was widest across dimension 1 and narrowest across dimension 2. The ellipse for the medium level collection intensity was pulling towards the positive section of dimension 2 while otherwise being generally neutrally aligned across positive and negative dimension 1 with C28, C34, and C38 contributing most to the pull of this ellipse. The ellipse for the high level collection intensity was generally neutrally aligned across all positive and negative dimensions 1 and 2 with C26, C38, and C61 contributing most to the shape of this ellipse.

#### Correlation Matrices of Compounds of Interest and Standards

The correlation matrices were generated with the initial compounds of interest that made it above the  $\pm 0.3$  loading cutoff (Tables 1.3) and all standards. These matrices were made for all samples within the study and the subsets corresponding to each PCA

(Figures 1.10 and 1.11) and were used to identify the two strongest positive correlation clusters and two strongest negative correlation clusters among the treatment groups based on  $r^2$  values (Appendix E). In general, the control treatment had the strongest positive correlations and were less variable within each cluster and the chronic treatment had the strongest negative correlations and were more variable within each cluster. The control ( $n = 60$ ), acute ( $n = 58$ ), and chronic ( $n = 58$ ) treatments had similar numbers of positively correlated values with an  $r^2 > 0.4$ , but the chronic treatment had more negatively correlated values with an  $r^2 > -0.4$  ( $n = 17$ ) than control ( $n = 5$ ) or acute ( $n = 1$ ) treatments (Table 1.4). Positive correlation values of paired compounds where at least one treatment group had an  $r^2 > 0.4$  did not differ among treatment groups ( $\chi^2_{(2, 222)} = 2.704$ ,  $P = 0.259$ , Table 1.6). However, the negative correlation values did differ among groups ( $\chi^2_{(2, 60)} = 18.798$ ,  $P = <0.001$ , Table 1.6) where the chronic treatment had more negatively correlated compounds than control ( $P_{\text{chronic-control}} = 0.0017$ ) and acute ( $P_{\text{chronic-acute}} = <0.001$ ) treatments, but control and acute did not differ ( $P_{\text{control-acute}} = 0.153$ , Table 1.7).

Overall, there were reoccurring patterns of clusters of correlated compounds with only minor differences across treatment groups. There were two strongly positive and two strongly negative correlation clusters that occurred relatively consistently throughout the control, acute, and chronic subsets (Figure 1.10, Table 1.5, Appendix F).

The first positive correlation cluster was observed among C5, C7, C28, C32, and C34 (Appendix E). The positive correlations occurring in this cluster were fairly consistent throughout each subsetted treatment group with minimal differences observed. There was no difference in the overall strength of positive correlations within this cluster among treatment groups ( $\chi^2_{(2, 27)} = 2.5497$ ,  $P = 0.280$ , Table 1.8). The strongest positive

correlations across all treatment groups within this cluster were between C5 and C7 ( $r^2 > 0.97$ ) (Table 1.5).

The second positive correlation cluster was observed among C8, C10, C11, C22, C24, and C44 (Appendix E). The correlations observed within this cluster were also fairly consistent in strength throughout each subsetted treatment group ( $\chi^2_{(2, 42)} = 1.617$ ,  $P = 0.446$ , Table 1.8). The strongest positive correlations across all treatment groups were between C8 and C11 ( $r^2 > 0.97$ ). The control treatment had consistently higher positive correlations, but each treatment had a different combination of minimum negative correlated values (Table 1.5).

The first negative correlation cluster was observed among C8, C10, C11, C22, C24 (which comprise our second positively correlated cluster) and C28, C32, and C34 (which comprise our first positively correlated cluster). The negative correlations occurring in this cluster were significantly different among treatment groups ( $\chi^2_{(2, 42)} = 10.12$ ,  $P = 0.006$ , Table 1.8) where the chronic treatment had more negatively correlated compounds than control ( $P_{\text{chronic-control}} = 0.011$ ) and acute ( $P_{\text{chronic-acute}} = 0.011$ ) treatments, but control and acute did not differ ( $P_{\text{control-acute}} = 0.935$ ) (Table 1.9). All groups had different combinations of minimum and maximum negatively correlated values (Table 1.5). The strongest negative correlations were between C22 and C32 for the chronic treatment ( $r^2 > -0.59$ ), between C8 and C34 for the acute treatment ( $r^2 > -0.39$ ), and between C24 and C28 for the control treatment ( $r^2 > -0.37$ ) (Table 1.5).

The second negative cluster was observed among C8, C26, C37, and C38 with the chronic treatment being the most variable. There was no difference in the overall strength of negative correlations within this cluster among treatment groups ( $\chi^2_{(2, 9)} = 1.500$ ,  $P =$

0.4724, Table 1.8). Chronic and acute treatments shared the same combinations of minimum and maximum negatively correlated values (Table 1.5). The strongest negative correlation was between C37 and C38 for both chronic ( $r^2 = -0.53$ ) and acute treatments ( $r^2 = -0.41$ ) and the strongest negative correlation was between C26 and C38 for the control treatment ( $r^2 = -0.44$ ) (Table 1.5).

#### Selection of Compounds of Interest Based on Correlations

Compounds C18, C26, and C33 were correlated (mean  $r^2 = 0.623$ ; SEM = 0.225) with C26 chosen due to it appearing in nearly every PCA above the +/-0.3 loading cutoff and having the highest loading values among the correlated compounds. Compounds C5, C7, C9, and C28 were correlated (mean  $r^2 = 0.659$ ; SEM = 0.258) with C28 chosen due to it appearing in every PCA above the +/-0.3 loading cutoff and having the highest loading values among the correlated compounds. Compounds C32 and C34 were correlated (mean  $r^2 = 0.768$ ; SEM = 0.129) with C34 chosen due to it appearing in every PCA above the +/-0.3 loading cutoff, having the highest loading values among the correlated compounds, and having the lowest occurrence of zero values. Compounds C37 and C38 were correlated (mean  $r^2 = -0.414$ ; SEM = -0.260) with C38 chosen due to it being the standard terpinolene. Compounds C8 and C44 were correlated (mean  $r^2 = 0.665$ ; SEM = 0.098) with C44 chosen due to it appearing more often in PCAs above the +/-0.3 loading cutoff. Compound C44 did not appear as having a high PCA loading above the +/-0.3 cutoff in the collection intensity group and therefore was not included for subsequent analyses for collection intensity but was included for analyses for time points and treatment groups. Compound C61 was not strongly correlated with any of the other compounds of interest, but it was selected as a final compound of interest due to

its appearance in the collection intensity PCA loadings above the loading cutoff of +/-0.3. The resulting final compound of interest were therefore C26, C28, C34, C38, C44, and C61.

#### Comparing Time Points and Treatment Groups

We found that there was no statistically significant effect for any compound among time points or among treatment groups (Table 1.10, Figure 1.13, Appendix G). Although not significant, there were a few notable patterns with most chemicals in most treatments decreasing with time following the initial simulated browsing event. Concentrations of C26 were constant for both the control and acute treatments for the first three time points (T = 0 – 24 hr) and then both decreased at 48 hr. Concentrations of C28 also remained constant across time for acute treatment plants and then show a decrease at 48 hr that was 87.1% lower than control plants during this time point. Concentrations of C38 remained relatively constant with a slight increase at 1 hr for acute that was 1.97 times higher than control plants followed by a decrease in concentration at 24 and 48 hr with chronic plants having 1.83 times higher concentrations than control at 24 hr. Both acute and chronic groups showed a gradual decrease in concentrations of C44 over time with acute plants 60.3% lower than control at 48 hr and chronic plants 53.1% lower than control at 144 hr. Although it was not selected based on the previously mentioned criteria for the final compounds of interest, C18 also showed a decrease in concentration with time ( $P < 0.05$ ) across all treatments (Appendix H).

#### Comparing Collection Intensities

We did not find any statistically significant differences for any compounds of interest among collection intensity levels (Table 1.11, Figure 1.14). Although not

significant, there were a few notable patterns. Concentrations of C28 were 2.53 times higher for the low level of collection intensity and 2.01 times higher in the high level of collection intensity compared to the control plants at 144 hr. In addition, concentrations of C61 in the high level of collection intensity were 43.1% lower than plants in the low and 35.7% lower than plants in the medium level of collection intensity.

### **Discussion**

In this investigation we used a time-interval based approach to investigate induction of monoterpenes in sagebrush (*Artemisia tridentata* subsp. *wyomingensis*) in the winter in response to simulated browsing of an avian herbivore. This experiment was designed to detect changes in monoterpene profiles over a six-day period to identify if, when, and to what extent monoterpenes change in response to damage, thus signaling the onset of an induced chemical defense response (Zangerl and Rutledge 1996, Kant et al. 2004, Heil 2009, Heil and Karban 2010, Portillo-Estrada et al. 2015). Overall, we found substantial overlap in the ellipses of all generated PCAs subsetted either by time points within treatment groups, between treatment groups, and among levels of collection intensity (Figures 1.7, 1.8, 1.9). This strong ellipses overlap suggests that an induced defense response is not occurring in sagebrush in winter regardless of the level of damage to leaves. We found minimal evidence that the compounds of interest that best explained the variation within and among treatment groups and different levels of collection intensity changed following simulated browsing (Figures 1.10, 1.11, 1.13, 1.14, Tables 1.10, 1.11). Support for our hypotheses were inconsistent. Results did not support the emission hypothesis that monoterpenes concentrations would initially decrease at the start of the time course or the induction hypothesis that monoterpene concentrations would

increase as the time course progressed. We also did not support the hypothesis that treatment plants were less variable in the types of monoterpenes present compared to control plants (Figure 1.8). Our results also did not support the hypothesis that higher browsing intensity would cause greater changes in concentrations via chronic treatment (Figures 1.7, 1.13) or higher collection intensity (Figures 1.9, 1.14). One pattern of interest observed that was in support of the higher browsing intensity hypothesis was more negative correlations among compounds in the chronic treatment group than control and acute treatment groups (Table 1.4, 1.6, Table 1.8).

Results generally indicate very minimal changes in chemistry of sagebrush after damage in the winter for this subspecies in this specific location (Tables 1.10, 1.11, Figures 1.13, 1.14). These results differ from previous studies in sagebrush that found significant changes in monoterpenes released and levels of leaf palatability between undamaged control plants and damaged treatment plants in the summer during a single collection event (Karban et al. 2000, 2006, Karban and Baxter 2001) and various time courses (Karban and Maron 2002, Kessler et al. 2006, Shiojiri and Karban 2008). There are numerous plausible reasons why our results differ from other studies. First, we performed this study in the winter when there is less nitrogen availability and sunlight and temperatures are lower compared to the summer when resources are relatively higher. Lower resources could be a causative agent for the overall lack of induced defense response observed by limiting the production of monoterpenes and other defensive chemicals through glycolysis derivatives and enzymatic biosynthesis (Millard et al. 2001, Schultz et al. 2013). During the winter the process of detection of damage from herbivore browsing by plants may be slowed (Bilbrough and Richards 1993). It is

therefore possible that dormancy of chemical responses by sagebrush in the winter limits responses to browsing with the plants having little capacity to change their gene expression in response to damage (Kelsey et al. 1982, Morin et al. 2007, Lazarus et al. 2019). Our study suggests there may be limited chemical plasticity of sagebrush in the winter associated with a gene by browsing interaction. Analysis of monoterpene profiles of genetically distinct *Artemisia* subspecies (collected between May and October) within a common garden environment indicate that emission of monoterpenes in sagebrush is largely under genetic control but is also influenced by the environment (Jaeger et al. 2016). Given that monoterpenes can classify taxa of sagebrush relative to the environment, further understanding of chemical plasticity relative to gene by winter environment may advance our knowledge of the functional role of monoterpenes in the ecology and evolution of sagebrush.

The specific leaf type present on sagebrush could also impact the induced defense response. Ephemeral leaves, which are present during the spring and early summer, are larger in size compared to persistent leaves which are present all year (Miller and Schultz 1987). Due to ephemeral leaves only being produced in the productive growing season of summer where it is expected that they are more digestible, they may possess different chemical defense mechanisms than the persistent leaves that may instead rely on a constitutive defense mechanism with higher concentration of chemicals (Karban and Myers 1989, Zangerl and Rutledge 1996, Ito and Sakai 2009). Insect herbivores that are more prevalent in the summer may have a preference for leaf type, feeding more heavily on ephemeral rather than persistent due to the lower antioxidant levels (Pu et al. 2015), thus leading to heavier herbivore browsing and greater need for induced defense in this

leaf type. In support, ephemeral leaves have higher crude protein digestibility (2.4% higher), lower total phenolics (30.1% lower), and lower total monoterpenes (2.1% lower) compared to persistent leaves (unpublished data, Forbey). It is also possible that because the persistent leaves are the only leaf type present in the winter that they are dormant and are not able to respond to damage (Kelsey et al. 1982, Morin et al. 2007, Lazarus et al. 2019). This potential dormancy could be assessed by measuring the photosynthesis rate of the leaves during the winter. The enzymes responsible for sagebrush photosynthesis are functional at an approximate optimal temperature of 24°C, with large variation in temperature causing a decrease in enzyme functionality and subsequent photosynthesis rate (DePuit and Caldwell 1973, Hansen et al. 2008, Kleinhesselink and Adler 2018). During our study period and site, the average minimum temperature was 0.1°C and the maximum temperature never increasing above 22.4°C which suggests that the observed stability of monoterpenes during winter may be due to a complete lack of photosynthesis occurring in these leaves.

Results may also be related to the species of plant used in our study. The plant species for this study, Wyoming big sagebrush (*Artemisia tridentata* subsp. *wyomingensis*), was selected because of its high prevalence in the sagebrush steppe ecosystem that is currently threatened by fires, drought, and human encroachment (Kelsey et al. 1983, Takahashi and Huntly 2010, Reisner et al. 2013, Kleinhesselink and Adler 2018). Previous studies used *A. t. cana*, *A. t. vaseyana*, *A. douglasiana* or sagebrush (*A. tridentata*) without indicating subspecies (Karban et al. 2000, 2004, 2014b, 2016, Karban and Baxter 2001, Shiojiri and Karban 2008). This study may represent the first test of induced defenses in Wyoming big sagebrush. It is possible that Wyoming big

sagebrush relies on constitutive defenses rather than induce defenses (Karban and Myers 1989, Zangerl and Rutledge 1996, Ito and Sakai 2009) in the winter that are already highly deterrent to herbivores which may explain avoidance of this species by sage-grouse compared to *A. nova* (Frye et al. 2013). Wyoming big sagebrush is slow growing and located in environments that are relatively low in resources (Bilbrough and Richards 1993). Moreover, the synthesis of volatile chemicals may come at a cost to the plant in the form of reduced growth and increasing resource allocation (Engelberth and Engelberth 2019). For example, maize seedlings (*Zea mays*) that were exposed to volatiles to promote an induced defense response showed a significantly reduced growth when compared to the control seedlings over a period of approximately two weeks (Engelberth and Engelberth 2019). The use of volatiles in an induced defense rather than constitutive defense can be an efficient strategy due to its minimization of overall plant cost during times of stress and an increase in plant fitness (Raffa and Berryman 1982, Karban and Myers 1989, Heil and Karban 2010, Neilson et al. 2013, Backmann et al. 2019). However, when a plant is under constant herbivore pressure, it may rely on constitutive defense strategies to provide continual protection against herbivores using a more stable chemical profile (Underwood 1998, Ito and Sakai 2009, Karban 2011).

Although not required in summer, the application of the enzymes found in herbivore saliva that remains after a bite has occurred may be required to properly simulate an induced defense response in sagebrush in the winter (Paré et al. 2005). The simulated browsing that was performed in this experiment was done using scissors to snip and imitate the beak cuts on sagebrush leaves for each treatment plant to mimic natural herbivore browsing by sage-grouse and thereby produce a defensive chemical

response (Heil and Karban 2010, Fremgen 2015, Moreira et al. 2018, Bouwmeester et al. 2019, Moreira and Abdala-Roberts 2019) (Figure 1.2). It is possible that this form of mechanical damage may not have been sufficient to produce an induced defense response in sagebrush due to the lack of herbivore biotic factors co-occurring with the physical damage which would occur under natural browsing conditions (Paré et al. 2005, Kessler and Halitschke 2007). The lack of herbivore biotic factors, such as the saliva left behind after any bites have been made or oviposition fluids from insects, could potentially be the reason why there were generally no significant differences between the treatment groups when observing the generated PCAs (Figure 1.7, Figure 1.8).

Various abiotic environmental factors could also contribute to the lack of changes observed with wind being a major contributor. The degree and directionality of any wind present across the experimental landscape (e.g., average wind speed 24.0 mph at our site) could influence potential interactions between study plants and the variation in detection and induced response to emitted signals (Murlis et al. 2000, Aartsma et al. 2017). This study was performed in Wyoming, which is notoriously windy and could have complicated our ability to detect changes if they were occurring. Other studies were done in very controlled areas that were less impacted by windy conditions (Karban et al. 2000, 2004, Karban and Baxter 2001). The presence of wind could impact neighboring eavesdropping even if they are distanced over 60 cm apart by increasing the airflow between plants, thus potentially complicating the results (Karban et al. 2006, Aartsma et al. 2017). Wind can also cause turbulence within an area that mixes blends of emitted volatiles, further contributing to the chemical variation while simultaneously causing chemical breakdown and signal misinterpretation (Aartsma et al. 2017). Other abiotic

environmental factors such as temperature or snow depths could also contribute to the lack of change observed. The lower temperatures during our study (average minimum temperature 0.1°C, average maximum temperature 15.4°C) could cause enzymatic chemical synthesis to slow or stop entirely (Hulten et al. 2006, Neilson et al. 2013). It could also be that each time point could have had collections taken at different minimum or maximum temperatures, leading to potentially different reactions to these conditions and confounding the results. The accumulation of snow could create micro-climates depending on where it lands throughout a landscape and the resulting depths (average snow depth 1.27 mm during our study). Snow covering plants could potentially cause temperature discrepancies through insulation and partial coverage from browsing herbivores (Nobrega and Grogan 2007, Kelsey et al. 2021).

Regardless of the reason for lack of induced defense, our results indicate that there is overall stability of monoterpenes in Wyoming big sagebrush in this landscape irrespective of treatment group or damage level. Results suggest that after damage, plants are not becoming more vulnerable through loss of volatiles from leaves associated with emission or more chemically defended within 144 hr after damage through synthesis of new chemicals. Due to this lack of chemical induction, herbivores may not have to respond to temporal variation in the plant chemistry. Both sage-grouse (Frye et al. 2013, Wing and Messmer 2016) and pygmy rabbits (Ulappa et al. 2014, Pu et al. 2015, Nobler et al. 2019) detect and respond to chemical concentrations in Wyoming big sagebrush. As such, lack of induced defenses may allow these vertebrate herbivores to consistently return to plants originally selected based on lower chemical defenses. The stability of chemistry after being browsed is beneficial for foraging herbivores because they will not

have to search for new plants that have not been previously browsed in the winter. The high fidelity at winter sites by sage-grouse (Fischer et al. 1993, Gibson et al. 2014) may be encouraged by lack of induced defenses of sagebrush in the winter. Foraging fidelity (Fischer et al. 1993, Gibson et al. 2014) versus tracking of foraging resources (van der Graaf et al. 2006, Aikens et al. 2020) has been observed in a diversity of herbivores and could be partially linked not only to plant availability but also stability versus induction of chemical traits associated with historical browsing events.

However, we did discover some chemical patterns that deserve further attention, mainly revolving around the general decreases detected in compounds of interest (C26, C28, C34, C38, C44, and C61) (Figures 1.13, 1.14). Detection of subtle changes in chemical concentration or gain of specific chemicals, even if in low concentrations, can have biological effects in herbivores. For example, the odds that pygmy rabbits (*Brachylagus idahoensis*) will browse sagebrush (*Artemisia* spp.) decreases by 1.03 times for every 100  $\mu\text{g/gDW}$  increase in artemiseole concentration, which was 17.1% higher in unbrowsed than browsed plants (Ulappa et al. 2014). An increase in 1,8-cineole and an unidentified monoterpene decreased the odds of patch use by 18% and 40%, respectively, for each 1 AUC/100  $\mu\text{gDW}$  increase in concentration for Greater Sage-grouse (*Centrocercus urophasianus*) (Frye et al. 2013). This implies that the chemical changes do not necessarily need to be large to have an impact on diet selection of herbivores. We found that the largest concentration differences were seen in C28 and C38. The low and high levels of collection intensity had 2.53 times and 2.01 times higher concentrations of C28 respectively compared to the zero level control plants (Figure 1.14). Acute treatment plants had 1.97 times higher concentration of C38 at 1 hr after damage than control

plants. Chronic treatment plants also had 1.83 times higher concentration of C38 at 24 hr after damage than control plants (Figure 1.13). In addition, we found a general reduction over time of the main compounds of interest in the acute treatment group which may be indicative of a release in volatile chemicals following stimulated browsing. We also observed more variable responses in the AUC/gDW concentrations of the compounds of interest in the chronic treatment group (Figure 1.13) which may be influential for central placed foragers, like pygmy rabbits, because unpredictable chemistry may prevent them from accurately assessing concentrations while foraging. These concentration changes are larger than the concentration difference that caused a decrease in odds of use by pygmy rabbits (*Brachylagus idahoensis*) and sage-grouse (*Centrocercus urophasianus*) (Frye et al. 2013, Ulappa et al. 2014). Although we did detect small changes in concentrations, the overall stable chemistry observed at our study site suggests that foraging behavior of herbivores would not be severely influenced by previous damage by herbivores. We predict that herbivores at our site will have high foraging fidelity at this site and that stability of PSMs relative to browsing may be a novel factor contributing to the stability of herbivore populations (Fischer et al. 1993, Gibson et al. 2014). However, in another location where induction does occur, herbivores are expected to have higher movement within and among foraging patches to find a plant that has not been induced.

The second pattern we observed that may contribute to understanding plant-herbivore interactions is associated with patterns in correlated compounds. Patterns of compounds that are more negatively or positively correlated can help identify specific biochemical pathways involved in induced defenses that may prime plants to respond to future stressors. The various correlation matrices (Figure 1.10) can help identify which

compounds are substrates and products within biosynthetic pathways based on either strong positive values, when compounds are occurring together, or strong negative values, when compounds are occurring in the absence of the other. Correlated compounds may occur in the same biosynthetic pathways, possess similar biological functions, or be common biomarkers of stress. For example, alpha-pinene (C10) is produced in the methylerythritol pathway (MEP) which receives its substrates from the pyruvate product from glycolysis. The MEP pathway converts pyruvate into isopentenyl pyrophosphate (IPP) and Dimethylallyl pyrophosphate (DMAPP), which can both be further modified to create geranyl diphosphate (GPP) where all monoterpenes are derived. GPP can be converted into linalyl diphosphate that can further undergo enzymatic conversion to produce alpha-pinene (Schwab et al. 2001, Mahmoud and Croteau 2002, Chang and Keasling 2006, Muhlemann et al. 2014, Risner et al. 2020). Changes in correlation strength or direction can potentially link known standards and their pathways to the production and function of unknown monoterpenes (Muhlemann et al. 2014, Cofer et al. 2018). For example, stronger negative correlation between alpha-pinene (C10) and C34 in the chronic treatment ( $r^2 = -0.42$ ) compared to control ( $r^2 = -0.16$ ) might indicate that our unknown C34 is a chemical in the same biosynthetic pathway as alpha-pinene (Appendix E). With the chronic treatment group having significantly more negative correlations below the -0.4 threshold, it implies that these plants are converting one monoterpene into another. It is therefore necessary to investigate which compounds are negatively correlated in the chronic treatment group, but not in the control to better understand how browsing might influence these biosynthetic pathways. Many of the strongly correlated compounds were either not detected or had generally low

concentrations within the samples that would normally have been ignored. Correlation patterns could therefore lead to further exploration that could specifically identify the compounds of interest that have shared biological, defensive, or metabolic significance (Dudareva et al. 2004, Clavijo McCormick et al. 2014, Bouwmeester et al. 2019).

With the advancement of multivariate techniques, it is now possible to examine the nuances of defensive chemicals (Wallestad and Eng 1975, Heil and Karban 2010, Frye et al. 2013, Moreira et al. 2018, Bouwmeester et al. 2019, Moreira and Abdala-Roberts 2019). We examined multiple variables of time points, treatment groups, and damage level through collection intensity to determine when and how entire monoterpene profiles are changing in response to damage. This approach was useful because it allowed for the detection of potentially rare compounds and those with low concentrations that were previously likely to be overlooked to be examined as potential biomarkers of induction. Multivariate approaches can also help in identifying low concentration chemicals that should be reassessed in existing studies on diet selection (Zangerl and Rutledge 1996, Kant et al. 2004, Portillo-Estrada et al. 2015). Analytical limitations in detecting compounds that are at or below detection limits may cause some compounds to be overlooked or excluded (Lavagnini and Magno 2007, Myrick and Baker 2018). Our approach allows us to identify which compounds to quantify that may be involved in potential induced defense strategies (Wold and Marquis 1997, Karban et al. 2000, Thaler et al. 2002). We can use the knowledge gained from determining the compounds of interest and correlation patterns by investigating other types of defensive chemicals that may further advance our understanding of induced defense mechanisms. For example, high-performance liquid chromatography (HPLC) could be used to assess how phenolic

compounds that are produced through a different metabolic pathway are changing in the leaf tissue (Mattila et al. 2000, Koricheva 2002, Wing and Messmer 2016, Bouwmeester et al. 2019). We could also run further analyses such as mass-spectrometry (MS) and Nuclear Magnetic Resonance spectroscopy (NMR) that help identify unknowns and couple data on mixtures of chemicals with linear discriminant analysis (LDA), Nonmetric multidimensional scaling (NMDS), and random forest to reduce dimensionality to better understand the patterns of chemical change occurring (Angelini et al. 2010, Hervé et al. 2018, Papanas et al. 2021).

By understanding how plants respond, either by chemicals that remain stable or through emission or induction, may help inform management decisions. Our approach should be applied to other populations of sagebrush, other herbivores, and other highly important forage shrubs to better understand unique chemical patterns and responses associated with each plant-herbivore system (Agrell et al. 2003, Clavijo McCormick 2016). A more comprehensive understanding of what biotic stressors affect chemical profiles of plants could also help determine what types of plants may be better adapted for a specific area in regard to certain management decisions. For example, restoration efforts should consider plants that can adapt to local environmental conditions and remain stable to local and native herbivores (Provenza et al. 2003, Heil 2009, Heil and Karban 2010). To do this requires that monoterpene profiles within species are examined before and after they are placed on new landscapes. Having a diverse array of monoterpene profiles and knowledge surrounding how they are responding to their environmental factors will create a more adaptable, diverse population (Karbon et al. 2014a, Hussain et al. 2019). For example, a plant that is chemically dynamic may help it establish in a new

environment because it is less palatable to herbivores. However, a chemically dynamic plant may not adequately support a local herbivore population. These herbivores may avoid the newly established plants because they do not recognize the chemical signals or do not have the ability to detoxify the chemicals in the plant which could complicate recovery of the herbivore population (Koricheva 2002, Neilson et al. 2013, Veblen et al. 2015) (See Chapter 2). Overall, there are many opportunities for future studies to elucidate the complex and temporally dynamic chemical dance between plants and herbivores through observing the subtle changes in chemical concentrations using our multivariate approach. Moreover, the discovery of the correlated chemicals in response to herbivore damage could reveal novel biosynthetic pathways and help uncover the biological importance of correlated compounds for plant defense (Hervé et al. 2018) with novel pharmacological purposes (McLean et al. 2007, Clavijo McCormick et al. 2012, Li et al. 2017) (See Chapter 2).

### References

- Aartsma, Y., F. J. J. A. Bianchi, W. van der Werf, E. H. Poelman, and M. Dicke. 2017. Herbivore-induced plant volatiles and tritrophic interactions across spatial scales. *New Phytologist* 216:1054–1063.
- Agrawal, A. A. 2000. Benefits and costs of induced plant defense for *Lepidium virginicum* (Brassicaceae). *Ecology* 81:1804–1813.
- Agrell, J., W. Oleszek, A. Stochmal, M. Olsen, and P. Anderson. 2003. Herbivore-induced responses in alfalfa (*Medicago sativa*). *Journal of Chemical Ecology* 29:303–320.
- Aikens, E. O., K. L. Monteith, J. A. Merkle, S. P. H. Dwinell, G. L. Fralick, and M. J. Kauffman. 2020. Drought reshuffles plant phenology and reduces the foraging benefit of green-wave surfing for a migratory ungulate. *Global Change Biology* 26:4215–4225.

- Ameye, M., S. Allmann, J. Verwaeren, G. Smagghe, G. Haesaert, R. C. Schuurink, and K. Audenaert. 2018. Green leaf volatile production by plants: a meta-analysis. *New Phytologist* 220:666–683.
- Angelini, L., M. de Tommaso, D. Marinazzo, L. Nitti, M. Pellicoro, and S. Stramaglia. 2010. Redundant variables and Granger causality. *Physical Review E* 81:037201.
- Backmann, P., V. Grimm, G. Jetschke, Y. Lin, M. Vos, I. T. Baldwin, and N. M. van Dam. 2019. Delayed chemical defense: Timely expulsion of herbivores can reduce competition with neighboring plants. *The American Naturalist* 193:125–139.
- Baldwin, I. T., R. Halitschke, A. Paschold, C. C. von Dahl, and C. A. Preston. 2006. Volatile signaling in plant-plant interactions: “Talking trees” in the genomics era. *Science* 311:812–815.
- Baldwin, I. T., and J. C. Schultz. 1983. Rapid changes in tree leaf chemistry induced by damage: Evidence for communication between plants. *Science* 221:277–279.
- Basey, J. M., S. H. Jenkins, and P. E. Busher. 1988. Optimal central-place foraging by beavers: Tree-size selection in relation to defensive chemicals of quaking aspen. *Oecologia* 76:278–282.
- Bates, D., M. Mächler, B. Bolker, and S. Walker. 2015. Fitting linear mixed-effects models using lme4. *Journal of Statistical Software* 67:1–48.
- Becerra, J. X., K. Noge, and D. L. Venable. 2009. Macroevolutionary chemical escalation in an ancient plant-herbivore arms race. *Proceedings of the National Academy of Sciences* 106:18062–18066.
- Bilbrough, C. J., and J. H. Richards. 1993. Growth of sagebrush and bitterbrush following simulated winter browsing: Mechanisms of tolerance. *Ecology* 74:481–492.
- Birnbaum, S. S. L., and P. Abbot. 2018. Insect adaptations toward plant toxins in milkweed–herbivores systems – a review. *Entomologia Experimentalis et Applicata* 166:357–366.

- Bouwmeester, H., R. C. Schuurink, P. M. Bleeker, and F. Schiestl. 2019. The role of volatiles in plant communication. *The Plant Journal* 100:892–907.
- Bryant, J. P., K. Joly, F. S. C. Iii, D. L. DeAngelis, and K. Kielland. 2014. Can antibrowsing defense regulate the spread of woody vegetation in arctic tundra? *Ecography* 37:204–211.
- Bryant, J. P., and P. J. Kuropat. 1980. Selection of winter forage by subarctic browsing vertebrates: The tole of plant chemistry. *Annual Review of Ecology and Systematics* 11:261–285.
- Chang, M. C. Y., and J. D. Keasling. 2006. Production of isoprenoid pharmaceuticals by engineered microbes. *Nature Chemical Biology* 2:674–681.
- Chen, S., L. Zhang, X. Cai, X. Li, L. Bian, Z. Luo, Z. Li, Z. Chen, and Z. Xin. 2020. (E)-Nerolidol is a volatile signal that induces defenses against insects and pathogens in tea plants. *Horticulture Research* 7:1–15.
- Clavijo McCormick, A. 2016. Can plant–natural enemy communication withstand disruption by biotic and abiotic factors? *Ecology and Evolution* 6:8569–8582.
- Clavijo Mccormick, A., J. Gershenzon, and S. B. Unsicker. 2014. Little peaks with big effects: Establishing the role of minor plant volatiles in plant–insect interactions. *Plant, Cell & Environment* 37:1836–1844.
- Clavijo McCormick, A., S. B. Unsicker, and J. Gershenzon. 2012. The specificity of herbivore-induced plant volatiles in attracting herbivore enemies. *Trends in Plant Science* 17:303–310.
- Cofer, T. M., I. Seidl-Adams, and J. H. Tumlinson. 2018. From acetoin to (Z)-3-hexen-1-ol: The diversity of volatile organic compounds that induce plant responses. *Journal of Agricultural and Food Chemistry* 66:11197–11208.
- Cometto-Muñiz, J. E., W. S. Cain, M. H. Abraham, and R. Kumarsingh. 1998. Sensory properties of selected terpenes: Thresholds for odor, nasal pungency, nasal localization, and eye irritation. *Annals of the New York Academy of Sciences* 855:648–651.

- Dearing, M. D., W. J. Foley, and S. McLean. 2005. The influence of plant secondary metabolites on the nutritional ecology of herbivorous terrestrial vertebrates. *Annual Review of Ecology, Evolution, and Systematics* 36:169–189.
- DePuit, E. J., and M. M. Caldwell. 1973. Seasonal pattern of net photosynthesis of *Artemisia tridentata*. *American Journal of Botany* 60:426–435.
- Dudareva, N., A. Klemptien, J. K. Muhlemann, and I. Kaplan. 2013. Biosynthesis, function and metabolic engineering of plant volatile organic compounds. *New Phytologist* 198:16–32.
- Dudareva, N., E. Pichersky, and J. Gershenzon. 2004. Biochemistry of plant volatiles. *Plant Physiology* 135:1893–1902.
- Dussourd, D. E., and T. Eisner. 1987. Vein-cutting behavior: insect counterploy to the latex defense of plants. *Science* 237:898–901.
- Dwinnell, S. P. H., H. Sawyer, J. E. Randall, J. L. Beck, J. S. Forbey, G. L. Fralick, and K. L. Monteith. 2019. Where to forage when afraid: Does perceived risk impair use of the foodscape? *Ecological Applications* 29:e01972.
- Ehrlich, P. R., and P. H. Raven. 1964. Butterflies and plants: A study in coevolution. *Evolution* 18:586–608.
- Eisenring, M., M. Meissle, S. Hagenbucher, S. E. Naranjo, F. Wettstein, and J. Romeis. 2017. Cotton defense induction patterns under spatially, temporally and quantitatively varying herbivory levels. *Frontiers in Plant Science* 8:234.
- Engelberth, J., and M. Engelberth. 2019. The costs of green leaf volatile-induced defense priming: Temporal diversity in growth responses to mechanical wounding and insect herbivory. *Plants* 8:1–13.
- Fall, R., T. Karl, A. Hansel, A. Jordan, and W. Lindinger. 1999. Volatile organic compounds emitted after leaf wounding: On-line analysis by proton-transfer-reaction mass spectrometry. *Journal of Geophysical Research: Atmospheres* 104:15963–15974.

- Farmer, E. E., and C. A. Ryan. 1990. Interplant communication: Airborne methyl jasmonate induces synthesis of proteinase inhibitors in plant leaves. *Proceedings of the National Academy of Sciences* 87:7713–7716.
- Fine, P. V. A., Z. J. Miller, I. Mesones, S. Irazuzta, H. M. Appel, M. H. H. Stevens, I. Sääksjärvi, J. C. Schultz, and P. D. Coley. 2006. The growth–defense trade-off and habitat specialization by plants in Amazonian forests. *Ecology* 87:S150–S162.
- Fischer, R., A. Apa, W. Wakkinen, K. Reese, and J. Connelly. 1993. Nesting-area fidelity of sage grouse in southeastern Idaho. *The Condor* 95:1038–1041.
- Forbey, J. S., A. L. Harvey, M. A. Huffman, F. D. Provenza, R. Sullivan, and D. Tasmimir. 2009. Exploitation of secondary metabolites by animals: A response to homeostatic challenges. *Integrative and Comparative Biology* 49:314–328.
- Freeland, W. J., and D. H. Janzen. 1974. Strategies in herbivory by mammals: The role of plant secondary compounds. *The American Naturalist* 108:269–289.
- Fremgen, M. 2015. Plant toxins influence diet selection and intestinal parasites in a specialist herbivore. Boise State University Theses and Dissertations.
- Frye, G. G., J. W. Connelly, D. D. Musil, and J. S. Forbey. 2013. Phytochemistry predicts habitat selection by an avian herbivore at multiple spatial scales. *Ecology* 94:308–314.
- Gibson, D., E. J. Blomberg, M. T. Atamian, and J. S. Sedinger. 2014. Lek fidelity and movement among leks by male greater sage-grouse *Centrocercus urophasianus*: a capture-mark-recapture approach. *Ibis* 156:729–740.
- Glinwood, R., V. Ninkovic, J. Pettersson, and E. Ahmed. 2004. Barley exposed to aerial allelopathy from thistles (*Cirsium* spp.) becomes less acceptable to aphids. *Ecological Entomology* 29:188–195.
- Godard, K.-A., R. White, and J. Bohlmann. 2008. Monoterpene-induced molecular responses in *Arabidopsis thaliana*. *Phytochemistry* 69:1838–1849.

- Greenhalgh, R., M. L. Holding, T. J. Orr, J. B. Henderson, T. L. Parchman, M. D. Matocq, M. D. Shapiro, and M. D. Dearing. 2022. Trio-binned genomes of the woodrats *Neotoma bryanti* and *Neotoma lepida* reveal novel gene islands and rapid copy number evolution of xenobiotic metabolizing genes. *Molecular Ecology Resources* 22:2713–2731.
- Hansen, L. D., L. K. Farnsworth, N. K. Itoga, A. Nicholson, H. L. Summers, M. C. Whitsitt, and E. D. McArthur. 2008. Two subspecies and a hybrid of big sagebrush: Comparison of respiration and growth characteristics. *Journal of Arid Environments* 72:643–651.
- Heil, M. 2008. Indirect defence via tritrophic interactions. *New Phytologist* 178:41–61.
- Heil, M. 2009. Damaged-self recognition in plant herbivore defence. *Trends in Plant Science* 14:356–363.
- Heil, M., and J. C. S. Bueno. 2007. Within-plant signaling by volatiles leads to induction and priming of an indirect plant defense in nature. *Proceedings of the National Academy of Sciences* 104:5467–5472.
- Heil, M., and R. Karban. 2010. Explaining evolution of plant communication by airborne signals. *Trends in Ecology & Evolution* 25:137–144.
- Hervé, M. R., F. Nicolè, and K.-A. Lê Cao. 2018. Multivariate analysis of multiple datasets: a practical guide for chemical ecology. *Journal of Chemical Ecology* 44:215–234.
- Holopainen, J. K. 2004. Multiple functions of inducible plant volatiles. *Trends in Plant Science* 9:529–533.
- Hulten, M. van, M. Pelsler, L. C. van Loon, C. M. J. Pieterse, and J. Ton. 2006. Costs and benefits of priming for defense in *Arabidopsis*. *Proceedings of the National Academy of Sciences* 103:5602–5607.
- Hussain, A., J. C. Rodriguez-Ramos, and N. Erbilgin. 2019. Spatial characteristics of volatile communication in lodgepole pine trees: Evidence of kin recognition and intra-species support. *Science of The Total Environment* 692:127–135.

- Ito, K., and S. Sakai. 2009. Optimal defense strategy against herbivory in plants: Conditions selecting for induced defense, constitutive defense, and no-defense. *Journal of Theoretical Biology* 260:453–459.
- Jaeger, D. M., J. B. Runyon, and B. A. Richardson. 2016. Signals of speciation: Volatile organic compounds resolve closely related sagebrush taxa, suggesting their importance in evolution. *New Phytologist* 211:1393–1401.
- Jeffries, M. I., and S. P. Finn. 2019. The sagebrush biome range extent, as derived from classified landsat imagery: U.S. Geological Survey data release.
- Kant, M. R., K. Ament, M. W. Sabelis, M. A. Haring, and R. C. Schuurink. 2004. Differential timing of spider mite-induced direct and indirect defenses in tomato plants. *Plant Physiology* 135:483–495.
- Karban, R. 2011. The ecology and evolution of induced resistance against herbivores. *Functional Ecology* 25:339–347.
- Karban, R., I. T. Baldwin, K. J. Baxter, G. Laue, and G. W. Felton. 2000. Communication between plants: induced resistance in wild tobacco plants following clipping of neighboring sagebrush. *Oecologia* 125:66–71.
- Karban, R., and K. J. Baxter. 2001. Induced resistance in wild tobacco with clipped sagebrush neighbors: The role of herbivore behavior. *Journal of Insect Behavior* 14:147–156.
- Karban, R., M. Huntzinger, and A. C. McCall. 2004. The specificity of eavesdropping on sagebrush by other plants. *Ecology* 85:1846–1852.
- Karban, R., and J. Maron. 2002. The fitness consequences of interspecific eavesdropping between plants. *Ecology* 83:1209–1213.
- Karban, R., and J. H. Myers. 1989. Induced plant responses to herbivory. *Annual Review of Ecology, Evolution, and Systematics* 20:331–348.
- Karban, R., K. Shiojiri, M. Huntzinger, and A. C. McCall. 2006. Damage-induced resistance in sagebrush: Volatiles are key to intra- and interplant communication. *Ecology* 87:922–930.

- Karban, R., W. C. Wetzel, K. Shiojiri, S. Ishizaki, S. R. Ramirez, and J. D. Blande. 2014a. Deciphering the language of plant communication: volatile chemotypes of sagebrush. *New Phytologist* 204:380–385.
- Karban, R., W. C. Wetzel, K. Shiojiri, E. Pezzola, and J. D. Blande. 2016. Geographic dialects in volatile communication between sagebrush individuals. *Ecology* 97:2917–2924.
- Karban, R., L. H. Yang, and K. F. Edwards. 2014b. Volatile communication between plants that affects herbivory: a meta-analysis. *Ecology Letters* 17:44–52.
- Kassambara, A., and F. Mundt. 2020. Factoextra: Extract and visualize the results of multivariate data analyses. R Package Version 1.0.7. <https://CRAN.R-project.org/package=factoextra>
- Kelsey, K. C., S. H. Pedersen, A. J. Leffler, J. O. Sexton, M. Feng, and J. M. Welker. 2021. Winter snow and spring temperature have differential effects on vegetation phenology and productivity across Arctic plant communities. *Global Change Biology* 27:1572–1586.
- Kelsey, R. G., J. R. Stephens, and F. Shafizadeh. 1982. The chemical constituents of sagebrush foliage and their isolation. *Journal of Range Management* 35:617.
- Kelsey, R. G., W. E. Wright, F. Sneva, A. Winward, and C. Britton. 1983. The concentration and composition of big sagebrush essential oils from Oregon. *Biochemical Systematics and Ecology* 11:353–360.
- Kessler, A., and R. Halitschke. 2007. Specificity and complexity: the impact of herbivore-induced plant responses on arthropod community structure. *Current Opinion in Plant Biology* 10:409–414.
- Kessler, A., R. Halitschke, C. Diezel, and I. T. Baldwin. 2006. Priming of plant defense responses in nature by airborne signaling between *Artemisia tridentata* and *Nicotiana attenuata*. *Oecologia* 148:280–292.
- Kleinhesselink, A. R., and P. B. Adler. 2018. The response of big sagebrush (*Artemisia tridentata*) to interannual climate variation changes across its range. *Ecology* 99:1139–1149.

- Koricheva, J. 2002. Meta-analysis of sources of variation in fitness costs of plant antiherbivore defenses. *Ecology* 83:176–190.
- Kost, C., and M. Heil. 2006. Herbivore-induced plant volatiles induce an indirect defence in neighbouring plants. *Journal of Ecology* 94:619–628.
- Kost, C., M. Tremmel, and R. Wirth. 2011. Do leaf cutting ants cut undetected? Testing the effect of ant-induced plant defences on foraging decisions in *Atta colombica*. *PLOS ONE* 6:e22340.
- Lavagnini, I., and F. Magno. 2007. A statistical overview on univariate calibration, inverse regression, and detection limits: Application to gas chromatography/mass spectrometry technique. *Mass Spectrometry Reviews* 26:1–18.
- Lazarus, B. E., M. J. Germino, and B. A. Richardson. 2019. Freezing resistance, safety margins, and survival vary among big sagebrush populations across the western United States. *American Journal of Botany* 106:922–934.
- Li, S., X. Cheng, and C. Wang. 2017. A review on traditional uses, phytochemistry, pharmacology, pharmacokinetics and toxicology of the genus *Peganum*. *Journal of Ethnopharmacology* 203:127–162.
- Mahmoud, S. S., and R. B. Croteau. 2002. Strategies for transgenic manipulation of monoterpene biosynthesis in plants. *Trends in Plant Science* 7:366–373.
- Malenke, J. R., E. Magnanou, K. Thomas, and M. D. Dearing. 2012. Cytochrome P450 2B diversity and dietary novelty in the herbivorous, desert woodrat (*Neotoma lepida*). *PLOS ONE* 7:e41510.
- Mattila, P., J. Astola, and J. Kumpulainen. 2000. Determination of flavonoids in plant material by HPLC with diode-array and electro-array detections. *Journal of Agricultural and Food Chemistry* 48:5834–5841.
- McCall, A. C., and R. Karban. 2006. Induced defense in *Nicotiana attenuata* (Solanaceae) fruit and flowers. *Oecologia* 146:566–571.

- McLean, S., R. R. Boyle, S. Brandon, N. W. Davies, and J. S. Sorensen. 2007. Pharmacokinetics of 1,8-cineole, a dietary toxin, in the brushtail possum (*Trichosurus vulpecula*): Significance for feeding. *Xenobiotica* 37:903–922.
- Merenda, P. F. 1997. A guide to the proper use of factor analysis in the conduct and reporting of research: Pitfalls to avoid. *Measurement and Evaluation in Counseling and Development* 30:156–164.
- Millard, P., A. Hester, R. Wendler, and G. Baillie. 2001. Interspecific defoliation responses of trees depend on sites of winter nitrogen storage. *Functional Ecology* 15:535–543.
- Miller, R. F., and L. M. Schultz. 1987. Development and longevity of ephemeral and perennial leaves on *Artemisia tridentata* Nutt. ssp. *wyomingensis*. *Great Basin Naturalist* 47.
- Moreira, X., and L. Abdala-Roberts. 2019. Specificity and context-dependency of plant–plant communication in response to insect herbivory. *Current Opinion in Insect Science* 32:15–21.
- Moreira, X., C. S. Nell, A. Katsanis, S. Rasmann, and K. A. Mooney. 2018. Herbivore specificity and the chemical basis of plant–plant communication in *Baccharis salicifolia* (Asteraceae). *New Phytologist* 220:703–713.
- Morin, X., T. Ameglio, R. Ahas, C. Kurz-Besson, V. Lanta, F. Lebourgeois, F. Miglietta, and I. Chuine. 2007. Variation in cold hardiness and carbohydrate concentration from dormancy induction to bud burst among provenances of three European oak species. *Tree Physiology* 27:817–825.
- Muhlemann, J. K., A. Klempien, and N. Dudareva. 2014. Floral volatiles: from biosynthesis to function. *Plant, Cell & Environment* 37:1936–1949.
- Murlis, J., M. A. Willis, and R. T. Cardé. 2000. Spatial and temporal structures of pheromone plumes in fields and forests. *Physiological Entomology* 25:211–222.
- Myrick, A. J., and T. C. Baker. 2018. Increasing signal-to-noise ratio in gas chromatography - Electroantennography using a Deans switch effluent chopper. *Journal of Chemical Ecology* 44:111–126.

- Neilson, E., J. Goodger, I. Woodrow, and B. Møller. 2013. Plant chemical defense: At what cost? *Trends in plant science* 18:250–258.
- Niemelä, P., A. Em, and H. E. 1979. Birch leaves as a resource for herbivores: Damage-induced increase in leaf phenols with trypsin-inhibiting effects. *Reports from the Kevo Subarctic Research Station* 15:37–40.
- Nobler, J. D. 2016. Risky business: Tradeoffs between nutrition, toxicity, and predation by a specialist mammalian herbivore. *Boise State University Theses and Dissertations*.
- Nobler, J. D., M. J. Camp, M. M. Crowell, L. A. Shipley, C. Dadabay, J. L. Rachlow, L. James, and J. S. Forbey. 2019. Preferences of specialist and generalist mammalian herbivores for mixtures versus individual plant secondary metabolites. *Journal of Chemical Ecology* 45:74–85.
- Nobrega, S., and P. Grogan. 2007. Deeper snow enhances winter respiration from both plant-associated and bulk soil carbon pools in birch hummock tundra. *Ecosystems* 10:419–431.
- Nykänen, H., and J. Koricheva. 2004. Damage-induced changes in woody plants and their effects on insect herbivore performance: a meta-analysis. *Oikos* 104:247–268.
- Oksanen, J., F. G. Blanchet, M. Friendly, R. Kindt, P. Legendre, D. McGlenn, P. R. Minchin, R. B. O'Hara, G. L. Simpson, P. Solymos, M. H. H. Stevens, E. Szoecs, and H. Wagner. 2020. *vegan: Community Ecology Package*. R package version 2.5-7.
- Ottensmann M., M. A. Stoffel, H. J. Nichols, J. I. Hoffman. 2018. GCalignR: An R package for aligning gas-chromatography data for ecological and evolutionary studies. *PLOS ONE*. doi:10.1371/journal.pone.0198311.
- Papana, A., E. Siggiridou, and D. Kugiuntzis. 2021. Detecting direct causality in multivariate time series: A comparative study. *Communications in Nonlinear Science and Numerical Simulation* 99:105797.

- Paré, P. W., M. A. Farag, V. Krishnamachari, H. Zhang, C.-M. Ryu, and J. W. Kloepper. 2005. Elicitors and priming agents initiate plant defense responses. *Photosynthesis Research* 85:149–159.
- Peterson, R. A. 2000. A meta-analysis of variance accounted for and factor loadings in exploratory factor analysis. *Marketing Letters* 11:261–275.
- Portillo-Estrada, M., T. Kazantsev, E. Talts, T. Tosens, and Ü. Niinemets. 2015. Emission timetable and quantitative patterns of wound-induced volatiles across different leaf damage treatments in aspen (*Populus Tremula*). *Journal of Chemical Ecology* 41:1105–1117.
- Provenza, F. D., J. J. Villalba, L. E. Dziba, S. B. Atwood, and R. E. Banner. 2003. Linking herbivore experience, varied diets, and plant biochemical diversity. *Small Ruminant Research* 49:257–274.
- Pu, X., L. Lam, K. Gehlken, A. C. Ulappa, J. L. Rachlow, and J. S. Forbey. 2015. Antioxidant capacity of Wyoming big sagebrush (*Artemisia tridentata* spp. *wyomingensis*) varies spatially and is not related to the presence of a sagebrush dietary specialist. *Western North American naturalist/Brigham Young University* 75:78–87.
- R Core Team. 2021. R: A language and environment for statistical computing. R Foundation for Statistical Computing, Vienna, Austria. <https://www.R-project.org/>.
- Raffa, K. F., and A. A. Berryman. 1982. Accumulation of monoterpenes and associated volatiles following inoculation of grand fir with a fungus transmitted by the fir engraver, *Scolytus ventralis* (Coleoptera: Scolytidae). *The Canadian Entomologist* 114:797–810.
- Raghava, T., P. Ravikumar, R. Hegde, and A. Kush. 2010. Spatial and temporal volatile organic compound response of select tomato cultivars to herbivory and mechanical injury. *Plant Science* 179:520–526.

- Reisner, M. D., J. B. Grace, D. A. Pyke, and P. S. Doescher. 2013. Conditions favouring *Bromus tectorum* dominance of endangered sagebrush steppe ecosystems. *Journal of Applied Ecology* 50:1039–1049.
- Risner, D., M. L. Marco, S. A. Pace, and E. S. Spang. 2020. The potential production of the bioactive compound pinene using whey permeate. *Processes* 8:263.
- Rosentreter, R., B. C. Robb, and J. S. Forbey. 2021. Using an ultraviolet light test to improve sagebrush identification and predict forage quality for wildlife. *Western North American Naturalist* 81:191–200.
- RStudio Team. 2021. RStudio: Integrated development environment for R. RStudio, PBC, Boston, MA. <http://www.rstudio.com/>.
- Schultz, J., H. Appel, A. Ferrieri, and T. Arnold. 2013. Flexible resource allocation during plant defense responses. *Frontiers in Plant Science* 4:324.
- Schwab, W., D. C. Williams, E. M. Davis, and R. Croteau. 2001. Mechanism of monoterpene cyclization: Stereochemical aspects of the transformation of noncyclizable substrate analogs by recombinant (–)-limonene synthase, (+)-bornyl diphosphate synthase, and (–)-pinene synthase. *Archives of Biochemistry and Biophysics* 392:123–136.
- Shiojiri, K., and R. Karban. 2008. Seasonality of herbivory and communication between individuals of sagebrush. *Arthropod-Plant Interactions* 2:87–92.
- Sorensen, J. S., E. Heward, and M. D. Dearing. 2005. Plant secondary metabolites alter the feeding patterns of a mammalian herbivore (*Neotoma lepida*). *Oecologia* 146:415–422.
- Steppuhn, A., and I. T. Baldwin. 2007. Resistance management in a native plant: nicotine prevents herbivores from compensating for plant protease inhibitors. *Ecology Letters* 10:499–511.
- Swanson, D. K. 2015. Environmental limits of tall shrubs in Alaska’s arctic national parks. *PLOS ONE* 10:e0138387.

- Takahashi, M., and N. Huntly. 2010. Herbivorous insects reduce growth and reproduction of big sagebrush (*Artemisia tridentata*). *Arthropod-Plant Interactions* 4:257–266.
- Thaler, J. S., A. L. Fidantsef, and R. M. Bostock. 2002. Antagonism between jasmonate- and salicylate-mediated induced plant resistance: Effects of concentration and timing of elicitation on defense-related proteins, herbivore, and pathogen performance in tomato. *Journal of Chemical Ecology* 28:1131–1159.
- Tuomi, J., P. Niemelä, E. Haukioja, S. Sirén, and S. Neuvonen. 1984. Nutrient stress: an explanation for plant anti-herbivore responses to defoliation. *Oecologia* 61:208–210.
- Tuomi, J., P. Niemela, M. Rousi, S. Siren, and T. Vuorisalo. 1988. Induced accumulation of foliage phenols in mountain birch: Branch response to defoliation? *The American Naturalist* 132:602–608.
- Tzin, V., Y. Hojo, S. R. Strickler, L. J. Bartsch, C. M. Archer, K. R. Ahern, S. Zhou, S. A. Christensen, I. Galis, L. A. Mueller, and G. Jander. 2017. Rapid defense responses in maize leaves induced by *Spodoptera exigua* caterpillar feeding. *Journal of Experimental Botany* 68:4709–4723.
- Ulappa, A. C., R. G. Kelsey, G. G. Frye, J. L. Rachlow, L. A. Shipley, L. Bond, X. Pu, and J. S. Forbey. 2014. Plant protein and secondary metabolites influence diet selection in a mammalian specialist herbivore. *Journal of Mammalogy* 95:834–842.
- Underwood, N. C. 1998. The timing of induced resistance and induced susceptibility in the soybean-Mexican bean beetle system. *Oecologia* 114:376–381.
- Unsicker, S. B., G. Kunert, and J. Gershenzon. 2009. Protective perfumes: the role of vegetative volatiles in plant defense against herbivores. *Current Opinion in Plant Biology* 12:479–485.
- van der Graaf, S. (A. J. ), J. Stahl, A. Klimkowska, J. P. Bakker, and R. H. Drent. 2006. Surfing on a green wave – how plant growth drives spring migration in the Barnacle Goose *Branta leucopsis*. *Ardea* 94:567–577.

- Veblen, K. E., K. C. Nehring, C. M. McGlone, and M. E. Ritchie. 2015. Contrasting effects of different mammalian herbivores on sagebrush plant communities. *PLOS ONE* 10:e0118016.
- Wallestad, R., and R. L. Eng. 1975. Foods of adult sage grouse in central Montana. *The Journal of Wildlife Management* 39:628–630.
- Wei T., and V. Simko. 2021. R package 'corrplot': Visualization of a correlation matrix. (Version 0.92). <https://github.com/taiyun/corrplot>.
- Wiens, J. A., R. G. Cates, J. T. Rotenberry, N. Cobb, B. V. Horne, and R. A. Redak. 1991. Arthropod dynamics on sagebrush (*Artemisia tridentata*): Effects of plant chemistry and avian predation. *Ecological Monographs* 61:299–322.
- Wing, B., and T. Messmer. 2016. Impact of sagebrush nutrients and monoterpenes on greater sage-grouse vital rates. *Human–Wildlife Interactions* 10:157–168.
- Wold, E. N., and R. J. Marquis. 1997. Induced defense in white oak: Effects on herbivores and consequences for the plant. *Ecology* 78:1356–1369.
- Zandt, P. A. V. 2007. Plant defense, growth, and habitat: A comparative assessment of constitutive and induced resistance. *Ecology* 88:1984–1993.
- Zangerl, A. R., and C. E. Rutledge. 1996. The probability of attack and patterns of constitutive and induced defense: A test of optimal defense theory. *The American Naturalist* 147:599–608.
- Zinn, A. D., D. Ward, and K. Kirkman. 2007. Inducible defences in *Acacia sieberiana* in response to giraffe browsing. *African Journal of Range and Forage Science* 24:123–129.

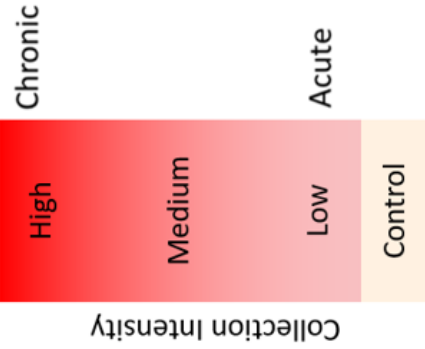
## Tables

**Table 1.1.** Sampling collection scheme. All sites (Figure 1.1) contained paired plants (Plant ID 1 - 5) with each being assigned to either a simulated browsed treatment (e.g., clipped, hereafter treatment, green left column) or serving as a control (e.g., was not clipped, tan top row). The treatment plants in each pair received a simulated browsing event (represented by the beak icon) at time zero (Hour 0) and then collections of the stems and leaves (represented by the scissors icon) were taken from the treatment plant at the designated time intervals after the simulated browsing event (Hour 1, Hour 24, Hour 48, Hour 144 hr). For each treatment plant's first collection of material, stems and leaves were also collected from the paired control plant. A collection intensity scale was assigned to each sample collection event throughout the time course for each treatment plant with a collection intensity of low indicating that no previous collection had taken place on that plant (low, light red representing acute level of simulated browsing) and a collection intensity of high indicating that three prior sequential collections had been taken on that plant (high, dark red, representing the highest chronic level of simulated browsing).

Controls	Plant 1 	Plant 2 	Plant 3 	Plant 4 	Plant 5 
Plant ID	Hour 0	Hour 1	Hour 24	Hour 48	Hour 144
Plant 1					
Plant 2*					
Plant 3					
Plant 4					
Plant 5					 **

 Browsed

 Collected



Collection Intensity

\* Plant 2 is chronically browsed and considered paired with all controls

\*\* Treatment Plant 5 at T = 144 hr was excluded from the analysis due to only having two samples

**Table 1.2.** Compound names with retention times (mins) acquired from gas chromatography. Naming the compounds was done to simplify the visualization of all compounds in the figures with known compounds in parentheses determined from co-chromatography with standards. The yellow highlighted compounds were included in the subsequent analyses because they were present in at least 10% of any treatment group. The unhighlighted compounds were excluded from the analyses.

Compound and Retention Times					
Compound Names	Retention Time	Compound Names	Retention Time	Compound Names	Retention Time
C1	3.084	C22 (p-cymene)	15.797	C43	19.177
C2	3.529	C23	15.948	C44	19.461
C3	4.316	C24 (1,8-cineole)	16.119	C45	19.585
C4	6.767	C25	16.176	C46	19.693
C5	10.732	C26	16.297	C47	19.859
C6	11.313	C27	16.428	C48	20.018
C7	11.677	C28	16.601	C49	20.250
C8	11.832	C29	16.763	C50	20.381
C9	12.061	C30	16.885	C51	20.476
C10 (alpha-pinene)	12.305	C31	17.070	C52	20.670
C11 (camphene)	12.890	C32	17.185	C53 (camphor)	20.763
C12	13.134	C33	17.410	C54	20.942
C13	13.296	C34	17.577	C55	21.102
C14	13.617	C35	17.692	C56	21.227
C15 (beta-pinene)	14.051	C36	17.773	C57	21.311
C16	14.328	C37	18.034	C58	21.436
C17	14.560	C38 (terpinolene)	18.132	C59	21.591
C18	14.815	C39	18.482	C60	21.688
C19	14.992	C40	18.664	C61	21.779
C20	15.259	C41	18.785	C62	21.877
C21 (3-carene)	15.496	C42	18.951		

**Table 1.3.** Principal Component Analysis (PCA) loadings cutoff tables for comparing time points (1, 24, 48, and 144 hr) within *a*) control, *b*) acute, or *c*) chronic treatment groups separately and comparing *d*) control versus acute, *e*) control versus chronic, and comparing *f*) varying levels of collection intensity at 144 hr. These tables were created from a threshold equation of  $\sqrt{1/n \text{col}(\text{dataframe})}$  that resulted in the value of 0.132 for all groups (Holland 2019). Similar loading values represent compounds that are correlated within the positive or negative quadrant of the PC dimensions (PC1 or PC2). Only loadings that are above the threshold of 0.132 (in bold) were included. Any loading in either PC1 or PC2 higher than +/-0.3 rounded were considered a compound of interest (indicated by red shading) as they signified a substantial contribution to the variation being observed among the groups being compared (Merenda 1997, Peterson 2000).

Time Points within Control			Time Points within Acute			Time Points within Chronic		
Compounds	PC1	PC2	Compounds	PC1	PC2	Compounds	PC1	PC2
C18	<b>-0.346</b>	<b>0.139</b>	C44	<b>-0.319</b>	<b>0.300</b>	C28	<b>-0.472</b>	<b>-0.016</b>
C26	<b>-0.334</b>	<b>0.224</b>	C38	<b>-0.293</b>	<b>-0.021</b>	C7	<b>-0.358</b>	<b>0.035</b>
C33	<b>-0.332</b>	<b>0.153</b>	C8	<b>-0.258</b>	<b>0.325</b>	C5	<b>-0.355</b>	<b>0.041</b>
C61	<b>-0.275</b>	<b>-0.021</b>	C60	<b>-0.148</b>	<b>0.027</b>	C34	<b>-0.339</b>	<b>0.283</b>
C16	<b>-0.275</b>	<b>0.023</b>	C61	<b>-0.135</b>	<b>0.223</b>	C32	<b>-0.211</b>	<b>0.190</b>
C37	<b>-0.241</b>	<b>0.229</b>	C12	<b>-0.101</b>	<b>0.154</b>	C18	<b>-0.041</b>	<b>0.389</b>
C45	<b>-0.221</b>	<b>0.139</b>	C33	<b>-0.057</b>	<b>0.196</b>	C29	<b>0.036</b>	<b>0.201</b>
C62	<b>-0.205</b>	<b>-0.071</b>	C16	<b>-0.010</b>	<b>0.221</b>	C45	<b>0.041</b>	<b>0.213</b>
C29	<b>-0.176</b>	<b>0.054</b>	C51	<b>0.028</b>	<b>0.187</b>	C44	<b>0.095</b>	<b>-0.138</b>
C32	<b>0.039</b>	<b>0.392</b>	C18	<b>0.032</b>	<b>0.255</b>	C33	<b>0.130</b>	<b>0.307</b>
C34	<b>0.069</b>	<b>0.355</b>	C26	<b>0.152</b>	<b>-0.072</b>	C37	<b>0.131</b>	<b>0.290</b>
C38	<b>0.102</b>	<b>-0.182</b>	C32	<b>0.152</b>	<b>0.406</b>	C19	<b>0.137</b>	<b>0.027</b>
C44	<b>0.131</b>	<b>-0.332</b>	C9	<b>0.160</b>	<b>0.381</b>	C38	<b>0.147</b>	<b>-0.313</b>
C9	<b>0.140</b>	<b>0.267</b>	C30	<b>0.171</b>	<b>-0.066</b>	C8	<b>0.156</b>	<b>0.039</b>
C7	<b>0.207</b>	<b>0.252</b>	C37	<b>0.216</b>	<b>-0.091</b>	C21	<b>0.165</b>	<b>-0.054</b>
C5	<b>0.245</b>	<b>0.290</b>	C7	<b>0.310</b>	<b>0.238</b>	C62	<b>0.166</b>	<b>-0.072</b>
C28	<b>0.329</b>	<b>0.363</b>	C5	<b>0.326</b>	<b>0.252</b>	C26	<b>0.171</b>	<b>0.482</b>
			C34	<b>0.374</b>	<b>-0.128</b>	C61	<b>0.175</b>	<b>0.188</b>
			C28	<b>0.384</b>	<b>0.124</b>	C39	<b>0.194</b>	<b>0.067</b>

a)

b)

c)

d)

Control versus Acute		
Compounds	PC1	PC2
C44	<b>-0.294</b>	<b>-0.176</b>
C38	<b>-0.227</b>	<b>-0.210</b>
C61	<b>-0.144</b>	<b>0.295</b>
C8	<b>-0.143</b>	-0.074
C62	-0.127	<b>0.168</b>
C33	-0.039	<b>0.316</b>
C16	-0.036	<b>0.247</b>
C18	-0.001	<b>0.352</b>
C45	0.037	<b>0.223</b>
C26	0.090	<b>0.428</b>
C37	<b>0.148</b>	<b>0.382</b>
C30	<b>0.149</b>	-0.021
C9	<b>0.232</b>	0.030
C32	<b>0.266</b>	0.023
C7	<b>0.341</b>	-0.103
C34	<b>0.357</b>	0.064
C5	<b>0.372</b>	-0.111
C28	<b>0.447</b>	<b>-0.189</b>

e)

Control versus Chronic		
Compounds	PC1	PC2
C28	<b>-0.472</b>	<b>0.165</b>
C5	<b>-0.345</b>	<b>0.146</b>
C7	<b>-0.325</b>	<b>0.149</b>
C34	<b>-0.244</b>	<b>0.295</b>
C9	<b>-0.228</b>	<b>0.132</b>
C32	<b>-0.203</b>	<b>0.326</b>
C38	-0.008	<b>-0.294</b>
C44	0.012	<b>-0.307</b>
C21	0.056	-0.096
C29	0.092	<b>0.143</b>
C45	0.102	<b>0.217</b>
C18	<b>0.158</b>	<b>0.346</b>
C37	<b>0.169</b>	<b>0.254</b>
C62	<b>0.204</b>	-0.031
C16	<b>0.205</b>	<b>0.145</b>
C33	<b>0.226</b>	<b>0.283</b>
C61	<b>0.239</b>	<b>0.153</b>
C26	<b>0.266</b>	<b>0.343</b>

f)

Collection Intensity		
Compounds	PC1	PC2
C61	<b>-0.301</b>	<b>-0.079</b>
C37	<b>-0.262</b>	<b>-0.393</b>
C18	-0.065	<b>-0.334</b>
C26	-0.063	<b>-0.427</b>
C33	-0.049	<b>-0.241</b>
C45	0.008	<b>-0.183</b>
C44	0.027	<b>0.291</b>
C51	0.097	-0.082
C38	<b>0.135</b>	<b>0.333</b>
C30	<b>0.148</b>	-0.080
C39	<b>0.172</b>	-0.102
C34	<b>0.267</b>	<b>-0.298</b>
C9	<b>0.277</b>	-0.068
C5	<b>0.327</b>	-0.075
C7	<b>0.338</b>	-0.051
C32	<b>0.340</b>	<b>-0.182</b>
C28	<b>0.477</b>	-0.058

**Table 1.4.** The number of correlated pairs (Figure 1.10, Figure 1.11) that were above the +/-0.4 threshold for control, acute, and chronic treatment group.

Treatment	Positive	Negative
Control	60	5
Acute	58	1
Chronic	58	17

**Table 1.5. Mean, Standard Error, minimum (Min), and maximum (Max) statistics for the two strongest positive and two strongest negative correlated clusters that occurred throughout the treatment groups.**

	Positive Clusters							
	C5, C7, C28, C32, C34			C8, C10, C11, C22, C24, C44				
	Mean	Standard Error	Min	Max	Mean	Standard Error	Min	Max
<b>Control</b>	0.72	0.19	0.54 (C5-C32)	0.99 (C5-C7)	0.65	0.24	0.48 (C10-C44)	0.99 (C8-C11)
<b>Acute</b>	0.65	0.21	0.49 (C5-C32)	0.90 (C5-C7)	0.54	0.43	0.30 (C11-C24)	0.98 (C8-C11)
<b>Chronic</b>	0.62	0.3	0.62 (C5-C32)	0.97 (C5-C7)	0.55	0.49	0.18 (C8-C24)	0.97 (C8-C11)
	Negative Clusters							
	C8, C10, C11, C22, C24, C28, C32, C34			C8, C26, C37, C38				
	Mean	Standard Error	Min	Max	Mean	Standard Error	Min	Max
<b>Control</b>	-0.25	-0.33	-0.07 (C10-C32)	-0.37 (C24-C28)	-0.34	-0.31	-0.21 (C8-C37)	-0.44 (C26-C38)
<b>Acute</b>	-0.22	-0.70	-0.02 (C8-C32)	-0.39 (C8-C34)	-0.52	-0.47	-0.13 (C26-C38)	-0.41 (C37-C38)
<b>Chronic</b>	-0.38	-0.34	-0.18 (C11-C32)	-0.59 (C22-C32)	-0.27	-0.85	-0.01 (C26-C38)	-0.53 (C37-C38)

**Table 1.6. Kruskal-Wallis test results comparing positive and negative correlated values among the control, acute, and chronic treatment groups where only pairs were included if at least one treatment group had an  $r^2 > +/-0.4$ .**

Positive Correlations

	Kruskal-Wallis Rank Sum Test		
	df	$\chi^2$	P
$r^2$ by Treatment	2, 222	2.7037	0.2588

Negative Correlations

	Kruskal-Wallis Rank Sum Test		
	df	$\chi^2$	P
$r^2$ by Treatment	2, 60	18.798	<0.001

**Table 1.7. Pairwise Wilcoxon Rank Sum test to determine which treatment groups of control, acute, and chronic were significantly different from each other when at least one treatment group had an  $r^2 > -0.4$ .**

Negative Correlations

Pairwise comparisons using Wilcoxon rank sum exact test

	Control	Acute
Acute	0.153	-
Chronic	0.0017	<0.001

**Table 1.8. Kruskal-Wallis test results on the correlation values between the strongest positive and negative correlation clusters to compare strength among the control, acute, and chronic treatment groups.**

Positive Correlation Cluster: C5, C7, C28, C32, C34

Kruskal-Wallis Rank Sum Test			
	df	$\chi^2$	P
$r^2$ by Treatment	2, 27	2.5497	0.2795

Positive Correlation Cluster: C8, C10, C11, C22, C24, C44

Kruskal-Wallis Rank Sum Test			
	df	$\chi^2$	P
$r^2$ by Treatment	2, 42	1.617	0.4455

Negative Correlation Cluster: C8, C10, C11, C22, C24, C28, C32, C34

Kruskal-Wallis Rank Sum Test			
	df	$\chi^2$	P
$r^2$ by Treatment	2, 42	10.12	0.0063

Negative Correlation Cluster: C8, C26, C37, C38

Kruskal-Wallis Rank Sum Test			
	df	$\chi^2$	P
$r^2$ by Treatment	2,9	1.5	0.4724

**Table 1.9. Pairwise Wilcoxon Rank Sum test to determine if the treatment groups of control, acute, and chronic were significantly different from each other when observing the strongest negative correlation cluster.**

Negative Correlation Cluster C8, C10, C11, C22, C24, C28, C32, C34

Pairwise comparisons using Wilcoxon rank sum exact test

	Control	Acute
Acute	0.935	-
Chronic	0.011	0.011

**Table 1.10. Two-way ANOVA results for the final compounds of interest identified from comparing treatment groups and time points.**

C26

Sources of Variation	ANOVA		
	df	F	P
Treatment	2, 139	1.368	0.258
Time Points	4, 139	1.163	0.330

C28

Sources of Variation	ANOVA		
	df	F	P
Treatment	2, 139	1.829	0.164
Time Points	4, 139	0.501	0.735

C34

Sources of Variation	ANOVA		
	df	F	P
Treatment	2, 139	1.169	0.314
Time Points	4, 139	0.283	0.889

C38

Sources of Variation	ANOVA		
	df	F	P
Treatment	2, 139	0.537	0.586
Time Points	4, 139	0.625	0.646

C44

Sources of Variation	ANOVA		
	df	F	P
Treatment	2, 139	1.272	0.284
Time Points	4, 139	0.318	0.865

**Table 1.11. One-way ANOVA results from the final compounds of interest from comparing the varying levels of collection intensity.**

C26

Sources of Variation	ANOVA		
	df	F	P
Collection Intensity	3, 49	0.561	0.643

C28

Sources of Variation	ANOVA		
	df	F	P
Collection Intensity	3, 49	0.463	0.709

C34

Sources of Variation	ANOVA		
	df	F	P
Collection Intensity	3, 49	0.272	0.845

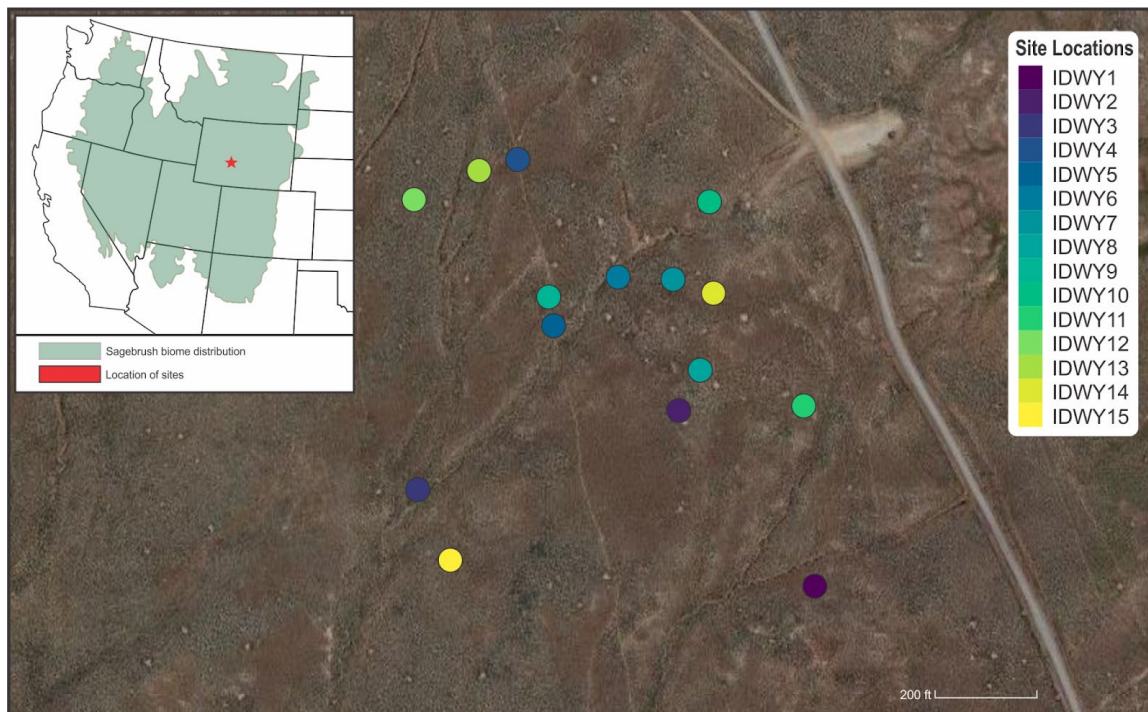
C38

Sources of Variation	ANOVA		
	df	F	P
Collection Intensity	3, 49	0.56	0.644

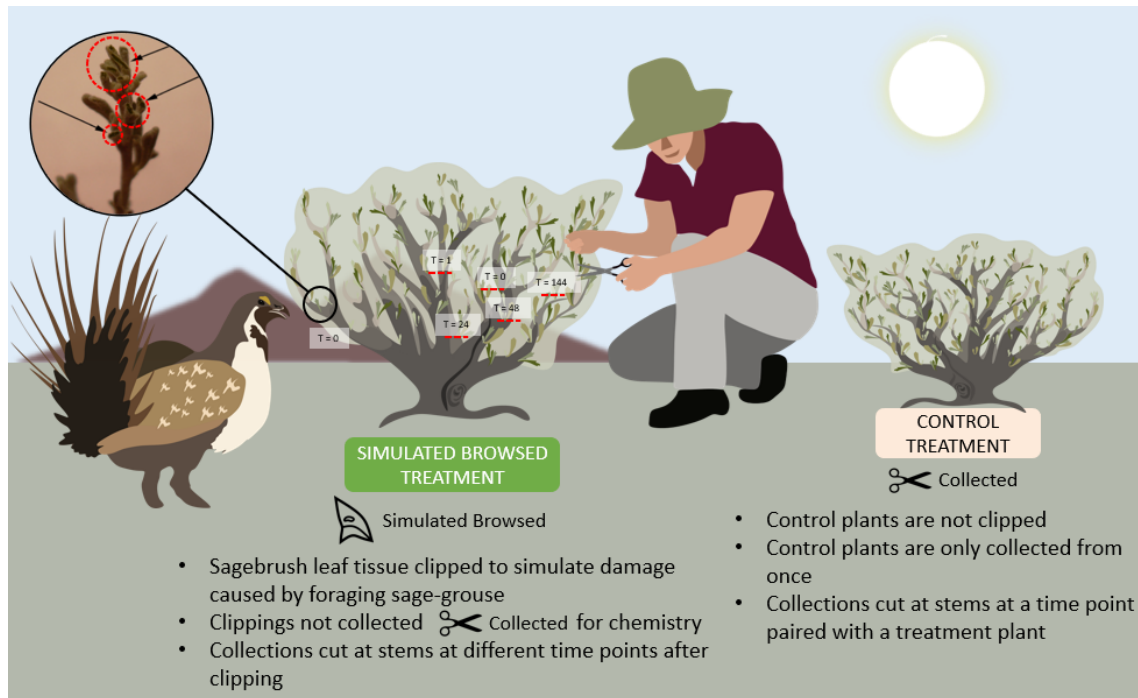
C61

Sources of Variation	ANOVA		
	df	F	P
Collection Intensity	3, 49	0.62	0.605

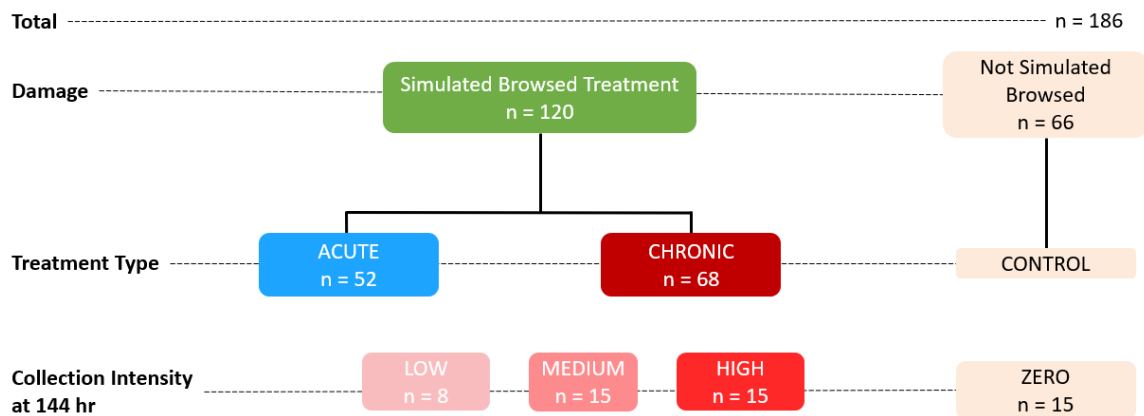
## Figures



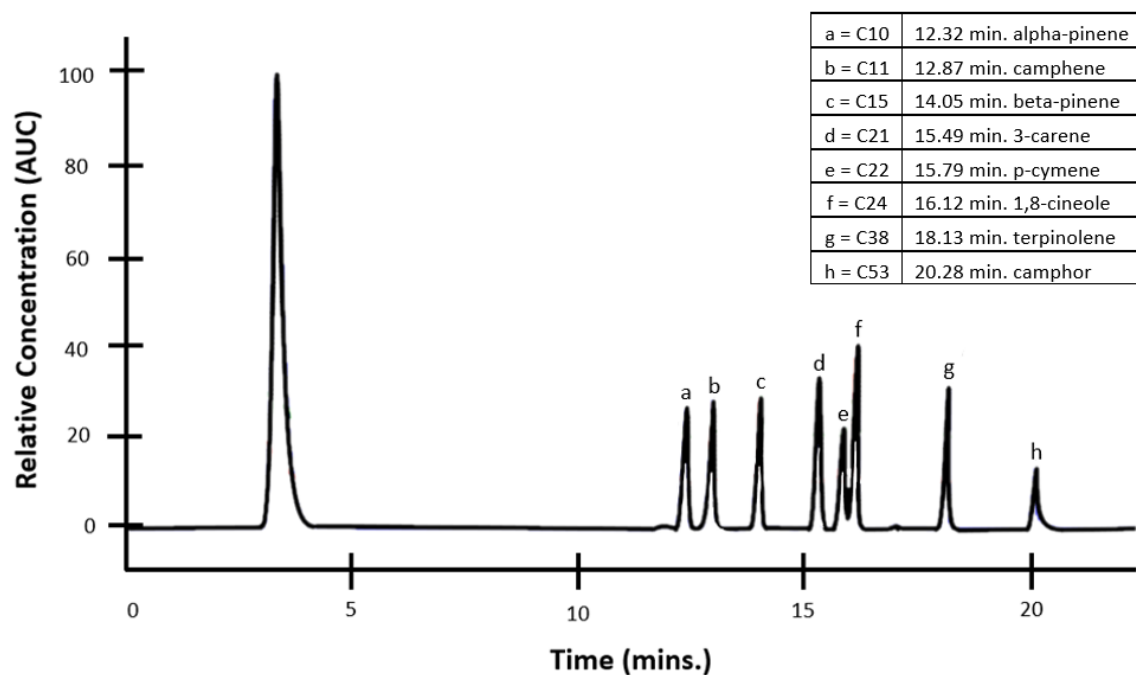
**Figure 1.1. Map of 15 collection patches in Fremont County, Wyoming, USA where the induced defense experiment was conducted. The overlay map in the upper left corner displays the sagebrush biome distribution throughout the western United States. The red star indicates the location of the study area. Sagebrush biome distribution map acquired from the USGS (Jeffries and Finn 2019).**



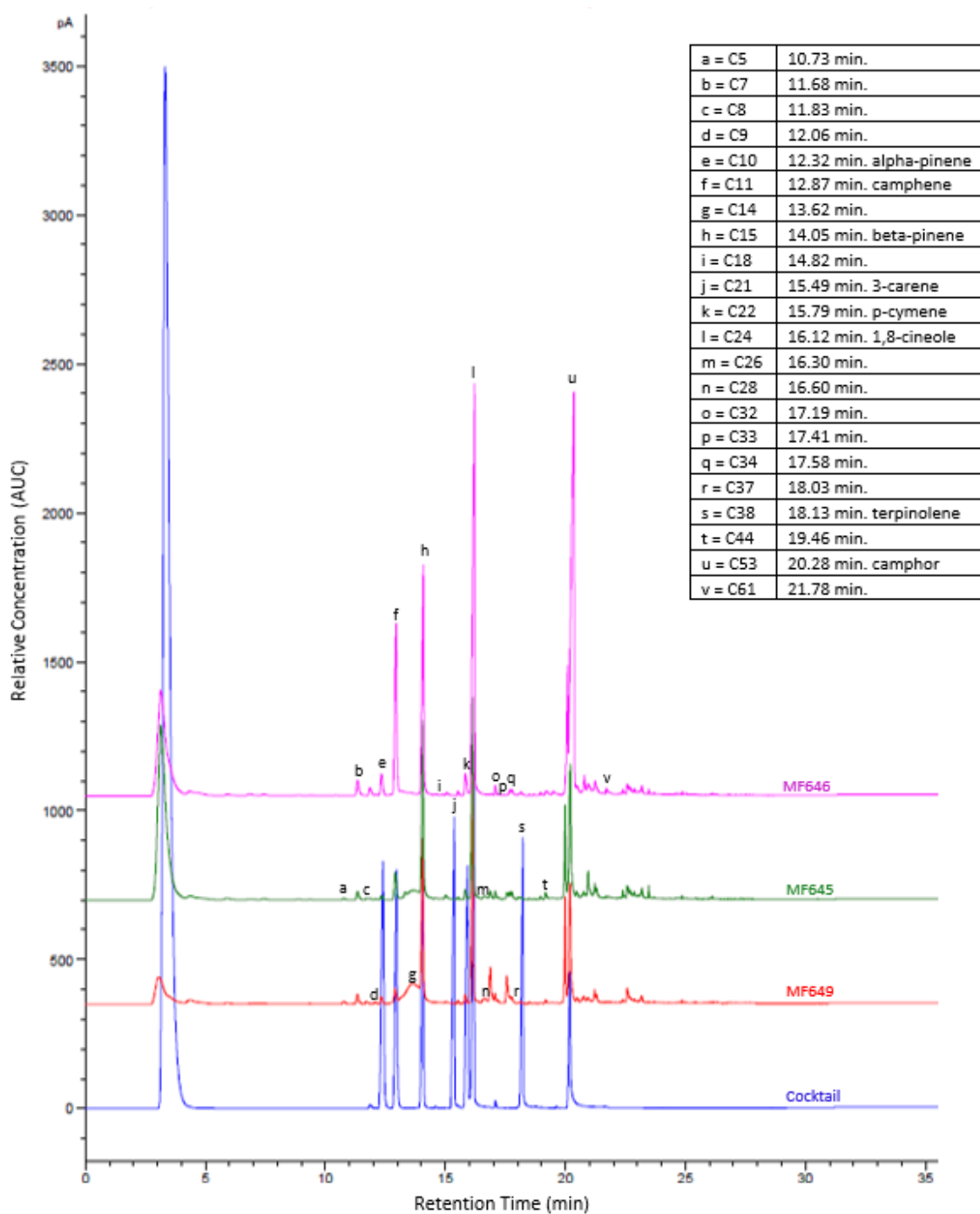
**Figure 1.2. (Left) Overview of induced defense experiment with treatments that mimic natural browsing by sage-grouse on sagebrush where distinct bite marks are made on the leaves. This browsing damage was simulated by cutting 50 leaves from each simulated browsed treatment plant (indicated by bird beak icon) in each collection site at zero hr ( $T = 0$  hr). After the simulated browsing treatment, leaf and stem material was collected using scissors at various time points (0, 1, 24, 48, and 144 hr). Collections were taken from treatment plants and (Right) a spatially and temporally paired control plant that was unique and had never received simulated browsing or prior collections. All paired treatment and control plants were positioned at a minimal distance of 1 m apart.**



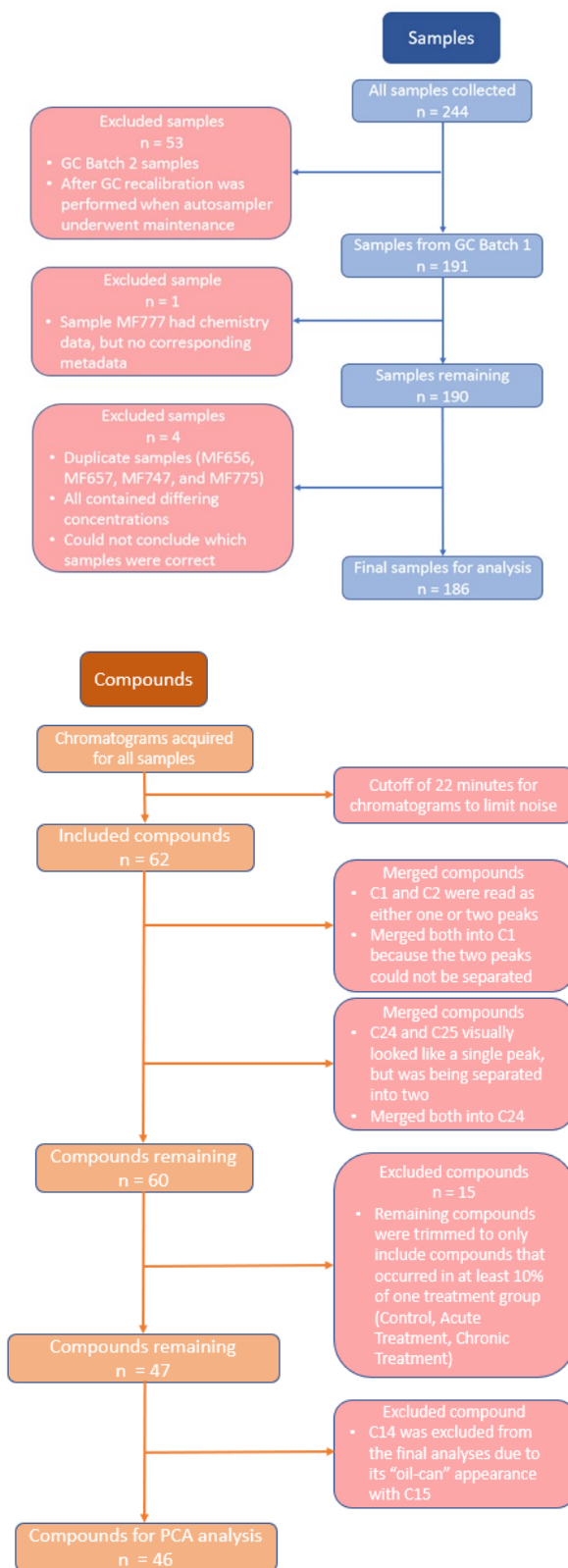
**Figure 1.3.** Diagram of induced defense data structure and the associated number of collection samples in each group.



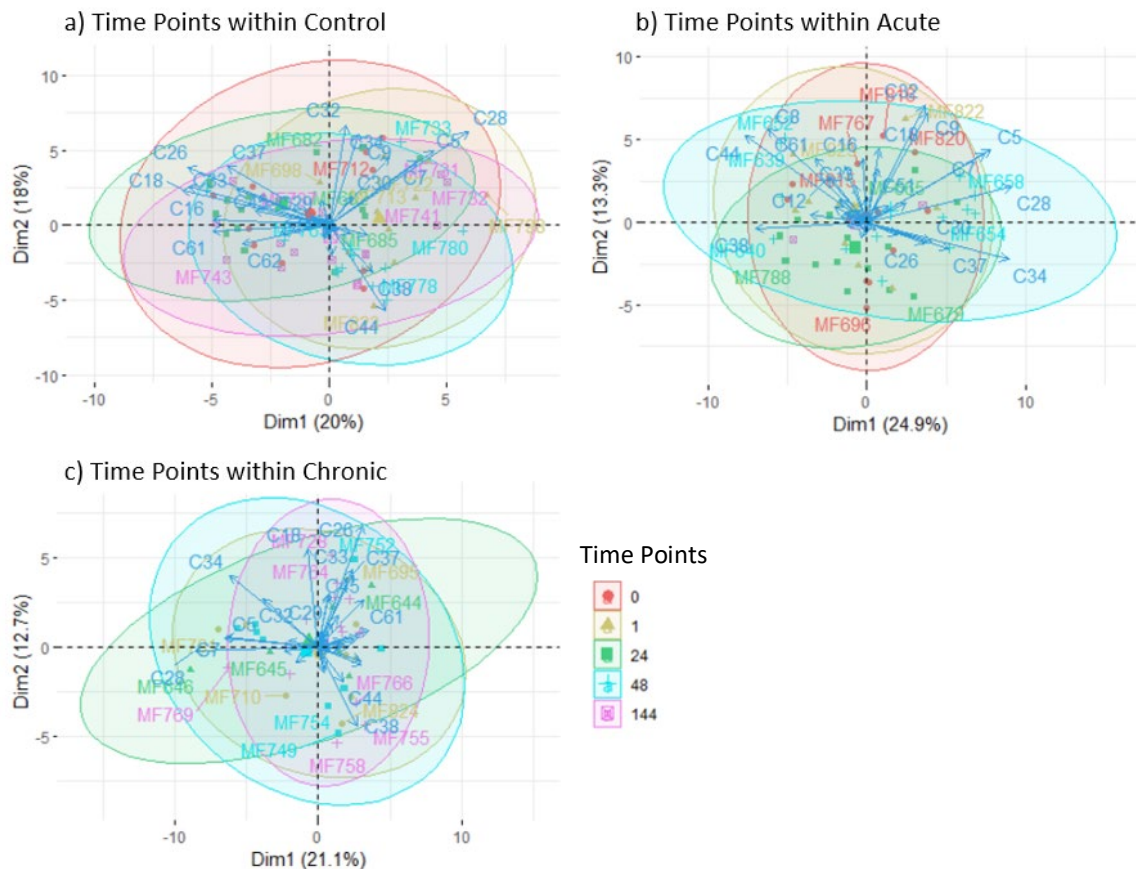
**Figure 1.4.** Chromatogram of a cocktail of monoterpene standards used for co-chromatography. The standards correspond to the compound names (inset) based on the retention times (mins) that they appear on the chromatogram. The first peak corresponds to the solvent methylene chloride used to combine standards into a single sample for gas chromatography.



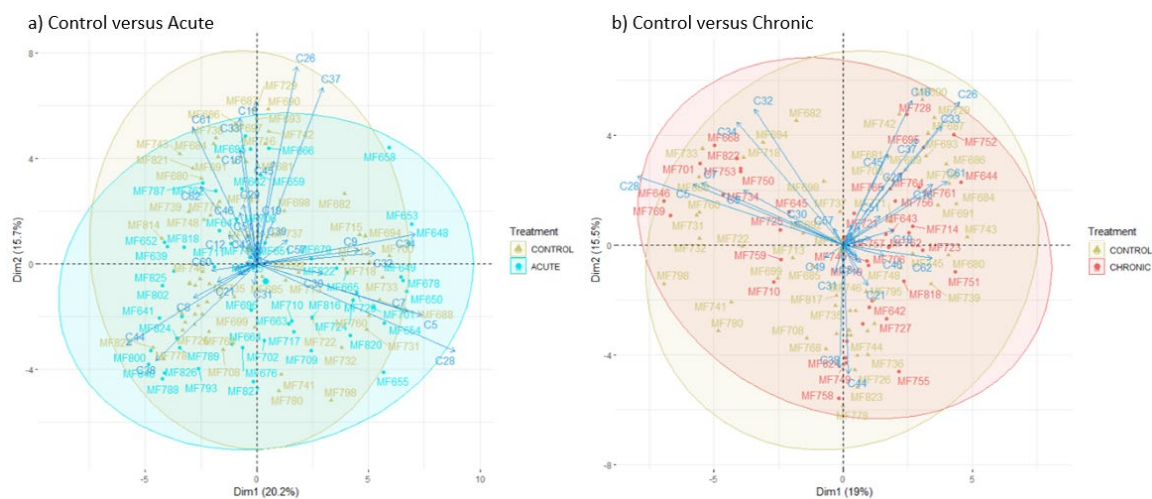
**Figure 1.5.** Representative monoterpene chromatograms for sagebrush (*Artemisia tridentata* subsp. *wyomingensis*) (top three lines) and the cocktail of monoterpene standards (bottom blue line). The peaks represent individual compounds with the relative abundance measured as area under the curve (AUC) with the corresponding retention time (RT) in mins. The main compounds of interest and standards are marked using compound names based on associated RTs (Table 1.2).



**Figure 1.6. Consort diagrams that details the decisions made for inclusion and exclusion of samples and monoterpene compounds into the analyses.**

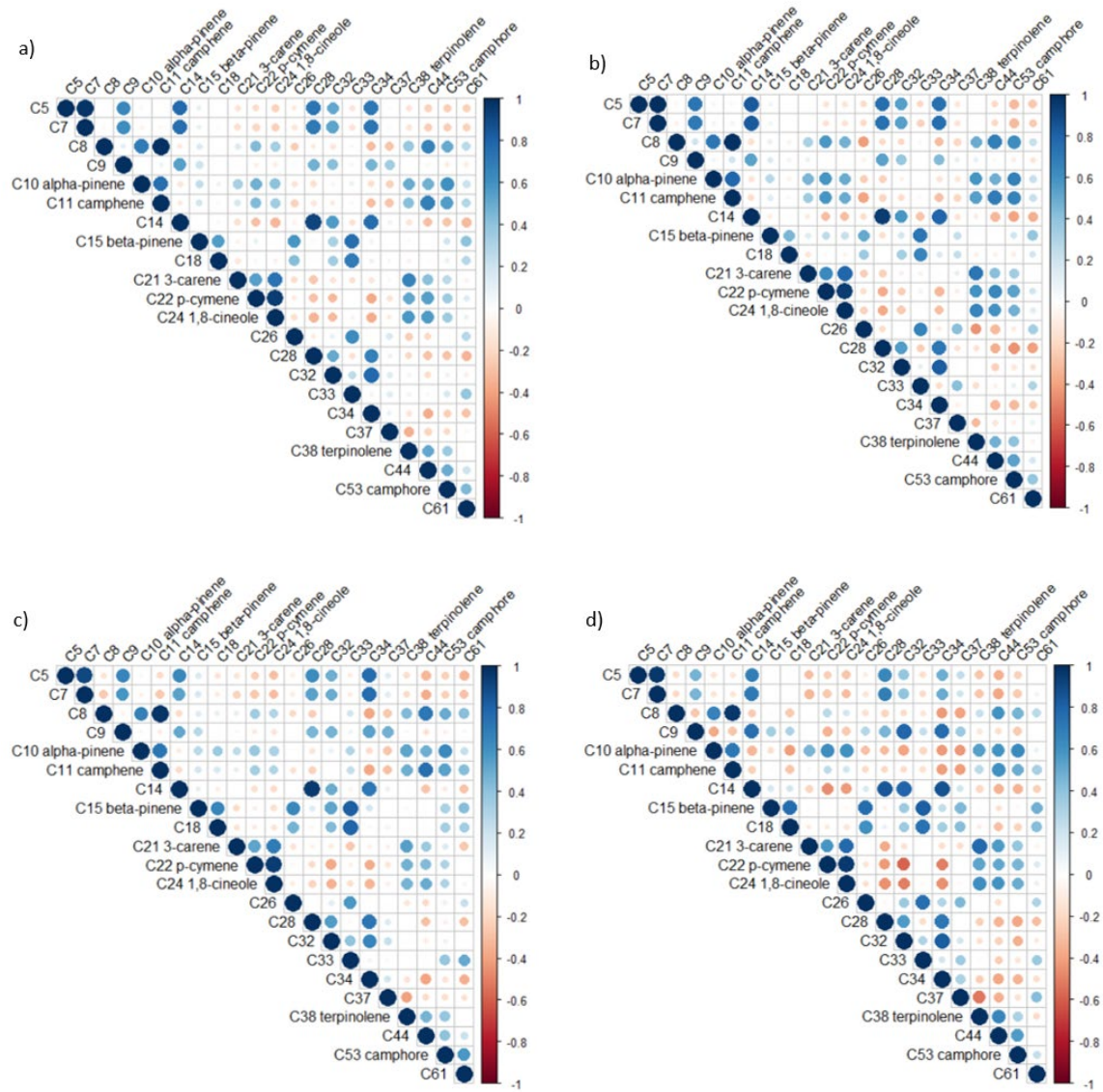


**Figure 1.7. Principal Component Analyses (PCAs) generated for comparing time points (1, 24, 48, and 144 hr) within a) control, b) acute, and c) chronic treatment groups separately using the calculated centered values. The colored ellipses represent the different time points (hr) after simulated browsing within each treatment and where time points fall across the different PC dimensions. The compounds are represented by the vectors of varying lengths with the longer vectors having a stronger influence on the variation among the samples within the time point category (see Table 1.3 for PCA loadings).**



**Figure 1.8.** PCAs generated for the *a)* control versus acute treatment for all time points and *b)* control versus chronic treatment for all time points using the calculated centered values. The colored ellipses represent the different treatment groups present and where they fall across the different PC dimensions. The compounds are represented by the vectors of varying lengths with the longer vectors having a stronger influence on the variation among the samples within the treatment category (see Table 1.3 for PCA loadings).





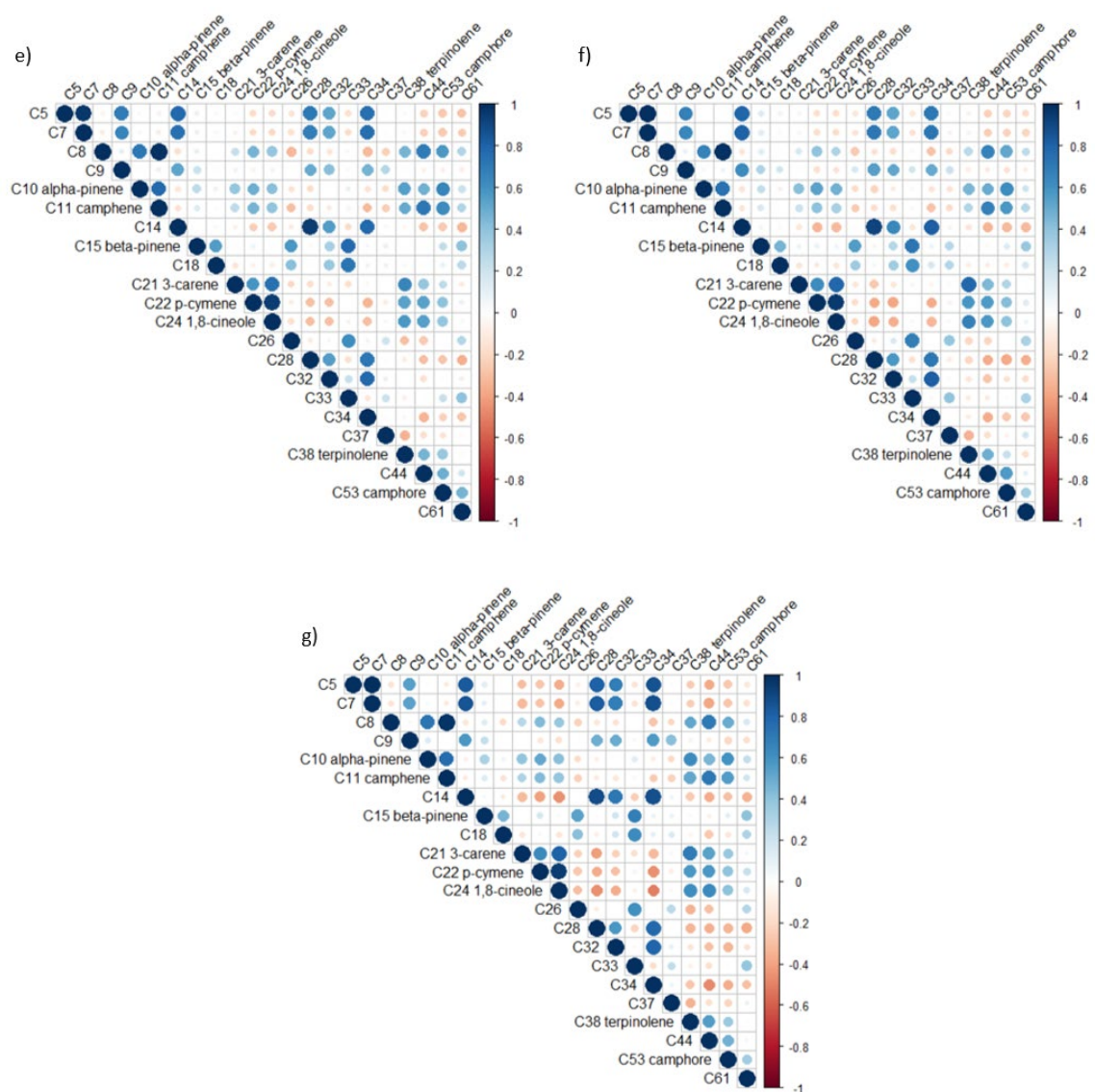


**Figure 1.10.** Correlation matrices generated from the area under the curve per gram dry weight (AUC/gDW) values of the fourteen main vector loadings that made the cutoff threshold of  $\pm 0.3$  (see Table 1.3) and the monoterpene standards. The size of each circle corresponds to the strength of the correlation represented by the correlation coefficients between  $-1.0$  and  $+1.0$  among the respective compounds while the color indicates either a positive (blue) or a negative (red) correlation. All compounds aside from the standards appeared in at least one of the PCA loading tables. The correlation matrices are created through comparing *a*) all samples in the experiment, *b*) time points within control, *c*) time points within acute, *d*) time points within chronic, *e*) control versus acute, *f*) control versus chronic, and *g*) collection intensity. Compound C14 was excluded in the subsequent analyses due to its “oil-can” appearance that bled into C15 (see Appendix C for details).

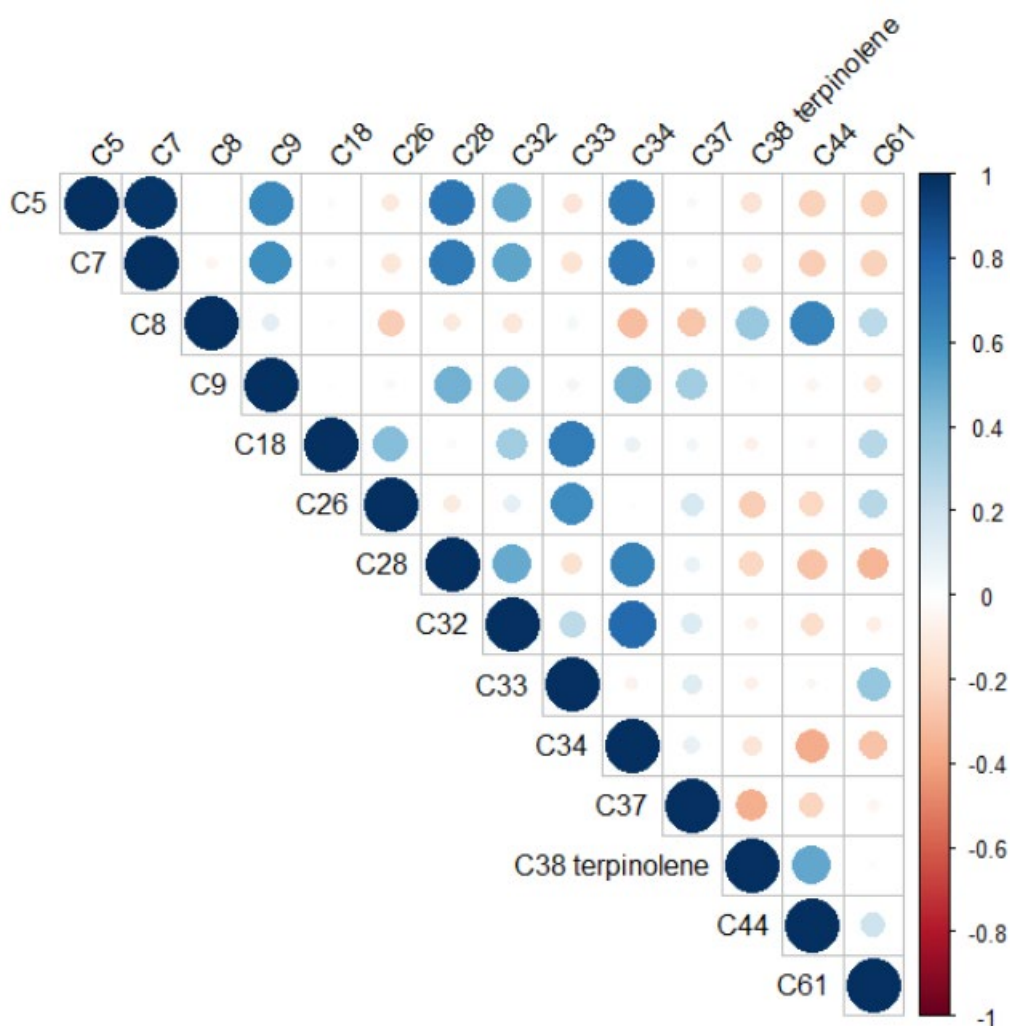


**Figure 1.11.** Correlation matrices generated from the area under the curve per gram dry weight (AUC/gDW) values of the compounds of interest that made it above the cutoff of  $\pm 0.3$  that signified a substantial contribution to the variation being observed among all samples within the experiment (see Table 1.3). The size of each circle corresponds to the strength of the correlation between  $-1.0$  and  $+1.0$  between the respective compounds while the color indicates either a positive (blue) or a negative (red) correlation. All compounds appeared in at least one of the PCA loading tables as having a loading value above the  $\pm 0.3$  cutoff.

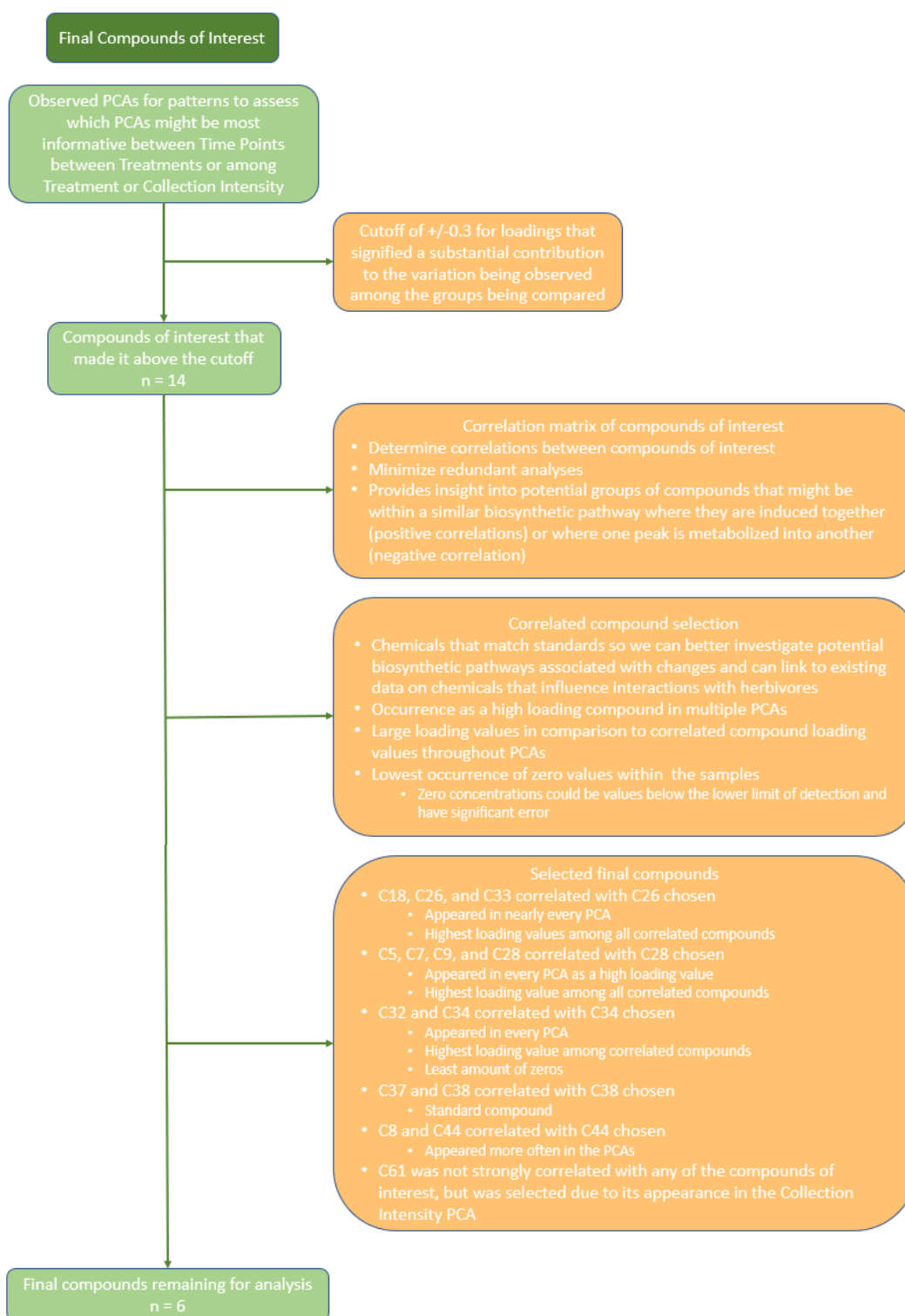


**Figure 1.12. Consort diagram that details the decisions made for inclusion and exclusion of the final compounds of interest that made it above the PCA loading cutoff of +/-0.3 for the final analyses (see Table 1.3).**

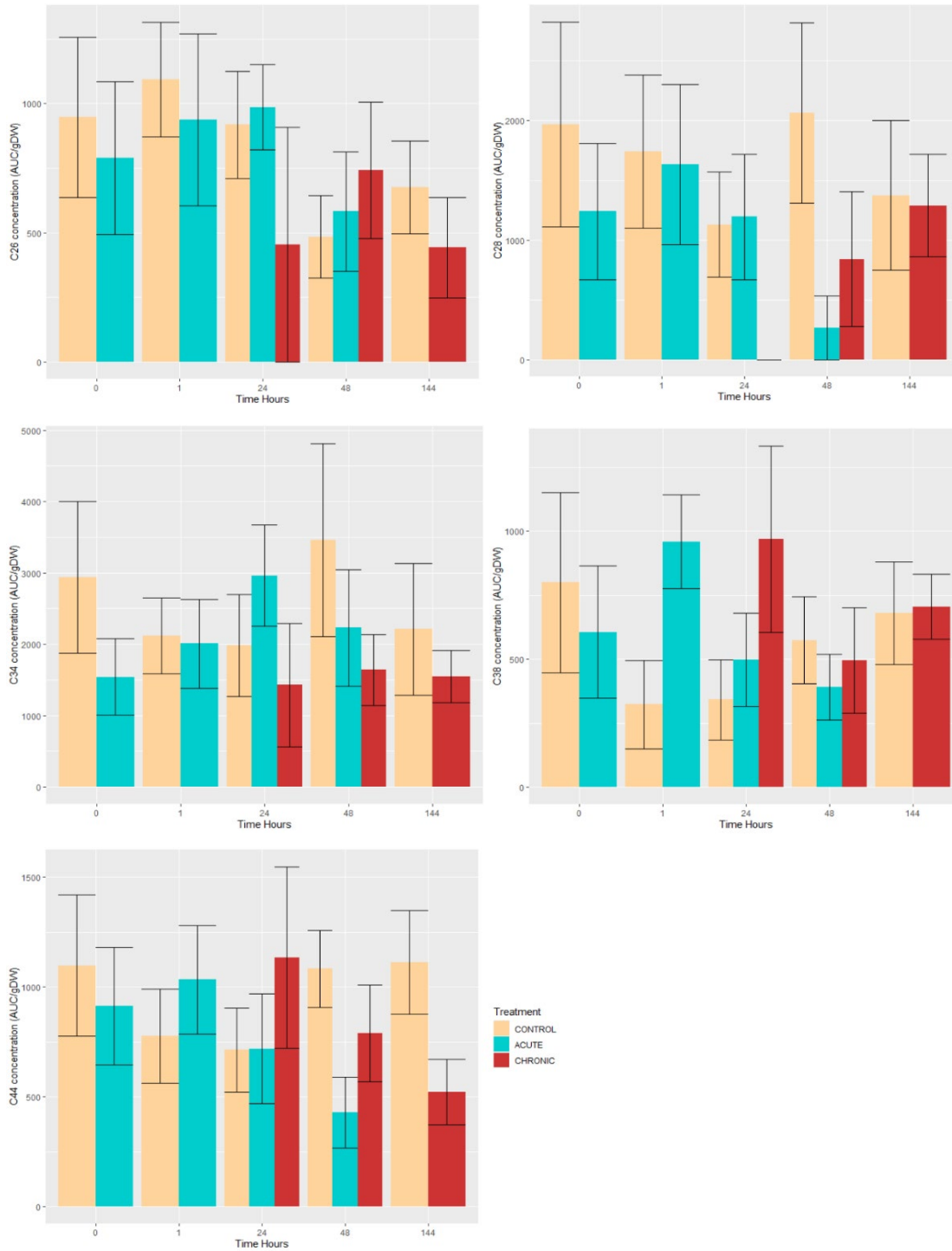


**Figure 1.13. Mean monoterpene concentrations (AUC/gDW) for the final compounds of interest when comparing treatment groups across the time points (hours) after the first simulated browsing event. Each bar graph has associated standard error bars.**

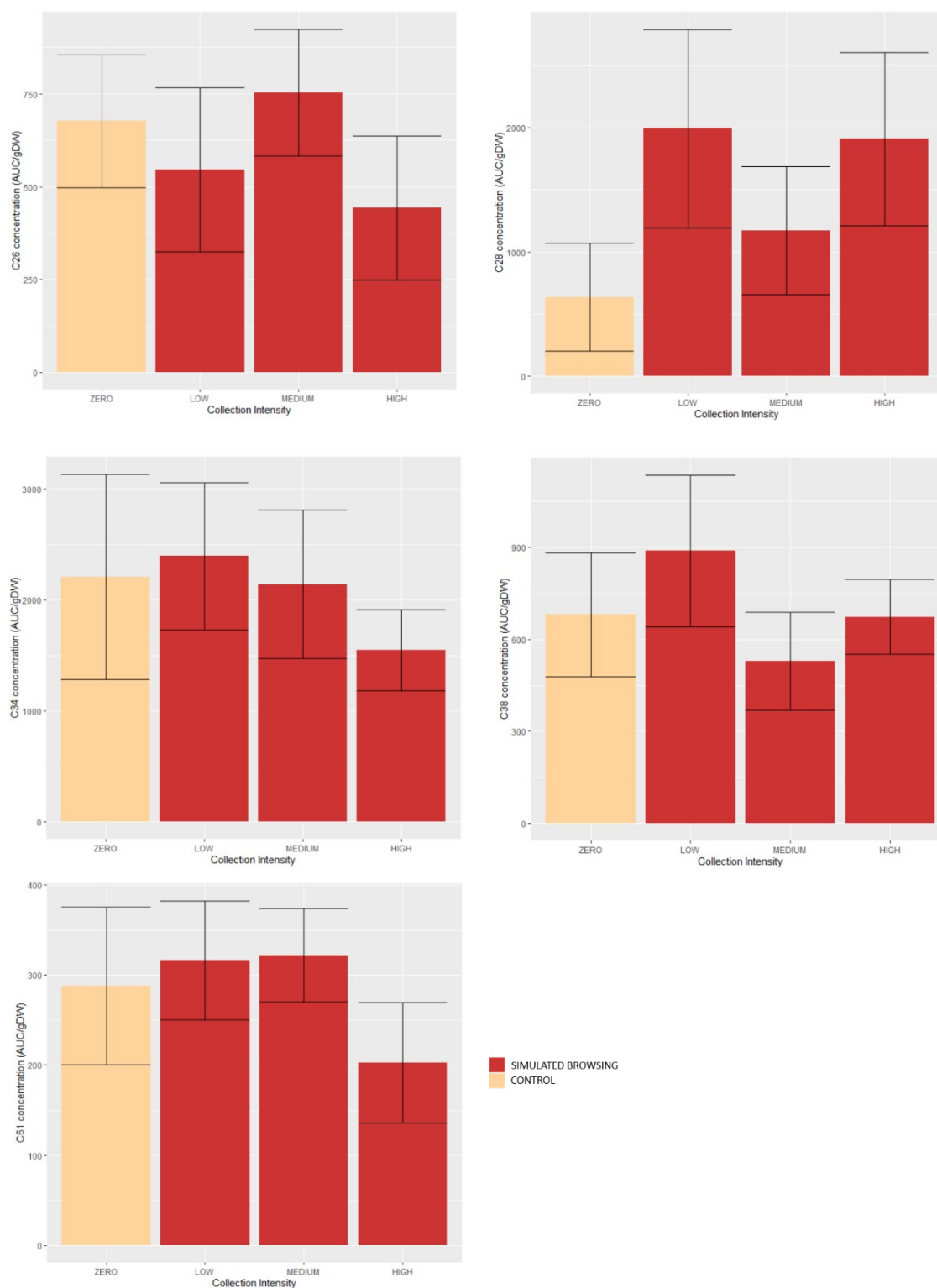


**Figure 1.14. Mean monoterpene concentrations (AUC/gDW) for the final compounds of interest when comparing across the varying levels of collection intensity for plants at 144 hr following the first simulated browsed event. Each bar graph has associated standard error bars.**

CHAPTER TWO: APPLYING KNOWLEDGE OF PLANT INDUCED DEFENSE TO  
ECOSYSTEM MANAGEMENT, AGRICULTURE, AND PHARMACOLOGY  
THROUGH USE-INSPIRED RESEARCH IN CHEMISTRY

The underlying mechanisms of plant communication at multiple levels are vital to understanding how organisms and ecosystems are linked. For example, the volatile communication of willow trees (*Salix eriocarpa*) is involved in the attraction of the natural predator ladybird (*Aiolocaria hexaspilota*) when damaged by a willow leaf beetle (*Plagioderia versicolora*), demonstrating a tritrophic interaction (Yoneya and Takabayashi 2013). However, uncovering these communication mechanisms that control these different levels of ecosystem interactions has yet to be fully investigated across various habitats and species (Aartsma et al. 2017, Takabayashi 2022). There are thousands of new plant species discovered every year, each with unique mechanisms by which they interact with other organisms to shape their survival (Christenhusz and Byng 2016). Simultaneously, we are losing species in threatened ecosystems such as the sagebrush steppe (Reisner et al. 2013), amazon rainforests (Codato et al. 2019), tropical ecosystems (Noh et al. 2020), and coral reefs (Mumby and Steneck 2008) that are reliant on chemical signals. The lack of knowledge of plant communication throughout an ecosystem is problematic because these chemical messages are what influence the responses of other organisms. Uncovering communication mechanisms in diverse ecosystems would help provide knowledge of the diversity that exists in plant systems by elucidating the multiple specific responses and chemicals for different organisms across

trophic levels. Chemical signals are not only used to map the distribution of new and existing species (Li et al. 2014, Olsoy et al. 2020), but also to predict interactions with other organisms (Kost and Heil 2006, Ninkovic et al. 2016). To uncover these communication mechanisms, chemicals must be monitored over time, across landscapes, and when exposed to different biotic and abiotic factors. For example, studies that investigate the communication dynamics of plants when exposed to herbivore damage (Chapter 1) lay the foundation for uncovering which chemicals are most likely to contribute to the interactions observed between sagebrush and sage-grouse and how these organisms and their interactions are impacted.

To understand how chemistry mediates interactions between organisms of interest in other fields and systems, applying the approach of a time course could be used to investigate the full chemical profile and the changes observed (Heil and Karban 2010, Clavijo McCormick et al. 2014, Bouwmeester et al. 2019). Detecting dynamics in chemicals would help identify how plants are able to communicate in specific environments and how chemical signaling in response to biotic or abiotic stimuli differs across plant taxa. Advances in detection technology allow chemical interactions to be investigated across larger spatial areas and time. For example, unmanned aerial systems have been used to map the different chemotypes in plants across space by linking phytochemical measurements in the field to sagebrush classification through machine learning and object based image analysis of shrub structural features (Olsoy et al. 2020). Gas chromatography has been used to examine the changes in chemical profiles across time (Lavagnini and Magno 2007, Clavijo McCormick 2016). We propose that a better understanding of the diversity and dynamics of chemicals in native and non-model plants

will benefit natural resources management, agriculture, and pharmacology through use-inspired research in chemistry.

Understanding how plants respond to damage by either herbivores or environmental conditions can inform how we manage ecosystems after disturbances (Koricheva 2002, Neilson et al. 2013, Veblen et al. 2015). For example, the chemical communication among successional plant communities arising after habitats are altered by abiotic disturbance, such as wildfires or floods, or by human decisions such as logging or conifer removal (Davies et al. 2012, Inderjit et al. 2017), may be asynchronous or disrupted and could influence the rate at which environments recover back to their original state (Huxel and Hastings 1999). In addition, chemical communication and the plasticity of chemicals that influence foraging of herbivores may depend on gene by environment conditions (Jaeger et al. 2016) that could influence the success of vegetative recovery by organizations such as the U.S. Fish and Wildlife Service and the Bureau of Land Management (BLM). These organizations reseed areas with key plant species that support the environment without knowing how chemical profiles that influence trophic interactions will respond to plant genotypes interacting with the local environment. For example, the BLM applied a suite of management responses to the 2015 Soda Fire in the sagebrush steppe along southern Idaho and eastern Oregon that primarily consisted of vegetation restoration through sagebrush reseedling of 3,637 average seedlings per acre over the 279,000 acres that were burned (Germino et al. 2022). Additional treatments included reseedling of other shrubs, forbs, and grasses and preemergent spraying of herbicide (Germino et al. 2022). This effort is consistent with other studies that reseeded disturbed areas with 0.25 pounds per acre of sagebrush seedlings after fire (Meyer and

Warren 2015, Grant-Hoffman and Plank 2021). In many of the historical reseeded efforts, seeds from plants adapted to the local environment are not used and instead randomly selected seeds from other areas within a seed bank are used (Shaw et al. 2005). The relatively low recovery of sagebrush after fires (Baker 2006) may have to do with the use of plants that are not locally adapted (Mahood and Balch 2019).

We propose that understanding complex chemical signals between both local and foreign seedlings may improve recovery. Specifically, understanding which plants respond fastest or more specifically to biotic and abiotic disturbances of a specific habitat could be used to more accurately determine which subspecies would be best chemically suited for a disturbed area to help the surrounding ecosystem recover (Kessler and Halitschke 2007, Moreira et al. 2015). Evidence that plants communicate better with closer relatives of the same subspecies (Karban et al. 2006, Heil and Karban 2010, Kigathi et al. 2013) could be used to identify chemotypes that are similar and allow for more precise decision making for reseeded actions and improve restoration efforts with plants of the same or similar chemotypes. Identifying which non-conspecifics eavesdrop on the emissions of other plants (Karban and Maron 2002, Karban et al. 2003, Karban 2011) could be used to help increase the adaptive resistance to herbivores. Identifying which chemical dialect neighboring plants respond best to (Karban et al. 2014, 2016) could be used to better reestablish an area with chemical dialects that are more locally adapted. Moreover, understanding the demographic differences of key plant species in their induced defense patterns in local communities compared to common garden experiments could prove beneficial in explaining variations in plant communities (Chaney et al. 2017, Germino et al. 2019, Zaiats et al. 2022). Application of these

approaches would help reestablish disturbed areas by using knowledge of how plants across different systems and populations are responding in different ways to various stressors, allowing for better management decisions on which plants may be better adapted to a specific area (Agrell et al. 2003, Clavijo McCormick 2016).

Identifying which PSMs change in response to herbivory and serve to deter future herbivores can prove useful in the field of agriculture (Kaplan and Lewis 2015, Brzozowski and Mazourek 2018). Specifically, identifying which PSMs contribute most to a plant's defensive capabilities could result in discovery and production of natural pesticides that could be applied to crops to deter herbaceous insects (Gish et al. 2015, Aartsma et al. 2017). Plant-derived pesticides could replace artificial herbicides or pesticides that can have negative effects on both the plant and the consumer (Altman and Campbell 1977, Souto et al. 2021). Volatile PSMs that are identified after damage could be used to attract natural predators from the surrounding environment to consume the herbivores causing damage (Peñaflor and Bento 2013). Intentional emission of specific PSMs could also be used as a method that naturally triggers induced defense mechanisms of plants (Brilli et al. 2019). For example, the volatile thujone from *Artemisia absinthium* L. (Asteraceae) plants offers a potential source of natural herbicide or pesticide that could be applied to an entire agricultural area (Höld et al. 2000, Souto et al. 2021). For all of these potential applications of defensive PSMs, the size of the area where the PSM would be applied must be considered. In predator-prey population simulations of natural chemical defenses of crops, it was found that larger areas of application of a chemical that attracts predators decreased the actual benefit of the applied chemical because predators could not properly cover the distances required to find the prey (Kaplan and

Lewis 2015). It also needs to be ensured that natural chemicals are not overused to reduce the potential of local predators becoming desensitized to chemical signals due to not receiving prey as a reinforcement (Glinwood et al. 2011, Kaplan and Lewis 2015). Environment conditions such as wind or rain should also be considered when applying natural chemicals because these factors may negate the effects of volatile chemicals (Murlis et al. 2000, Beyaert and Hilker 2014, Gish et al. 2015). In addition, PSM application at the agriculture-native landscape boundary might impact the interactions between native plants, herbivores, and predators through disrupting the natural balance among these organisms, driving more predators towards the agricultural environment rather than in their native area (Akter et al. 2018).

Finally, understanding the patterns of induced PSMs can open up the possibility of discovering novel natural products in plants that are most likely to have biological properties that could be used for pharmaceutical purposes (Kabera et al. 2014, Lautié et al. 2020). Many chemicals detected in plants do not have a known function, but could have pharmacological activity (Reumann et al. 2007, Dudareva et al. 2013). For example, a diterpenoid found naturally in yew species (*Taxus* spp.) is a drug that treats many types of cancer including breast, ovarian, and lung cancer (Patel 1998, Wang and Wu 2005). In addition, the yield of diterpenoids from yew plants can be increased by increasing the amount of water stress (Hoffman et al. 1999), decreasing shade intensity (FengJian et al. 2009), limiting the amount of damage to the plant tissue (Egan et al. 1996), and placing post-harvest containment samples in cold storage (Zhao et al. 2006), indicating the value of understanding changes in chemistry in plants responding to abiotic and biotic stressors. It is worth investigating if the monoterpenes found in this study or similar studies benefit

not only the plant of interest, but also have other biological targets for potential pharmaceutical use. Finally, identifying the biotic and abiotic conditions that maximize induction of chemicals could support methods that increase the yield of bioactive chemicals in plants prior to development of other forms of biosynthesis (Yukimune et al. 1996). For example, the yield of the anti-malaria drug artemisinin from sweet wormwood (*Artemisia annua*) increased following mechanical wounding on the plant tissue while also inducing several key genes in the biosynthesis pathway of artemisinin (Liu et al. 2010).

We propose several steps that could be used to apply knowledge of induced defense to improve restoration outcomes, benefit pest management in agriculture, and advance discovery and use of natural products for human health. First, better distribution maps of distinct chemotypes before disturbance to identify related and diverse taxonomic groups (Jaeger et al. 2016). For example, use of unmanned aerial systems could provide more accurate and extensive maps of chemically distinct plants across an entire landscape to better understand specific regional forage quality (Olsoy et al. 2020). Incorporating near-infrared spectroscopy (NIRS) could also assist in detecting different plant species, different chemical phenotypes among species, different populations of closely related species or subspecies, and various plant phenologies to gain a more accurate assessment of the chemotypic distribution across a landscape (Robb et al. 2022). For example, NIRS and unmanned aerial systems have been implemented in the study of both wheat (*Triticum* spp.) and poplar (*Populus* spp.), helping assess the nutritive and chemical qualities (Garnsworthy et al. 2000, Mazurek et al. 2022), detect and predict complex traits (Rincent et al. 2018), and classify different subtypes of each species (Rincent et al.

2018, Spoladore et al. 2021). Second, the approaches used to analyze the data obtained from gas chromatography (Chapter 1) can be applied and modified where needed for other systems other than the sagebrush and sage-grouse interaction in the winter season investigated in this study. The experimental design could easily be adapted to other plants of interest, the response of other herbivore browsing styles in timing or the manner in which damage occurs, how often collections are taken, in a variety of different environmental systems, or during different times of the year. The overall goal of any of these approaches should be to determine if the plants of interest are chemically stable or responding dynamically when exposed to different biotic and abiotic stressors. This information could be used for ecosystem management by allowing the detection of chemical plasticity for more strategic collection and reseeded that may improve restoration efforts to help the surrounding ecosystem recover. For agriculture, this knowledge could provide insight into how the size of the area where the PSM is applied can impact the desired response strength with secondary consequences of reducing predators to the native landscape. The discovery of chemicals with the most bioactivity could be better understood along with how to best simulate the biotic and abiotic conditions to maximize yield in cultivars and in culture for pharmaceutical use. However, none of these potential applications for induced defense chemistry are possible without conservation of diverse chemicals in native non-model organisms. Conservation of biodiversity is the first steps necessary to both identify the diversity of chemicals in plants and assess their dynamics.

## References

- Aartsma, Y., F. J. J. A. Bianchi, W. van der Werf, E. H. Poelman, and M. Dicke. 2017. Herbivore-induced plant volatiles and tritrophic interactions across spatial scales. *New Phytologist* 216:1054–1063.
- Agrell, J., W. Oleszek, A. Stochmal, M. Olsen, and P. Anderson. 2003. Herbivore-induced responses in alfalfa (*Medicago sativa*). *Journal of Chemical Ecology* 29:303–320.
- Akter, M. S., S. S. Siddique, R. Momotaz, M. Arifunnahar, K. M. Alam, and S. J. Mohiuddin. 2018. Biological control of insect pests of agricultural crops through habitat management was discussed. *Journal of Agricultural Chemistry and Environment* 8:1–13.
- Altman, J., and C. L. Campbell. 1977. Effect of herbicides on plant diseases. *Annual Review of Phytopathology* 15:361–385.
- Baker, W. L. 2006. Fire and restoration of sagebrush ecosystems. *Wildlife Society Bulletin* 34:177–185.
- Beyaert, I., and M. Hilker. 2014. Plant odour plumes as mediators of plant–insect interactions. *Biological Reviews* 89:68–81.
- Bouwmeester, H., R. C. Schuurink, P. M. Bleeker, and F. Schiestl. 2019. The role of volatiles in plant communication. *The Plant Journal* 100:892–907.
- Brilli, F., F. Loreto, and I. Baccelli. 2019. Exploiting plant volatile organic compounds (VOCs) in agriculture to improve sustainable defense strategies and productivity of crops. *Frontiers in Plant Science* 10:1–8.
- Brzozowski, L., and M. Mazourek. 2018. A sustainable agricultural future relies on the transition to organic agroecological pest management. *Sustainability* 10:1–25.
- Chaney, L., B. A. Richardson, and M. J. Germino. 2017. Climate drives adaptive genetic responses associated with survival in big sagebrush (*Artemisia tridentata*). *Evolutionary Applications* 10:313–322.

- Christenhusz, M. J. M., and J. W. Byng. 2016. The number of known plants species in the world and its annual increase. *Phytotaxa* 261:201–217.
- Clavijo McCormick, A. 2016. Can plant–natural enemy communication withstand disruption by biotic and abiotic factors? *Ecology and Evolution* 6:8569–8582.
- Clavijo McCormick, A., J. Gershenzon, and S. B. Unsicker. 2014. Little peaks with big effects: Establishing the role of minor plant volatiles in plant–insect interactions. *Plant, Cell & Environment* 37:1836–1844.
- Codato, D., S. E. Pappalardo, A. Diantini, F. Ferrarese, F. Gianoli, and M. De Marchi. 2019. Oil production, biodiversity conservation and indigenous territories: Towards geographical criteria for unburnable carbon areas in the Amazon rainforest. *Applied Geography* 102:28–38.
- Davies, G. M., J. D. Bakker, E. Dettweiler-Robinson, P. W. Dunwiddie, S. A. Hall, J. Downs, and J. Evans. 2012. Trajectories of change in sagebrush steppe vegetation communities in relation to multiple wildfires. *Ecological Applications* 22:1562–1577.
- Dudareva, N., A. Klempien, J. K. Muhlemann, and I. Kaplan. 2013. Biosynthesis, function and metabolic engineering of plant volatile organic compounds. *New Phytologist* 198:16–32.
- Egan, T. P., N. D. Danielson, and D. L. Gorchov. 1996. Effects of wounding on taxol and baccatin III levels in *Taxus media* cv Hicksii. *Ohio Journal of Science* 96:41–44.
- FengJian, Y., Z. Rui, P. HaiHe, Z. XueKe, and Z. YuanGang. 2009. Seasonal dynamic of the yield of taxol in the branches and leaves of *Taxus chinensis* var. *mairei* with different shade intensities. *Bulletin of Botanical Research* 29:471–474.
- Garnsworthy, P. C., J. Wiseman, and K. Fegeros. 2000. Prediction of chemical, nutritive and agronomic characteristics of wheat by near infrared spectroscopy. *The Journal of Agricultural Science* 135:409–417.
- Germino, M. J., A. M. Moser, and A. R. Sands. 2019. Adaptive variation, including local adaptation, requires decades to become evident in common gardens. *Ecological Applications* 29:e01842.

- Germino, M. J., P. Torma, M. R. Fisk, and C. V. Applestein. 2022. Monitoring for adaptive management of burned sagebrush-steppe rangelands: Addressing variability and uncertainty on the 2015 Soda Megafire. *Rangelands* 44:99–110.
- Gish, M., C. M. De Moraes, and M. C. Mescher. 2015. Herbivore-induced plant volatiles in natural and agricultural ecosystems: open questions and future prospects. *Current Opinion in Insect Science* 9:1–6.
- Glinwood, R., E. Ahmed, E. Qvarfordt, and V. Ninkovic. 2011. Olfactory learning of plant genotypes by a polyphagous insect predator. *Oecologia* 166:637–647.
- Grant-Hoffman, M. N., and H. L. Plank. 2021. Practical postfire sagebrush shrub restoration techniques. *Rangeland Ecology & Management* 74:1–8.
- Heil, M., and R. Karban. 2010. Explaining evolution of plant communication by airborne signals. *Trends in Ecology & Evolution* 25:137–144.
- Hoffman, A., C. Shock, and E. Feibert. 1999. Taxane and ABA production in yew under different soil water regimes. *HortScience* 34:882–885.
- Höld, K. M., N. S. Sirisoma, T. Ikeda, T. Narahashi, and J. E. Casida. 2000.  $\alpha$ -Thujone (the active component of absinthe):  $\gamma$ -Aminobutyric acid type A receptor modulation and metabolic detoxification. *Proceedings of the National Academy of Sciences* 97:3826–3831.
- Huxel, G. R., and A. Hastings. 1999. Habitat loss, fragmentation, and restoration. *Restoration Ecology* 7:309–315.
- Inderjit, J. A. Catford, S. Kalisz, D. Simberloff, and D. A. Wardle. 2017. A framework for understanding human-driven vegetation change. *Oikos* 126:1687–1698.
- Jaeger, D. M., J. B. Runyon, and B. A. Richardson. 2016. Signals of speciation: Volatile organic compounds resolve closely related sagebrush taxa, suggesting their importance in evolution. *New Phytologist* 211:1393–1401.
- Kabera, J. N., E. Semana, A. R. Mussa, and X. He. 2014. Plant secondary metabolites: Biosynthesis, classification, function and pharmacological properties. *Journal of Pharmacy and Pharmacology* 2:377–392.

- Kaplan, I., and D. Lewis. 2015. What happens when crops are turned on? Simulating constitutive volatiles for tritrophic pest suppression across an agricultural landscape. *Pest Management Science* 71:139–150.
- Karban, R. 2011. The ecology and evolution of induced resistance against herbivores. *Functional Ecology* 25:339–347.
- Karban, R., and J. Maron. 2002. The fitness consequences of interspecific eavesdropping between plants. *Ecology* 83:1209–1213.
- Karban, R., J. Maron, G. W. Felton, G. Ervin, and H. Eichenseer. 2003. Herbivore damage to sagebrush induces resistance in wild tobacco: evidence for eavesdropping between plants. *Oikos* 100:325–332.
- Karban, R., K. Shiojiri, M. Huntzinger, and A. C. McCall. 2006. Damage-induced resistance in sagebrush: Volatiles are key to intra- and interplant communication. *Ecology* 87:922–930.
- Karban, R., W. C. Wetzel, K. Shiojiri, S. Ishizaki, S. R. Ramirez, and J. D. Blande. 2014. Deciphering the language of plant communication: volatile chemotypes of sagebrush. *New Phytologist* 204:380–385.
- Karban, R., W. C. Wetzel, K. Shiojiri, E. Pezzola, and J. D. Blande. 2016. Geographic dialects in volatile communication between sagebrush individuals. *Ecology* 97:2917–2924.
- Kessler, A., and R. Halitschke. 2007. Specificity and complexity: the impact of herbivore-induced plant responses on arthropod community structure. *Current Opinion in Plant Biology* 10:409–414.
- Kigathi, R. N., W. W. Weisser, D. Veit, J. Gershenson, and S. B. Unsicker. 2013. Plants suppress their emission of volatiles when growing with conspecifics. *Journal of Chemical Ecology* 39:537–545.
- Koricheva, J. 2002. Meta-analysis of sources of variation in fitness costs of plant antiherbivore defenses. *Ecology* 83:176–190.

- Kost, C., and M. Heil. 2006. Herbivore-induced plant volatiles induce an indirect defence in neighbouring plants. *Journal of Ecology* 94:619–628.
- Lautié, E., O. Russo, P. Ducrot, and J. A. Boutin. 2020. Unraveling plant natural chemical diversity for drug discovery purposes. *Frontiers in Pharmacology* 11:1–37.
- Lavagnini, I., and F. Magno. 2007. A statistical overview on univariate calibration, inverse regression, and detection limits: Application to gas chromatography/mass spectrometry technique. *Mass Spectrometry Reviews* 26:1–18.
- Li, M., Q. Zhang, D. G. Streets, K. B. He, Y. F. Cheng, L. K. Emmons, H. Huo, S. C. Kang, Z. Lu, M. Shao, H. Su, X. Yu, and Y. Zhang. 2014. Mapping Asian anthropogenic emissions of non-methane volatile organic compounds to multiple chemical mechanisms. *Atmospheric Chemistry and Physics* 14:5617–5638.
- Liu, D., L. Zhang, C. Li, K. Yang, Y. Wang, X. Sun, and K. Tang. 2010. Effect of wounding on gene expression involved in artemisinin biosynthesis and artemisinin production in *Artemisia annua*. *Russian Journal of Plant Physiology* 57:882–886.
- Mahood, A. L., and J. K. Balch. 2019. Repeated fires reduce plant diversity in low-elevation Wyoming big sagebrush ecosystems (1984–2014). *Ecosphere* 10:e02591.
- Mazurek, S., M. Włodarczyk, S. Pielorz, P. Okińczyc, P. M. Kuś, G. Długosz, D. Vidal-Yañez, and R. Szostak. 2022. Quantification of salicylates and flavonoids in poplar bark and leaves based on IR, NIR, and Raman spectra. *Molecules* 27:3954.
- Meyer, S. E., and T. W. Warren. 2015. Seeding big sagebrush successfully on Intermountain rangelands. Great Basin Factsheet Series Number 10. Sage Grouse Initiative. 5 p. Online: <http://www.sagegrouseinitiative.com/seeding-big-sagebrush-successfully-on-intermountain-rangelands/>.

- Moreira, X., L. Abdala-Roberts, J. Hernández-Cumplido, M. A. C. Cuny, G. Glauser, and B. Benrey. 2015. Specificity of induced defenses, growth, and reproduction in lima bean (*Phaseolus lunatus*) in response to multispecies herbivory. *American Journal of Botany* 102:1300–1308.
- Mumby, P., and R. Steneck. 2008. Coral reef management and conservation in light of rapidly evolving ecological paradigms. *Trends in Ecology & Evolution* 23:555–563.
- Murlis, J., M. A. Willis, and R. T. Cardé. 2000. Spatial and temporal structures of pheromone plumes in fields and forests. *Physiological Entomology* 25:211–222.
- Neilson, E., J. Goodger, I. Woodrow, and B. Møller. 2013. Plant chemical defense: At what cost? *Trends in plant science* 18:250–258.
- Ninkovic, V., D. Markovic, and I. Dahlin. 2016. Decoding neighbour volatiles in preparation for future competition and implications for tritrophic interactions. *Perspectives in Plant Ecology, Evolution and Systematics* 23:11–17.
- Noh, J. K., C. Echeverria, J. Kleemann, H. Koo, C. Fürst, and P. Cuenca. 2020. Warning about conservation status of forest ecosystems in tropical Andes: National assessment based on IUCN criteria. *PLOS ONE* 15:e0237877.
- Olsoy, P. J., J. S. Forbey, L. A. Shipley, J. L. Rachlow, B. C. Robb, J. D. Nobler, and D. H. Thornton. 2020. Mapping foodscapes and sagebrush morphotypes with unmanned aerial systems for multiple herbivores. *Landscape Ecology* 35:921–936.
- Patel, R. N. 1998. Tour de paclitaxel: Biocatalysis for semisynthesis. *Annual Review of Microbiology* 52:361–395.
- Peñaflor, M. F. G. V., and J. M. S. Bento. 2013. Herbivore-induced plant volatiles to enhance biological control in agriculture. *Neotropical Entomology* 42:331–343.
- Reisner, M. D., J. B. Grace, D. A. Pyke, and P. S. Doescher. 2013. Conditions favouring *Bromus tectorum* dominance of endangered sagebrush steppe ecosystems. *Journal of Applied Ecology* 50:1039–1049.

- Reumann, S., L. Babujee, C. Ma, S. Wienkoop, T. Siemsen, G. E. Antonicelli, N. Rasche, F. Lüder, W. Weckwerth, and O. Jahn. 2007. Proteome analysis of *Arabidopsis* leaf peroxisomes reveals novel targeting peptides, metabolic pathways, and defense mechanisms. *The Plant Cell* 19:3170–3193.
- Rincent, R., J.-P. Charpentier, P. Faivre-Rampant, E. Paux, J. Le Gouis, C. Bastien, and V. Segura. 2018. Phenomic selection is a low-cost and high-throughput method based on indirect predictions: Proof of concept on wheat and poplar. *G3: Genes, Genomes, Genetics* 8:3961–3972.
- Robb, B. C., P. J. Olsoy, J. J. Mitchell, T. T. Caughlin, D. M. Delparte, S. J. Galla, M. R. Fremgen-Tarantino, J. D. Nobler, J. L. Rachlow, L. A. Shipley, and J. S. Forbey. 2022. Near-infrared spectroscopy aids ecological restoration by classifying variation of taxonomy and phenology of a native shrub. *Restoration Ecology* 30:e13584.
- Shaw, N. L., A. M. DeBolt, R. Rosentreter, and S. B. Monsen. 2005. Reseeding big sagebrush: techniques and issues. Pages 99–108 *Sage-Grouse Habitat Restoration Symposium Proceedings*; 2001 June 4-7, Boise, ID. Boise, ID.
- Souto, A. L., M. Sylvestre, E. D. Tölke, J. F. Tavares, J. M. Barbosa-Filho, and G. Cebrián-Torrejón. 2021. Plant-derived pesticides as an alternative to pest management and sustainable agricultural production: Prospects, applications and challenges. *Molecules* 26:4835.
- Spoladore, S. F., M. Brígida dos Santos Scholz, and E. Bona. 2021. Genotypic classification of wheat using near-infrared spectroscopy and PLS-DA. *Applied Food Research* 1:100019.
- Takabayashi, J. 2022. Herbivory-induced plant volatiles mediate multitrophic relationships in ecosystems. *Plant and Cell Physiology* 63:1344–1355.
- Veblen, K. E., K. C. Nehring, C. M. McGlone, and M. E. Ritchie. 2015. Contrasting effects of different mammalian herbivores on sagebrush plant communities. *PLOS ONE* 10:e0118016.

- Wang, J. W., and J. Y. Wu. 2005. Nitric oxide is involved in methyl jasmonate-induced defense responses and secondary metabolism activities of *Taxus* cells. *Plant and Cell Physiology* 46:923–930.
- Yoneya, K., and J. Takabayashi. 2013. Interaction–information networks mediated by plant volatiles: a case study on willow trees. *Journal of Plant Interactions* 8:197–202.
- Yukimune, Y., H. Tabata, Y. Higashi, and Y. Hara. 1996. Methyl jasmonate-induced overproduction of paclitaxel and baccatin III in *Taxus* cell suspension cultures. *Nature Biotechnology* 14:1129–1132.
- Zaiats, A., J. M. Requena-Mullor, M. J. Germino, J. S. Forbey, B. A. Richardson, and T. T. Caughlin. 2022. Spatial models can improve the experimental design of field-based transplant gardens by preventing bias due to neighborhood crowding. *Ecology and Evolution* 12:e9630.
- Zhao, C.-F., L.-J. Yu, Z. Liu, and Y.-P. Sun. 2006. The dynamic variation of several important taxane content in post-harvest *Taxus chinensis* clippings. *Journal of Asian Natural Products Research* 8:229–239.

APPENDIX A

**Original Sketch of Experimental Design**

The original sketch of the field experimental design demonstrating how each treatment and control plant were spatially selected and the approximate distances between them (Figure A.1). This is included to provide additional clarity for the setup for how collections were taken to create the different time points, treatment groups, and collection intensity levels through the paired plant design.

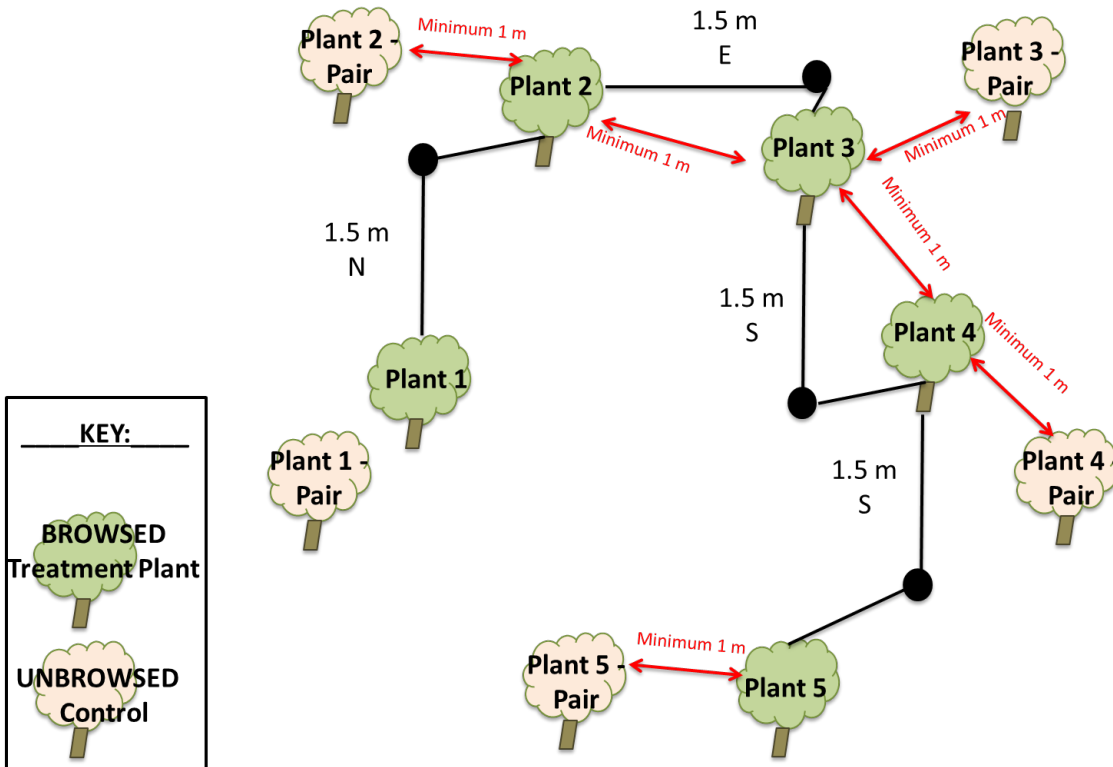


**Figure A.1.** Original sketch of the field experimental design showing the spatial extent by which plants were treated and how they were paired with control plants. Plant numbers match those in Table 1.1 and the overview layout of Figure 1.2.

## APPENDIX B

**Gas Chromatography Settings**

Concentrations of monoterpenes in sagebrush samples were quantified using a gas chromatograph (Agilent 6890N, Agilent Technologies; 5301 Stevens Creek Boulevard, Santa Clara, CA 95051, USA) with a headspace auto-sampler (Hewlett-Packard HP7694; 1501 Page Mill Road, Palo Alto, CA 94204, USA). One ml of headspace gas was injected into a J&W DB-5 capillary column (30m x 250 $\mu$ m x 0.25 $\mu$ m).

Headspace auto-sampler operating conditions were as follows: 100°C oven temperature, 110°C loop temperature, 120°C transfer line temperature, 20 min vial equilibrium time, 0.20 min pressurization time, 0.50 min loop fill time, 0.20 min loop equilibrium time, and a 0.50 min injection time.

Gas Chromatogram operating conditions were as follows: 250°C splitless injector temperature, 300°C flame ionization detector temperature, 40°C oven temperature for 2 min, then increasing 3°C/min to the temperature of 60°C, then increasing 5°C/min to the temperature of 120°C, then increasing 20°C/min to the temperature of 300°C, and held for 7 min at 300°C. Nitrogen was the make-up gas and helium was the carrier gas. The inlet pressure was set at 80 KPa with the flow rate of 1.0 mL/min (Nobler 2018).

## APPENDIX C

**Compound Inclusion, Exclusion, and Merging**

Compounds C1 and C2 received manual adjustment to merge the peaks together into C1 for all AUC values. The AUC values for each peak could not be separated in the samples that had only one peak being read. This merging of peaks was performed due to C1 and C2 being read as either one peak or two for each sample with nearly all samples possessing two peaks with the peak for C1 bleeding into the peak for C2 (Figure C.1).

Compounds C24 and C25 received manual adjustment to merge the peaks together into C24 (1,8-cineole) for all AUC values. The AUC values were being falsely separated into two peaks for C24 instead of as a single peak as indicated by manual review of the chromatograms (Figure C.2).

The appearance of C14 was investigated to determine that it needed to be excluded from the overall analyses. This was due to the questionable dilution of C14 into C15 in an “oil-can” shape in the chromatograms. It was determined that C14 appeared in random samples and run batches. C14 never occurred in blank runs or in standard cocktails which suggested that it was not a contaminant (Figure C.3).

The following figures of flow charts, chromatograms, PCAs, boxplots, and ANOVAs (Figures C.4 – C.10, Tables C.1 – C.3) were previously generated with C14 included in the analyzed compounds. The compound C14 needed to be excluded from the overall analyses due to the appearance of the peak diluting into C15 in an “oil-can” nature. It could not be determined if C14 was a true individual peak or an early elution of the sequential peak of C15. Analyses were previously conducted with the inclusion of C14 to attempt to account for the variation between the treatment groups, time points, and collection intensities. It was from these former analyses that it was determined that C14 should be excluded due to it supposedly accounting for the largest portion of the variation

within each subset. Due to its questionable appearance and nature in these analyses, it was concluded that excluding C14 was the best course of action for this study. Overall results for all PCA visualizations did not differ when C14 was excluded. Its exclusion did help to elucidate which compounds were contributing the most variation to the subsets and therefore which compounds to place focus on for analyses.

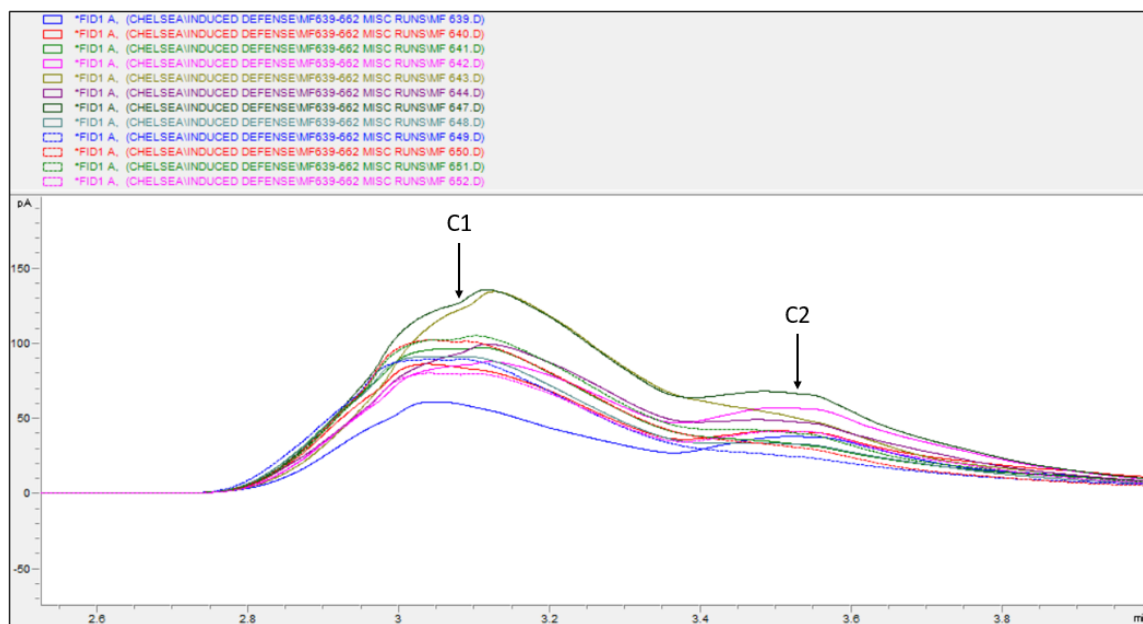


**Figure C.1.** Stacked chromatograms of randomly selected samples that contained either one or two peaks being recorded for AUC values of C1 and C2 (Table 1.2). C1 and C2 are indicated by their retention time (min). C1 is shown to constantly bleed into C2.

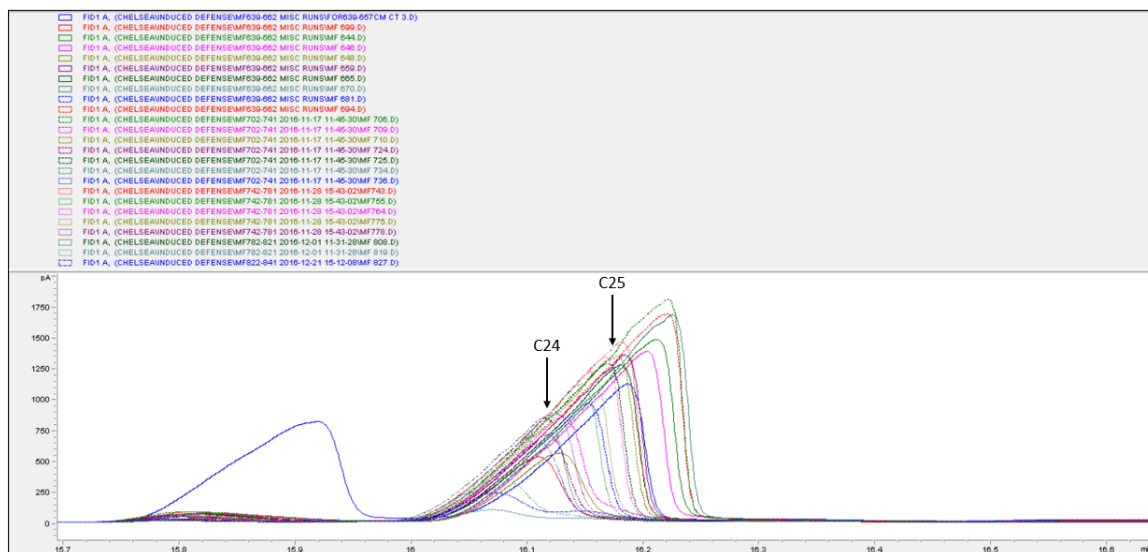


**Figure C.2.** Stacked chromatograms of randomly selected samples that contained either one or two peaks recorded for AUC values of C24 and C25 (Table 1.2). C24 and C25 are indicated by their retention time (min). The peak for C24 is shown to overlap the position for C25 due to its large peak size and range.

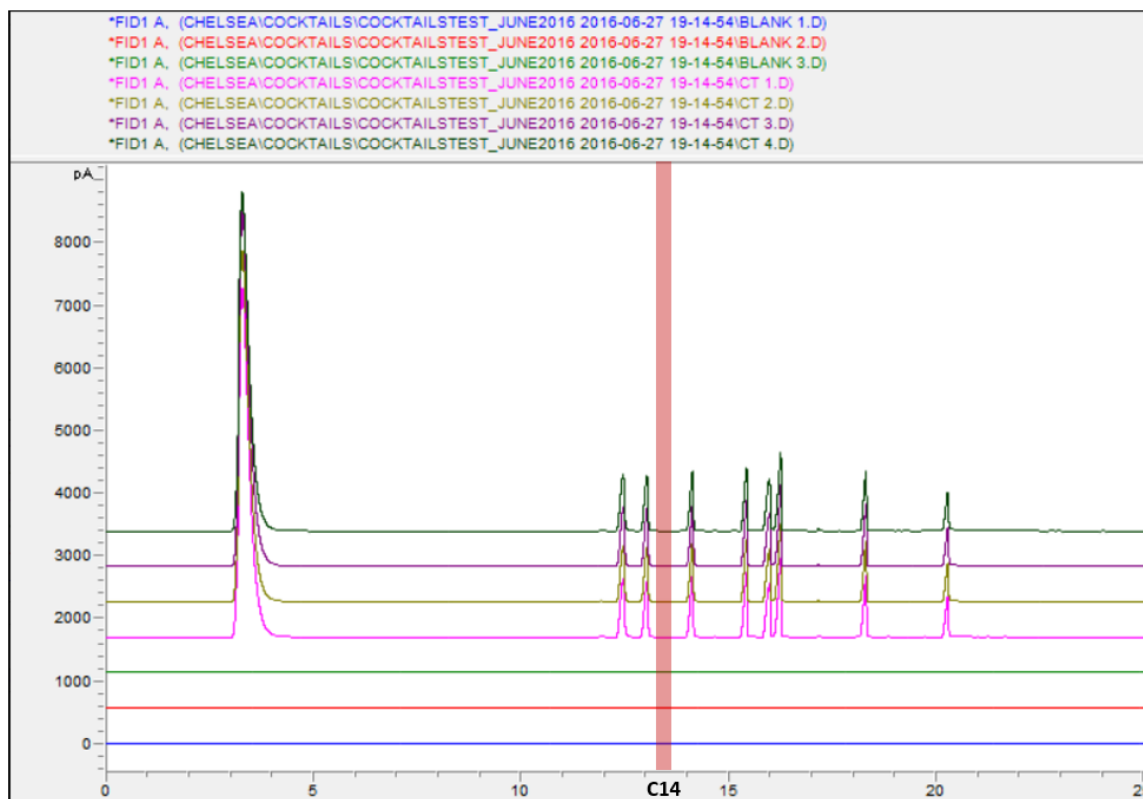


**Figure C.3. Representative chromatograms of monoterpene cocktail standard runs (top for chromatograms) and blanks (bottom 3 chromatograms). The red bar transecting each chromatogram at 13.62 min retention time indicates the location for C14 that appeared randomly throughout the samples with an “oil-can” shape (Figure 1.5, Figure C.4). C14 never occurred in any of the blank or standard cocktail runs suggesting it was not a contaminant.**

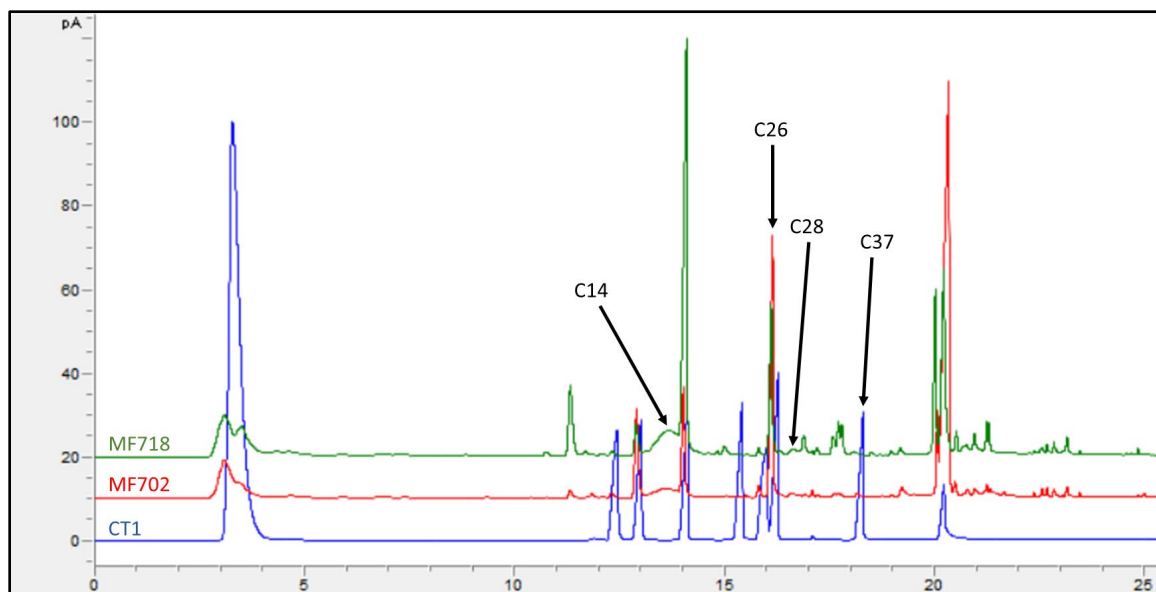


**Figure C.4.** Representative chromatograms of monoterpenes in sagebrush (*Artemisia tridentata* spp.) (top two lines) and the monoterpene cocktail standard (bottom line). The peaks represent the initial individual compounds with the relative abundance measured in area under the curve (AUC) with the corresponding retention time in minutes. The main compounds of interest are marked prior to C14 exclusion. Here the “oil-can” appearance of C14 (at 13.62 min) is clearly demonstrated.



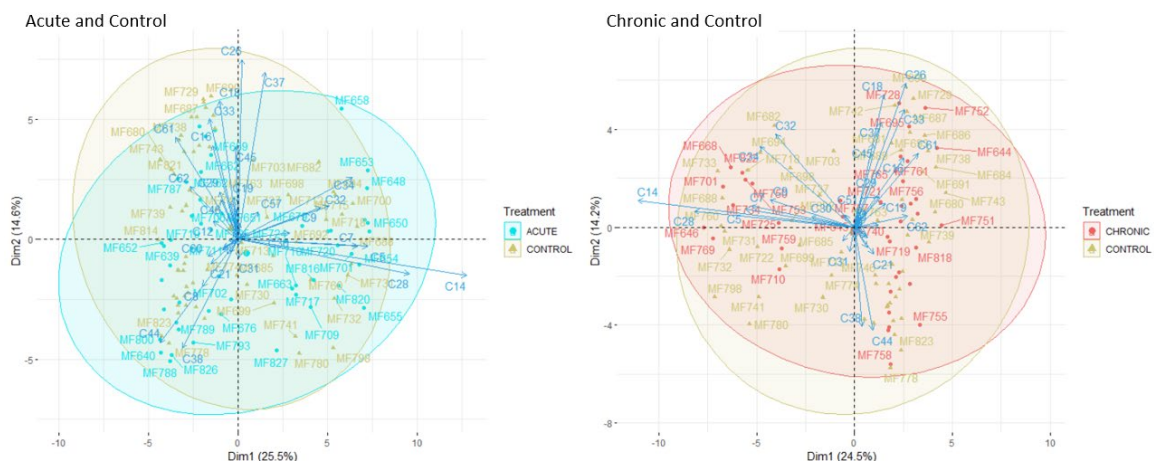


**Figure C.6.** PCAs generated for the *a)* control versus acute treatment for all time points and *b)* control versus chronic treatment for all time points using the calculated centered values with the inclusion of C14. The colored ellipses represent the different treatment groups present and where they fall across the different PC dimensions. The compounds are represented by the vectors of varying lengths with the longer vectors having a stronger influence on the variation among the samples within the treatment category. In each PCA, C14 is a strongly pulling vector.

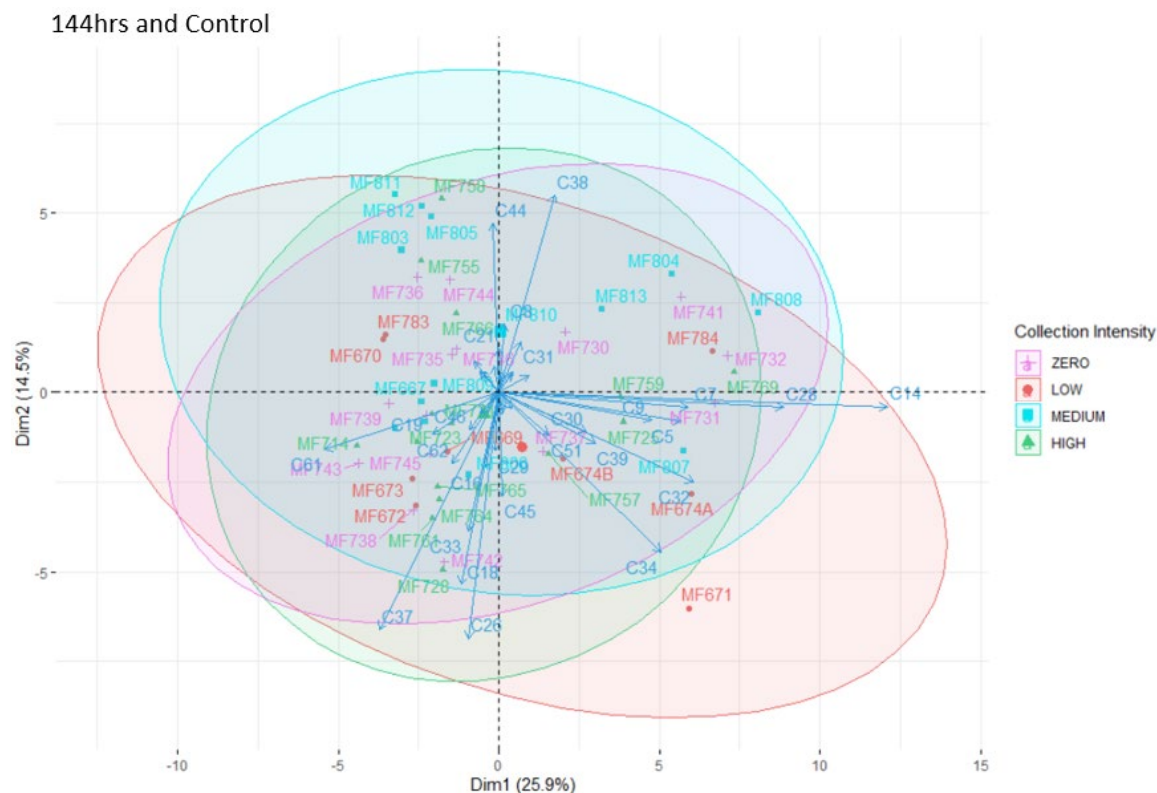


**Figure C.7** PCA generated for the different levels of collection intensity using the calculated centered values with the inclusion of C14. The colored ellipses represent the different levels of collection intensity (zero – high) and where they fall across the different PC dimensions. The compounds are represented by the vectors of varying lengths with the longer vectors having a stronger influence on the variation among the samples within the collection intensity category. In this PCA, C14 is a strongly pulling vector.



e.

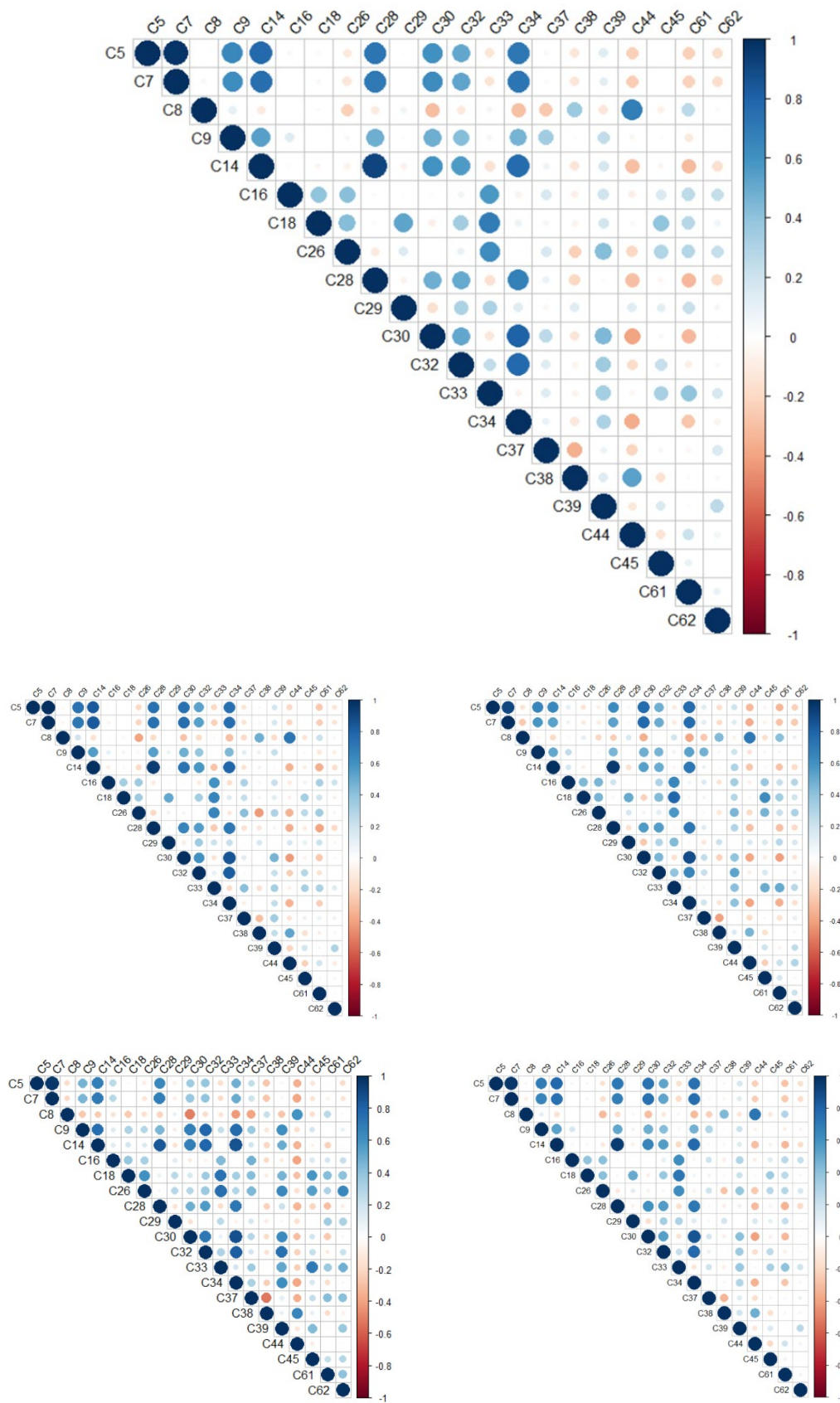
Chronic and Control		
Compound	PC1	PC2
C61	<b>0.170</b>	<b>0.206</b>
C62	<b>0.141</b>	0.030
C26	<b>0.137</b>	<b>0.403</b>
C33	<b>0.132</b>	<b>0.331</b>
C16	<b>0.132</b>	<b>0.194</b>
C32	<b>-0.210</b>	<b>0.261</b>
C9	<b>-0.225</b>	0.076
C34	<b>-0.253</b>	<b>0.226</b>
C7	<b>-0.275</b>	0.059
C5	<b>-0.292</b>	0.051
C28	<b>-0.427</b>	0.044
C14	<b>-0.578</b>	0.074
C18	0.077	<b>0.371</b>
C37	0.071	<b>0.294</b>
C45	0.049	<b>0.235</b>
C29	0.064	<b>0.158</b>
C38	0.020	<b>-0.278</b>
C44	0.048	<b>-0.289</b>

d.

Acute and Control		
Compound	PC1	PC2
C14	<b>0.559</b>	-0.088
C28	<b>0.420</b>	-0.083
C5	<b>0.317</b>	-0.017
C7	<b>0.292</b>	-0.017
C34	<b>0.279</b>	<b>0.150</b>
C32	<b>0.222</b>	0.081
C9	<b>0.201</b>	0.078
C38	<b>-0.136</b>	<b>-0.264</b>
C61	<b>-0.153</b>	<b>0.247</b>
C44	<b>-0.190</b>	<b>-0.250</b>
C26	0.010	<b>0.435</b>
C37	0.065	<b>0.405</b>
C18	-0.045	<b>0.335</b>
C33	-0.070	<b>0.292</b>
C16	-0.063	<b>0.228</b>
C45	-0.006	<b>0.224</b>

f.

144hrs and Control		
Compound	PC1	PC2
C14	<b>0.566</b>	-0.025
C28	<b>0.415</b>	-0.026
C32	<b>0.284</b>	<b>-0.156</b>
C7	<b>0.275</b>	-0.026
C5	<b>0.266</b>	-0.050
C34	<b>0.236</b>	<b>-0.278</b>
C9	<b>0.224</b>	-0.047
C39	<b>0.140</b>	-0.089
C37	<b>-0.175</b>	<b>-0.413</b>
C61	<b>-0.253</b>	-0.099
C38	0.081	<b>0.344</b>
C44	-0.009	<b>0.295</b>
C45	0.005	<b>-0.181</b>
C33	-0.044	<b>-0.242</b>
C18	-0.055	<b>-0.335</b>
C26	<b>-0.044</b>	<b>-0.429</b>



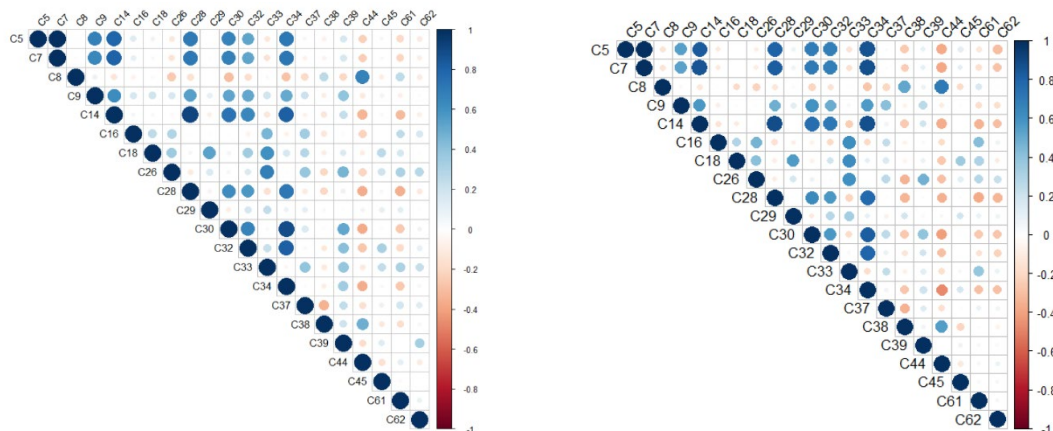


**Figure C.8.** Correlation matrices generated from the area under the curve per gram dry weight (AUC/gDW) values of the main vector loadings that made the cutoff threshold of  $\pm 0.3$  (see Table 1.3) with the inclusion of C14. The size of each circle corresponds to the strength of the correlation between  $-1.0$  and  $+1.0$  among the respective compounds while the color indicates either a positive (blue) or a negative (red) correlation. All compounds aside from the standards appeared in at least one of the PCA loading tables. The correlation matrices are creating through comparing *a)* all samples in the experiment, *b)* time points within control, *c)* time points within acute, *d)* time points within chronic, *e)* control versus acute, *f)* control versus chronic, and *g)* collection intensity.

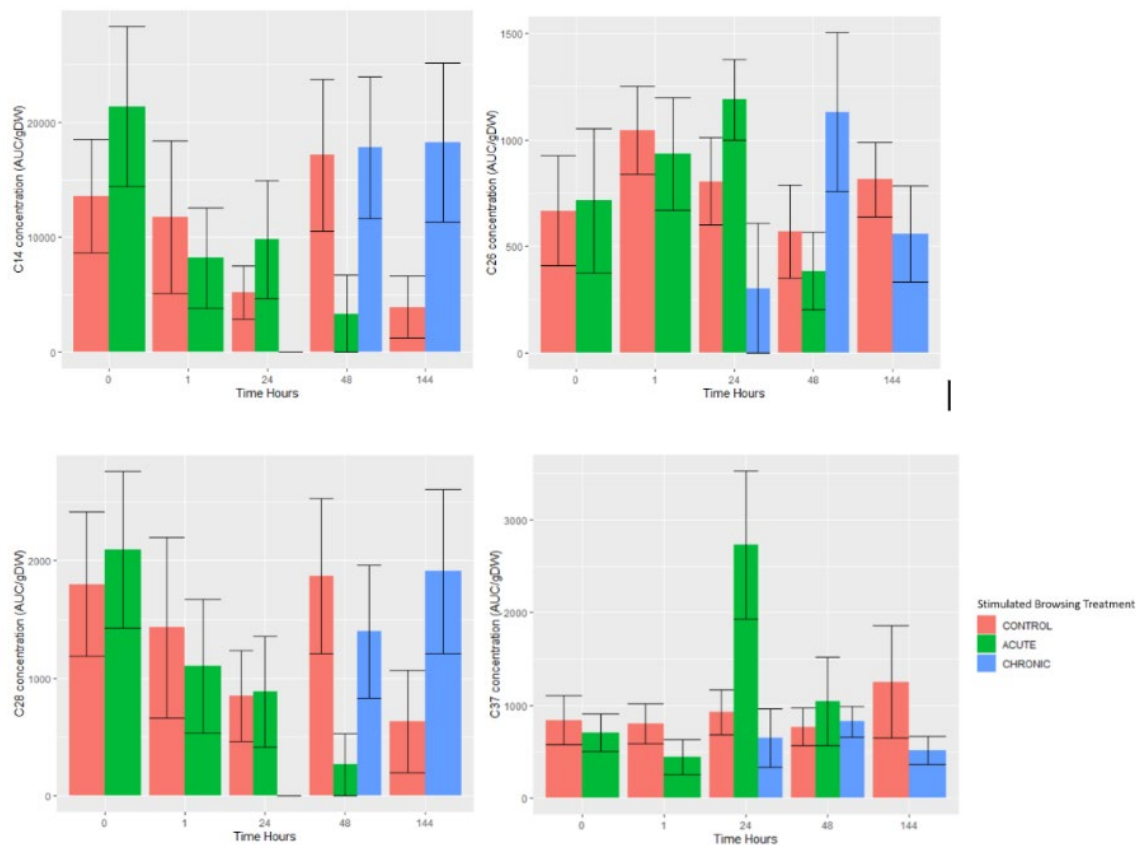


**Figure C.9.** Mean monoterpene concentrations (AUC/gDW) for the initial compounds of interest when comparing treatment groups across the time points (hours) after the first simulated browsing event. Each bar graph has associated standard error bars. These were generated using the four main compounds that displayed the highest vector loadings when C14 was included.

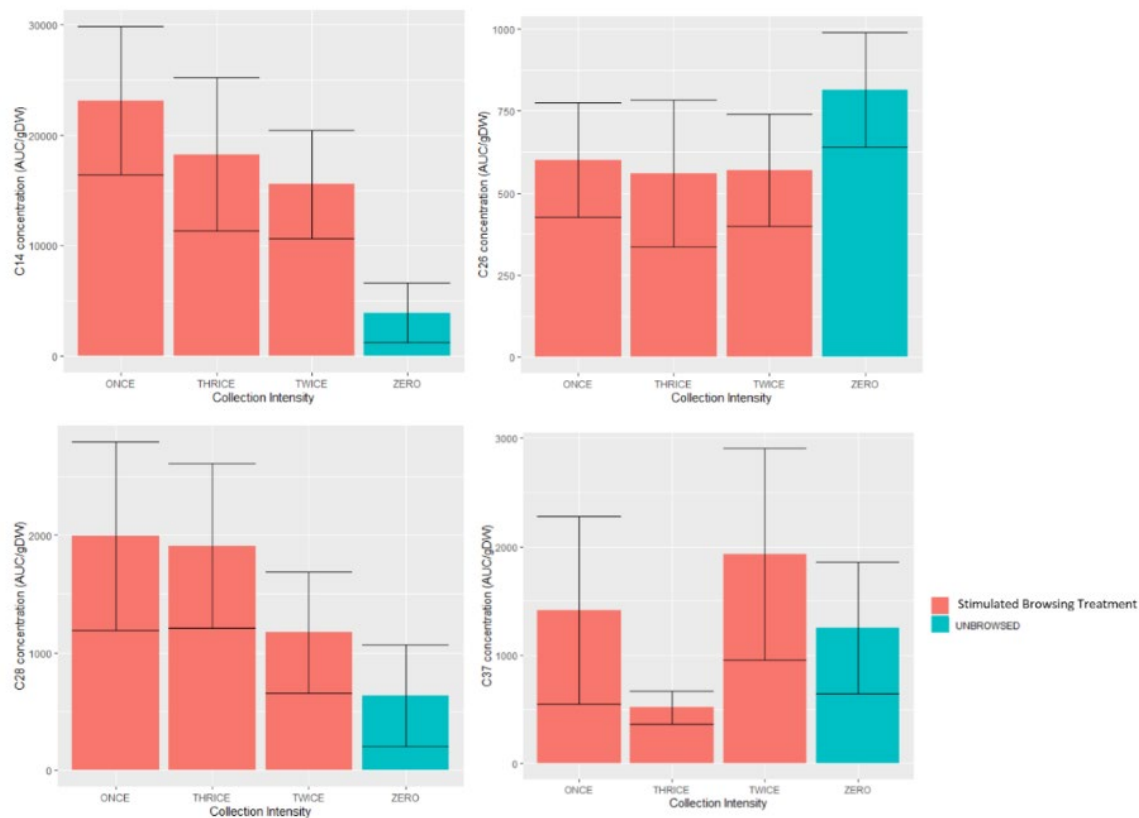


**Figure C.10. Mean monoterpene concentrations (AUC/gDW) for the initial compounds of interest when comparing treatment groups across the varying levels of collection intensity. Each bar graph has associated standard error bars. These were generated using the four main compounds that displayed the highest vector loadings when C14 was included.**

**Table C.2. Two-way ANOVA results for the initial compounds of interest identified from comparing treatment groups and time points. These were calculated when C14 was included in the analysis.**

Two-way ANOVA results for Figure 7					
Source of variation	<i>df</i>	Sum of Squares	MS	<i>F</i> ratio	<i>P</i> value
<b>C14</b>					
Treatment	2	4.55E+08	224535357	0.647	0.525
Time Hours	4	2.22E+09	555530730	1.58	0.183
Residuals	141	4.96E+10	351539094		
<b>C26</b>					
Treatment	2	3.42E+05	171217	0.241	0.786
Time Hours	4	2.12E+06	531147	0.749	0.56
Residuals	141	1.00E+08	709451		
<b>C28</b>					
Treatment	2	2.50E+06	125749	0.315	0.73
Time Hours	4	2.41E+07	6024132	1.516	0.201
Residuals	141	5.60E+08	3973241		
<b>C37</b>					
Treatment	2	8.72E+06	4360151	1.987	0.1409
Time Hours	4	2.02E+07	5047159	2.3	0.0617
Residuals	141	3.09E+08	2193958		
Significant Codes: 0 '****' 0.001 '***' 0.01 '**' 0.05 '*' 0.1 '.' 1 '' 1					

**Table C.3. One-way ANOVA results from the final compounds of interest from comparing the varying levels of collection intensity. These were calculated when C14 was included in the analysis.**

Two-way ANOVA results for Figure 8					
Source of variation	<i>df</i>	Sum of Squares	MS	<i>F</i> ratio	<i>P</i> value
<b>C14</b>					
Collection Intensity	3	2.57E+09	855871414	2.219	0.0974
Damage	1	4.93E+07	49278350	0.128	0.7223
Residuals	50	1.93E+10	385660090		
<b>C26</b>					
Collection Intensity	3	9.28E+05	309196	0.631	0.598
Damage	1	1.92E+05	192317	0.393	0.534
Residuals	50	2.45E+07	489830		
<b>C28</b>					
Collection Intensity	3	1.67E+07	5567232	1.17	0.33
Damage	1	1.64E+05	163605	0.034	0.854
Residuals	50	2.38E+08	4756503		
<b>C37</b>					
Collection Intensity	3	1.48E+07	4926168	0.794	0.503
Damage	1	5.38E+05	438192	0.071	0.791
Residuals	50	3.10E+08	6203084		
Significant Codes: 0 '****' 0.001 '***' 0.01 '**' 0.05 '.' 0.1 ' ' 1					

APPENDIX D

**Future Statistical Approaches**

Mixed linear models of PERMANOVAS that incorporate random effects to correct for correlated values will be used to compare AUC/gDW concentrations across time and treatment group for each final compound of influence. This analysis will be performed using the *lmer* function in the *lme4* package (Bates et al. 2015). To determine the statistical significance between the concentrations, Tukey's HSD post-hoc analysis will be performed.

To evaluate the effect of collection intensity at time 144 hr (T = 144 hr) of control and chronic treatment groups, alpha-diversity measurements will be calculated using the *diversity* function in the *vegan* package (Oksanen et al., 2020). The resulting alpha-diversity measurements will include the Simpson diversity index, Shannon diversity index, and Richness. To analyze these alpha-diversity measurements, linear mixed-effects models of each will be generated using the *lmer* function in the *lme4* package (Bates et al., 2015), with Site ID as a random effect to correct for correlated values. Beta-diversity measurements will be calculated to analyze the effect of collection intensity at time 144 hr (T = 144 hr) between the control and chronic to measure relatedness between groups.

A repeated measures analysis was not used for the approach for the repeated sample collection in this study because of the excluded batch 2 samples. This exclusion made it so that there was incomplete repeated data for each plant that did not allow for the appropriate statistical analyses. This is currently being remedied by rerunning the Batch 2 samples and comparing the AUC values to observe how much shift occurred between batches. The objective of this approach is to combine the newly aligned Batch 2 samples with the Batch 1 samples and then reanalyze chemicals of interest (Figures 1.13, 1.14) using a two-way repeated measures ANOVA where acute and chronic represent

treatment groups and monoterpene concentration at each time point is the repeated measure. Preliminary results of samples that were run repeatedly in Batch 1 and Batch 2 suggest high correlation and repeatability of AUC between batches (Figures D.1, D.2)

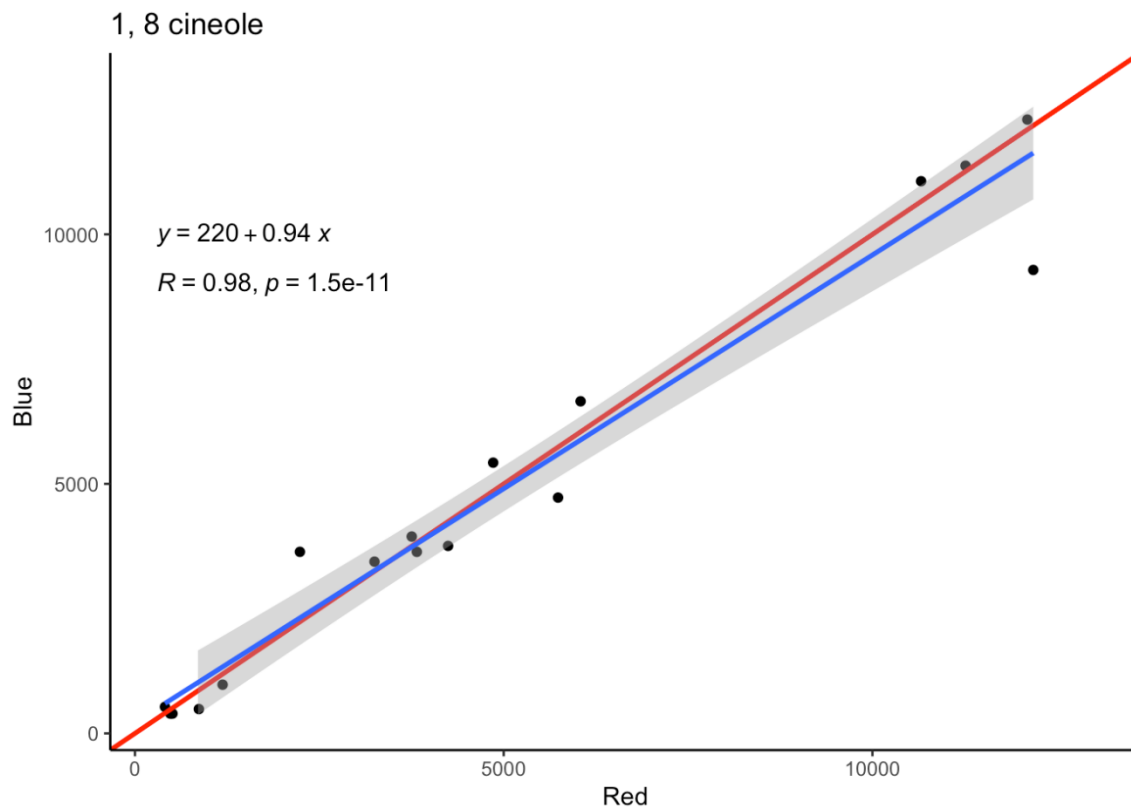


**Figure D.1.** Correlation plot of concentration (in area under the curve) for the monoterpene standard 1,8-cineole between Batch 1 (blue) and Batch 2 that occurred after recalibration of the gas chromatography machine (red) for the same 17 sagebrush samples.

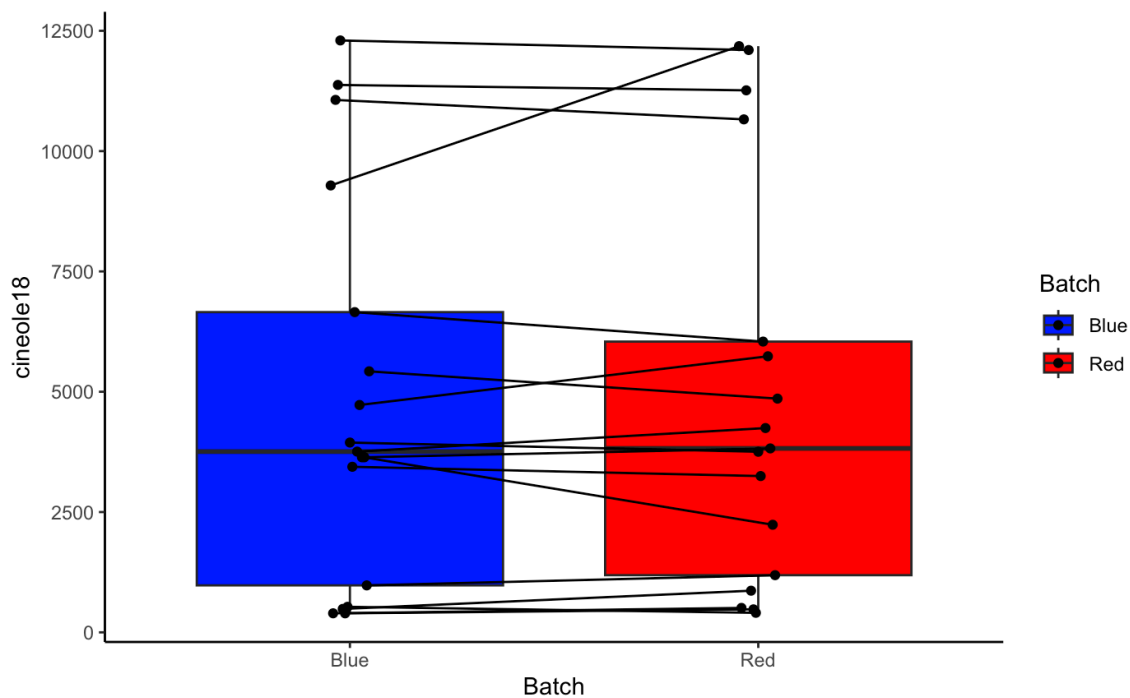


**Figure D.2.** Comparison of concentration (in area under the curve) for the monoterpene standard 1,8-cineole between Batch 1 (blue) and Batch 2 that occurred after recalibration of the gas chromatography machine (red) for the same 17 sagebrush samples. The repeat of each individual plant samples are connected between the two groups to show potential discrepancy.

APPENDIX E

**Correlation Matrices  $r^2$  Values for Each Treatment Group**

The correlation matrices for each of the subsetted treatment groups were further investigated for the  $r^2$  values between pairs of compounds. These correlations were filtered based on positive and negative  $r^2$  values. The following tables provide a visual representation of the three correlation matrices to better display the patterns being observed among the treatment groups. Any pair within any single treatment group with a correlated values  $r^2 > +/-0.4$  was included in additional analyses to compare strength of correlation among treatment groups (Table 1.4, 1.5, 1.6, 1.8). The sets of strongest positive and negative correlation clusters were determined by the strongest  $r^2$  values seen to appear in any one treatment group.







## APPENDIX F

**Boxplots of Subsetted Correlation Matrices  $r^2$  Values**

Boxplots of correlation  $r^2$  values among treatments where compounds were only included if at least one treatment had a compound correlations above  $\pm 0.4$  and for sets of the strongest positive and strongest negative correlation clusters based on the  $r^2$  values strengths (from Appendix F).

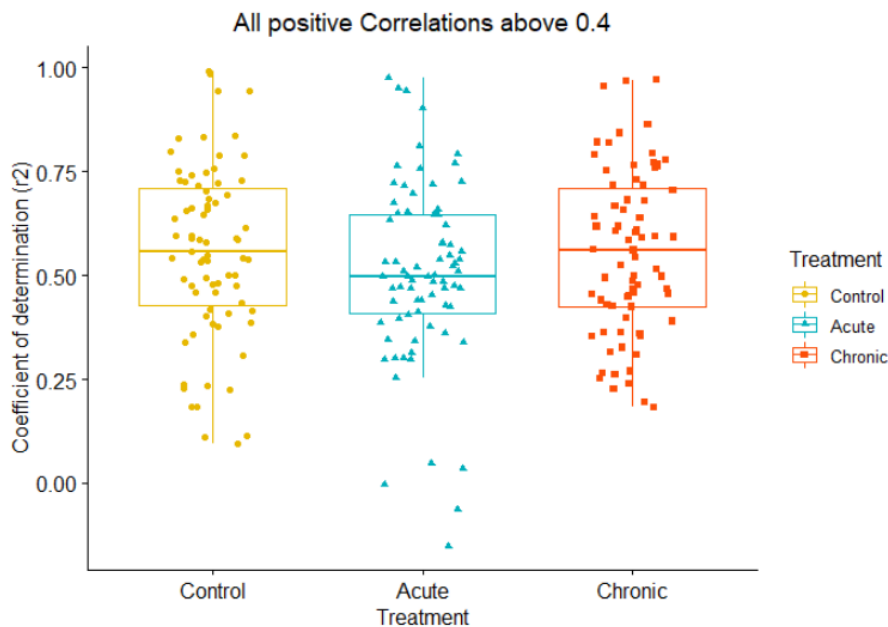


**Figure F.1. Boxplots of the positive correlation pairs for each treatment group where only pairs were included if at least one treatment group had an  $r^2 > 0.4$ . Each boxplot has an associated median and quartiles for each treatment group.**

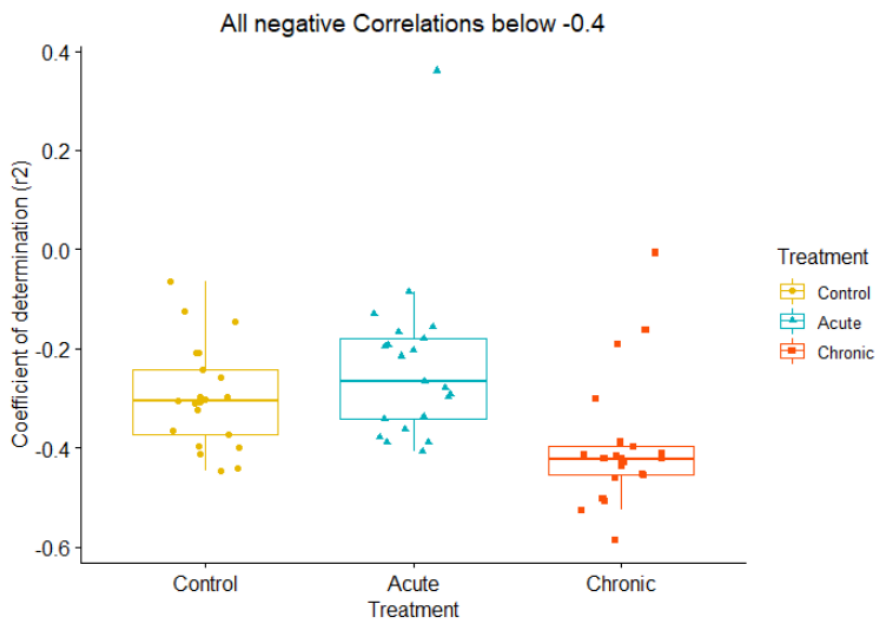


**Figure F.2. Boxplots of the negative correlation pairs for each treatment group where only pairs were included if at least one treatment group had an  $r^2 > -0.4$ . Each boxplot has an associated median and quartiles for each treatment group.**

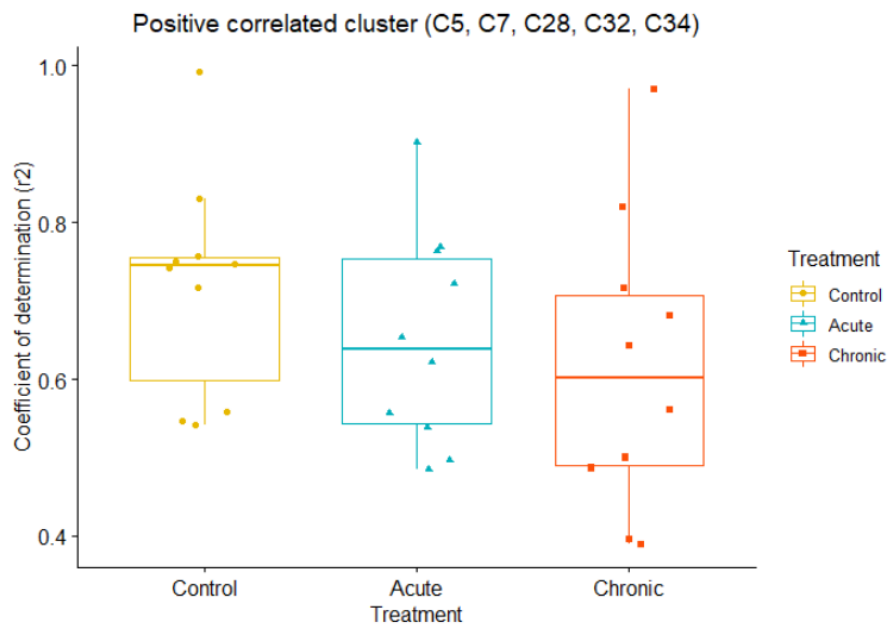


**Figure F.3. Boxplots of the strongest positive correlation cluster for each treatment group. Each boxplot has an associated median and quartiles for each treatment group.**

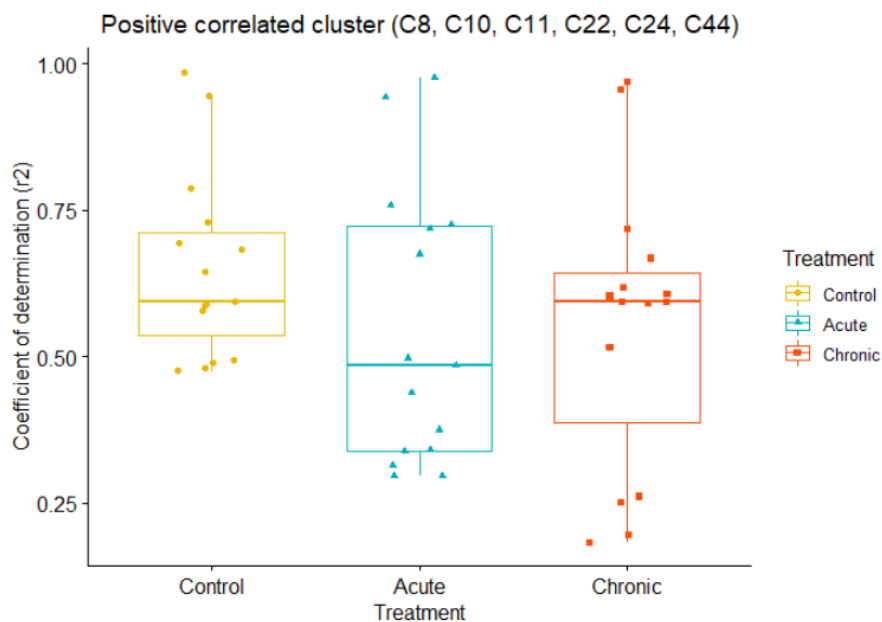


**Figure F.4. Boxplots of the second strongest positive correlation cluster for each treatment group. Each boxplot has an associated median and quartiles for each treatment group.**

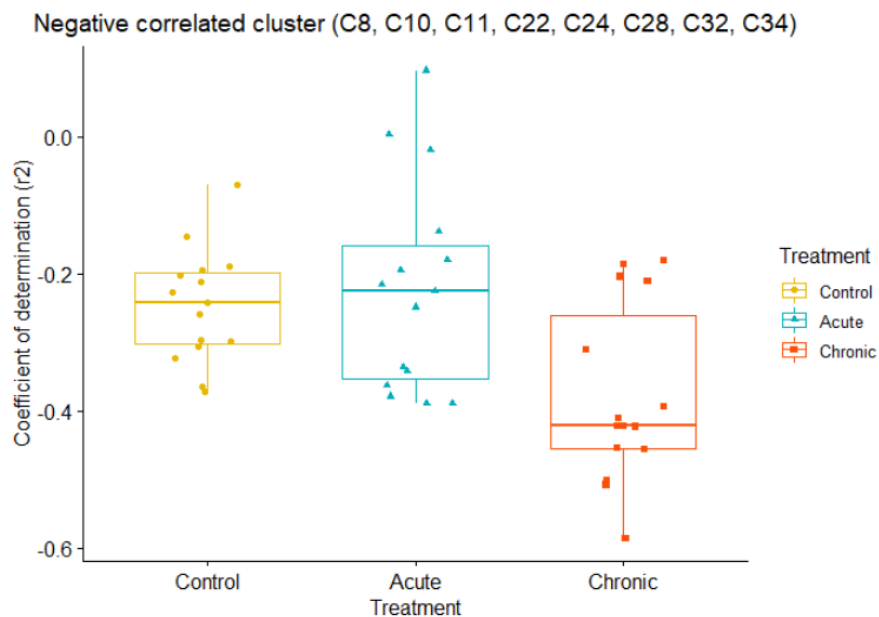


**Figure F.5.** Boxplots of the strongest negative correlation cluster for each treatment group. Each boxplot has an associated median and quartiles for each treatment group.

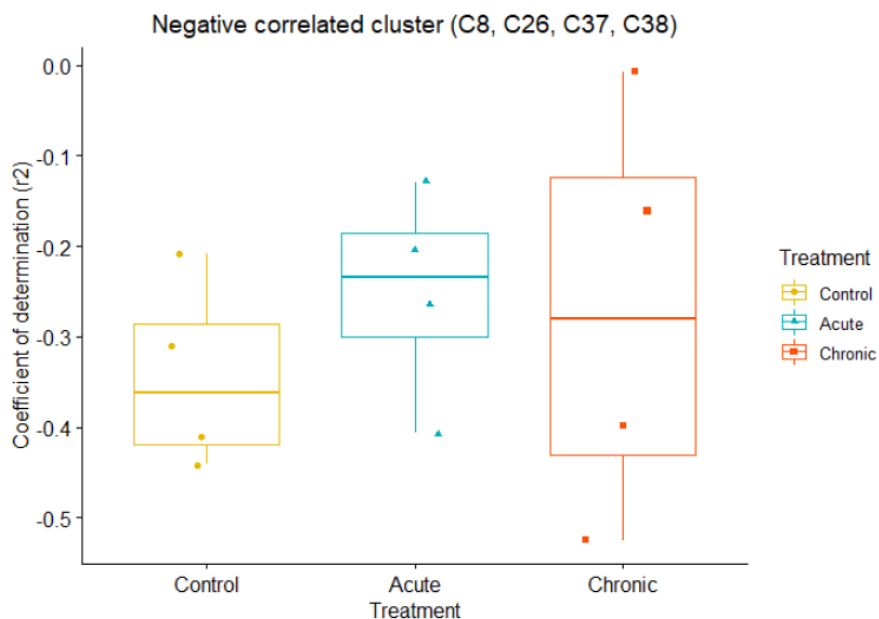


**Figure F.6.** Boxplots of the second strongest negative correlation cluster for each treatment group. Each boxplot has an associated median and quartiles for each treatment group.

APPENDIX G

**Effect of Treatment Groups, Time Points, and Treatment by Time Point  
Interactions**

An interaction effect of treatment groups and time points for chosen compounds of interest was evaluated with paired repeated two-way ANOVAs. For C26, there was no effect of treatment group ( $F_{2,134} = 1.346$ ,  $P = 0.264$ ) or an effect of time points ( $F_{2,134} = 1.144$ ,  $P = 0.339$ ), and there was no interaction between treatment group and time points ( $F_{2,134} = 0.550$ ,  $P = 0.738$ ) (Table G.1).

**Table G.1. Two-way ANOVA results for C26 comparing the effects of treatment group, time points, and treatment by time point interactions on the compound concentrations.**

Table G.1 - C26

Sources of Variation	ANOVA		
	df	F	P
Treatment	2, 134	1.346	0.264
Time Points	4, 134	1.144	0.339
Treatment * Time Points	5, 134	0.550	0.738

For C28, there was no effect of treatment group ( $F_{2,134} = 1.828$ ,  $P = 0.165$ ) or an effect of time points ( $F_{2,134} = 0.501$ ,  $P = 0.735$ ), and there also was no interaction between treatment group and time points ( $F_{2,134} = 0.975$ ,  $P = 0.435$ ) (Table G.2).

**Table G.2. Two-way ANOVA results for C28 comparing the effects of treatment group, time points, and treatment by time point interactions on the compound concentrations.**

Table G.2 - C28

Sources of Variation	ANOVA		
	df	F	P
Treatment	2, 134	1.828	0.165
Time Points	4, 134	0.501	0.735
Treatment * Time Points	5, 134	0.975	0.435

For C34, there was no effect of treatment group ( $F_{2,134} = 1.154$ ,  $P = 0.318$ ) or an effect of time points ( $F_{2,134} = 0.279$ ,  $P = 0.891$ ), and there also was no interaction between treatment group and time points ( $F_{2,134} = 0.638$ ,  $P = 0.671$ ) (Table G.3).

**Table G.3. Two-way ANOVA results for C34 comparing the effects of treatment group, time points, and treatment by time point interactions on the compound concentrations.**

Table G.3 - C34

Sources of Variation	ANOVA		
	df	F	P
Treatment	2, 134	1.154	0.318
Time Points	4, 134	0.279	0.891
Treatment * Time Points	5, 134	0.638	0.671

For C38, there was no effect of treatment group ( $F_{2,134} = 0.547$ ,  $P = 0.580$ ) or an effect of time points ( $F_{2,134} = 0.637$ ,  $P = 0.637$ ), and there also was no interaction between treatment group and time points ( $F_{2,134} = 1.536$ ,  $P = 0.183$ ) (Table G.4).

**Table G.4. Two-way ANOVA results for C38 comparing the effects of treatment group, time points, and treatment by time point interactions on the compound concentrations.**

Table G.4 - C38

Sources of Variation	ANOVA		
	df	F	P
Treatment	2, 134	0.547	0.580
Time Points	4, 134	0.637	0.637
Treatment * Time Points	5, 134	1.536	0.183

For C44, there was no effect of treatment group ( $F_{2,134} = 1.305$ ,  $P = 0.275$ ) or an effect of time points ( $F_{2,134} = 0.326$ ,  $P = 0.860$ ), and there also was no interaction between treatment group and time points ( $F_{2,134} = 1.728$ ,  $P = 0.132$ ) (Table G.5).

**Table G.5. Two-way ANOVA results for C44 comparing the effects of treatment group, time points, and treatment by time point interactions on the compound concentrations.**

Table G.5 - C44

Sources of Variation	ANOVA		
	df	F	P
Treatment	2, 134	1.305	0.275
Time Points	4, 134	0.326	0.860
Treatment * Time Points	5, 134	1.728	0.132

APPENDIX H

**Effect of Treatment Groups, Time Points, and Treatment by Time Point**

**Interactions for C18**

Although it was not selected based on the previously mentioned criteria for the final compounds of interest, C18 was also assessed in a basic two-way ANOVA due to this study being an exploratory approach (Tables H.1, H.2). We found C18 generally decreased in concentration with time ( $P = 0.0015$ ), but this decrease was consistent across treatments and therefore not associated with simulated browsing. This was considered a type I error but may represent a future compound of interest.

**Table H.1. Two-way ANOVA results for C18 comparing the effects of treatment group and time points on the compound concentrations.**

C18

Sources of Variation	ANOVA		
	df	F	P
Treatment	2, 139	1.925	0.1498
Time Points	4, 139	4.629	0.0015

**Table H.2. One-way ANOVA results for C18 comparing the effects of the varying levels of collection intensity on the compound concentrations.**

C18

Sources of Variation	ANOVA		
	df	F	P
Collection Intensity	3, 49	0.298	0.826

**Table H.3. Tukey's Honestly Significant Difference (HSD) test comparing the multiple means of each treatment group and time point in a pairwise manner for C18 to identify any differences that may be greater than the expected standard error.**

Treatment	Multiple comparisons of means 95% family-wise confidence level			
	Tukey's HSD			
	Difference	Lower bounds	Upper bounds	P
Acute-Control	14.3768	-181.5284	210.2821	0.9835
Chronic-Control	-170.3508	-400.4298	59.7283	0.1891
Chronic-Acute	-184.7276	-426.0365	56.5814	0.1689
Time Points	Difference	Lower bounds	Upper bounds	P
1-0	-412.127	-779.681	-44.2729	0.0196
24-0	-415.8565	-747.5292	-84.1839	0.0062
48-0	-404.0197	-732.2142	-75.8251	0.0077
144-0	-441.1443	-783.3185	-98.970	0.0045
24-1	-3.730	-335.4022	327.9431	0.9999
48-1	8.1073	-320.0873	336.3019	0.9999
144-1	-29.0173	-371.1915	313.1569	0.9993
48-24	11.8369	-275.6043	299.278	0.9999
144-24	-25.2877	-328.5927	278.0173	0.9994
144-48	-37.1246	-336.6223	262.3731	0.9970

A Tukey's Honestly Significant Difference (HSD) post-hoc test was performed on the two-way ANOVA for C18 to determine which time points showed significant differences that may be greater than the expected standard error (Table H.3). It revealed that zero h (T = 0 h) was significantly different when compared to all other time points of 1, 24, 48, and 144 hr (T = 1, 24, 48, 144 hr) ( $p = 0.02$ ,  $p = 0.006$ ,  $p = 0.008$ ,  $p = 0.005$ ).